Title

CHINA’S POWER SECTOR DECARBONIZATION: MODELING EMISSION REDUCTION POTENTIAL, TECHNICAL FEASIBILITY AND COST EFFICIENCY OF INTER-SECTORAL APPROACHES

Author

Avrin, Anne-Perrine Martine, Louise

Publication Date

2018

Peer reviewed|Thesis/dissertation

China's Power Sector Decarbonization: Modeling Emission Reduction Potential, Technical Feasibility and Cost Efficiency of Inter-sectoral Approaches

by

Anne-Perrine M. L. Avrin

A dissertation submitted in partial satisfaction of the

requirements for the degree of

Doctor of Philosophy

in

Energy and Resources

in the

Graduate Division

of the

University of California, Berkeley

Committee in Charge:

Professor Daniel M. Kammen, Chair
Professor Zechun Hu
Professor Ashok Gadgil
Professor Per F. Peterson

Summer 2018

CHINA'S POWER SECTOR DECARBONIZATION: MODELING EMISSION REDUCTION POTENTIAL, TECHNICAL FEASIBILITY AND COST EFFICIENCY OF INTER-SECTORAL APPROACHES

Abstract

China's Power Sector Decarbonization: Modeling Emission Reduction Potential, Technical Feasibility and Cost Efficiency of Inter-sectoral Approaches

by
Anne-Perrine M. L. Avrin

Doctor of Philosophy in Energy and Resources

University of California, Berkeley
Professor Daniel M. Kammen, Chair

China has become the "world's factory" and lifted up several millions of people out of poverty through decades of economic reforms. However, this socio-economic development, fueled by coal, has heavily impacted the energy landscape and the environment. Today, China is both the global largest polluter and largest developer of clean energy systems. The unprecedented extent of the country's power sector challenges and opportunities requires to refine current capacity planning models to better inform policy making. Focusing on climate urgency, this study contributes to filling this need by proposing new modeling frameworks. These models offer a fine-grain analysis of China's power sector decarbonization potential, by grounding long-term electricity mix expansion planning into inter-sectoral development. Using large datasets of technical, economic and social factors, levers of the clean power transition are analyzed by quantifying and comparing their decarbonization potential, technical feasibility, and cost efficiency over time and across regions and resources. The first lever lies in the coordinated expansion of a low-carbon electricity grid, resilient to renewable energy intermittency and disparities in space and time between energy resources and demand. The high-resolution model SWITCH-China is used to explore optimal capacity expansion pathways for China's electricity mix under various low-carbon policies. Results show that, while natural gas can become a bridge between the current coal-dominated grid and a future clean electricity mix, a deep decarbonization scenario mostly relies on the concomitant deployment of nuclear—inland, encouraged by advanced nuclear technology development—, wind, solar, energy storage, coal with carbon capture and storage, and an expanded transmission network. Meeting this long-term decarbonization goal increases electricity costs significantly compared to an unconstrained scenario. A modular approach, adaptable to traditional cost-minimizing tools used by planning agencies, is proposed to reduce uncertainty of future technological costs as well as costs resulting from electricity generation intermittency. The model finds that there exist alternatives to the least-cost strategy, which present slightly higher overall electricity costs, but much lower risks. In particular, given the predominance of fossil fuel in the current electricity mix, the deployment of low-carbon systems decreases the overall risk on future costs through diversification, even by accounting for increased operational complexity resulting from renewable energy intermittency. The second lever is the integration of linkages between power and water supply into the optimization framework, as China currently faces both severe water shortages and severe water pollution. Results show that, while total costs of the South to North Water Transfer Project are 2.5 times lower than nuclear desalination, the

latter emits six times less CO_2. In addition, fresh water from nuclear desalination is shown to be affordable even to the poorest households. Challenges posed by the construction and operation of interregional water diversion suggest that it should only be used in dry inland areas, while low-carbon desalination could be developed at larger scale near coastal economic centers. The DESEC model is developed to explore controllable desalination, powered by nuclear, wind, or solar energy, as a mean to alleviate water scarcity in coastal regions while enabling the wide deployment of a low-curtailment clean power base. Desalination, used as a deferrable load, can transform two low-value products, seawater and excess power from non-dispatchable energies, in a high-value product, fresh water. The DESEC model finds that the North China Grid region's entire water deficit—61.4 billion m^3—can be met entirely by deferrable desalination with a total cost of about \$1.5/m^3, less than the global average water price. Analyses conclude that there exist local alternatives to current national-scale power and water diversion projects, more adapted to regional characteristics, less prone to risks and disruptions. The third lever is the electrification of urban passenger cars, as the sector is poised for massive expansion in the next decade. Findings show that the near-term deployment of electric vehicles cannot be enabled by technology cost decrease alone. If the current impact from favorable policy is maintained but not amplified, CO_2 emissions from urban passenger cars will peak around 2040, or ten years past the official 2030 carbon peak target. In fact, although it demonstrates higher costs in the near term, large-scale vehicle electrification is the least-cost, least-CO_2-emission pathway for China's urban transportation expansion in the long run. Generally, model results reveal that massive investment is needed in R&D and infrastructure capacity deployment, and that utilities and institutions must be reformed to manage resources rationally, hand-in-hand. Many of the studied decarbonization options have not reached a mature stage or have not been deployed at utility-scale today, and future work is required to better account for modeling and data uncertainty. Yet, models developed, used and presented in this study all reveal the existence of viable, cost-efficient options to enable meaningful decarbonization while alleviating water scarcity and air pollution. These strategies can only be achieved by combining central-scale coordination with local-scale implementation, to take advantage of China's diverse and rich territory while minimizing risks. This dissertation provides new approaches for identifying realistic, affordable capacity expansion pathways, rigorously designed by mathematical optimization and large datasets, to reduce CO_2 emissions related to the power sector in line with climate targets. The impact that China will have on climate change and its ability to ensure its long-term sustainability will depend on actual decisions and actions undertaken by governmental and private entities. The success of the clean energy transition is contingent on the country's ability to encourage technological, economic and institutional innovation.

To the Chinese people.
A lifetime of research would not suffice to comprehend all the riches of their country.

ACKNOWLEDGMENTS

I am grateful to the many people that have helped me start, pursue, and complete this beautiful journey.

First and foremost, I would like to thank Nicolas Zweibaum. You have been an incredible support, both emotionally and intellectually, as this dissertation bears your print through the lot of valuable advice you provided me with over the years. First as a friend, then boyfriend, finally husband, you were on my side for the entire duration of this PhD, and I look forward to keeping you there for the rest of our lives.

Thanks to my wonderful parents, Catherine and Jérôme, for their unconditional love and support, which has remained as strong as ever since I decided to move to California. Thanks to Guillaume and Aude, the best siblings one could hope for. Their kindness, only, matches the depth of their thoughts. I owe, to you four, the courage it took me to dream about, then actually undertake, this adventure on the other side of the world.

This dissertation would not have been possible without the guidance and mentorship of Professors Daniel Kammen and Zechun Hu. Dan, your vision, fearlessness, and constant acknowledgement of the work of your students solidified my determination. Zechun, your meticulous review of my work and your intellectual contribution were decisive to my PhD.

I have greatly benefited from the advice of several researchers, including Professor Per Peterson, Professor Ashok Gadgil, Professor Scott Moura, Dr. Jiang Lin, Anthony Nahas. You have, at one point or another, be key to the progress of my PhD.

Thanks to my fellow ERGies, in particular Nikky Avila, Noah Kittner, Laura Moreno, Veronica Jacome, Kripa Jagannathan, Chris Hyun, Julia Szinai, and Jose Daniel Lara, for the countless discussions on campus or around a beer, sometimes both. You have helped me blur the line between working and understanding our world across countries, times and disciplines, a mindset that I hope to keep alive even as I move on from the academic world.

Thanks to Framatome (formerly Areva), without whom this PhD would not have been possible. I am grateful for the sponsorship (special kudos to Grégory Cherbuis for his patience in dealing with UC Berkeley's administrative process) and for the highly competent, visionary, and kind people I have met at the company, especially Lou Martinez Sancho, who has become a mentor and a friend.

Finally, as fun and friendship are essential ingredients of a successful PhD, huge thanks to the wonderful people I have met in the San Francisco Bay Area: Olivia Conjeaud, Soazig Kaam, Maxime Crépin, Arnaud de Régis, Simone Bochner, Justine Rey, Hugo Wagner, Laura Fontaine, Katya Cherukumilli, Karina Cucchi, Albert Yuen, Ahmed El Alaoui, Amine Kamel, Hubert and Meg Chaperon, Moana Reynau, Benjamin Fildier, Walid Mathlouthi & so many more. You have become my second family.

TABLE OF CONTENTS

Chapter 1 Introduction *1*

Chapter 2 System-Level Analysis of China's Electricity Mix Decarbonization *11*

2.1 Introduction **11**

2.2 Capacity Expansion Planning Modeling **19**

2.2.1 Methodology and Model Description 19
2.2.2 Scenarios 20
2.2.3 Results 22
2.2.4 Conclusion 28

2.3 Two-Step Uncertainty Minimization Approach **29**

2.3.1 Methodology and Model Description 31
2.3.2 Application to China's Power Sector and Results 33
2.3.3 Conclusion 38

Chapter 3 Decarbonized, Regional-Scale Alternatives for Fresh Water Supply in China *40*

3.1 Introduction **40**

3.2 Relevance of Nuclear Desalination as an Alternative to Water Transfer Geoengineering **42**

3.2.1 Methodology 43
3.2.2 Results 50
3.2.3 Conclusion 56

3.3 From Power Generation to Value Creation: De-Risking Clean Energy Investment via the Untapped Power-Water Coordination Opportunity in the North China Grid **57**

3.3.1 Concept, Applicability and Methodology 60
3.3.2 Results 73
3.3.3 Conclusion 81

Chapter 4 New Energy Vehicle Deployment in Urban China and Impacts on CO_2 Emissions, Costs and Energy Consumption *83*

4.1 Introduction **83**

4.2 Data and Methodology **86**

4.2.1 Vehicle Ownership Projections over the 2050 Horizon 86
4.2.2 CO_2 Emissions 87
4.2.3 New Energy Vehicle Deployment Scenarios 88
4.2.4 Economic Analysis 90
4.2.5 Electricity consumption 92

4.3 Results **94**

4.4 Conclusion..98

Chapter 5 Conclusion 100

References...104

List of Figures

Figure 1-1 Annual CO_2 emissions in China, the United States, France and Kenya at the national level (left) and per capita (right) in years 1990, 2010 and 2016. 2

Figure 1-2 Power generation share by source in China, end 2017. Total power generation in 2017: 6418 TWh. 6

Figure 2-1 Theoretical ramping profiles of Pressurized Water nuclear Reactors (PWR). 14

Figure 2-2 Count of operational storage systems per type of energy service provided worldwide in 2018. The color code indicates the level at which the storage system connects to the grid. 15

Figure 2-3 Carbon dioxide emission trajectory for China's power sector under the four scenarios (SWITCH-China results), as well as historical emissions in China and the United States until 2015. 23

Figure 2-4 Evolution of China's installed power generation capacity mix over time for the four scenarios (SWITCH-China results). 25

Figure 2-5 2050 dispatch schedule for the least-cost electricity mix in the IPCC Target Scenario (SWITCH-China results) 26

Figure 2-6 Infrastructure, generation and transmission capacity needed to achieve the IPCC target (SWITCH-China results). All represented lines are new transmission expansion 27

Figure 2-7 Feasible portfolios—including the Pareto efficient frontier from P_1 to P_2—characterized by expected LCOE and standard deviation of LCOE in the year 2030 (QP optimization results). P_S represents the least-cost electricity mix (SWITCH-China results from the BAU with Carbon Cap scenario). Pie charts represent generation shares for the five energy sources considered in portfolios P_S, P_1 and P_2. 35

Figure 2-8 Change in annual electricity generation per energy source for the two efficient portfolios P_1 (top) and P_2 (bottom) compared to the SWITCH-China least-cost portfolio in the year 2030 (QP results). 36

Figure 2-9 Change in annual CO_2 emissions for the two efficient portfolios P_1 and P_2 compared to the SWITCH portfolio in the four periods (QP results). 38

Figure 3-1 China's projected nuclear fleet in 2030 and Eastern, Central and Western routes of the SNWTP, as of 2015. The three routes are drawn in dark blue. Red crosses represent nuclear plants hosting reactors found appropriate to nuclear desalination in 2030, while yellow crosses indicate nuclear plants that, for geographic or age-related reasons, are considered not appropriate. 41

Figure 3-2 Nuclear capacity expansion in China until 2030. For nuclear reactors whose starting year is not known yet but that are planned to be built before 2030, first grid connection is assumed to be 2025. 46

Figure 3-3 Desalinated water supply cost in 2030 as a function of the quantity of water supplied per person per year in Beijing (model results). The blue dashed line indicates the threshold for the five-percent rule. Squared black markers represent quantities of water for which the capacity of an additional water plant is required (small quantities are supplied by nearby plants and cost increases as production from additional plants, farther from demand centers, is needed). 52

Figure 3-4 Annual renewable water resources (current: gray bars; model results for desalination: dashed bars) as well as total cost (production and transportation) from modeled nuclear desalination plants to the capitals of the eleven water-scarce provinces in 2030. The dashed blue line represents the threshold for absolute water scarcity. 53

Figure 3-5 Average specific desalinated water cost—including production and supply—for the SNWTP, nuclear desalination, and coal desalination in 2030, as a function of hypothetical carbon prices (model results). 56

Figure 3-6 Challenges and opportunities of VRE power generation and seawater desalination. Inter-resource synergies offer potential for value creation. 60

Figure 3-7 Location of capital cities of the NCG provinces (red crosses) used as proxies for water demand centers in the DESEC model. 72

Figure 3-8 Annual carbon dioxide emissions from power generation in NCG (gray bars) and desalination carbon footprint (blue dots), including desalination plant construction, production and transport of desalinated water (model results). 75

Figure 3-9 Simulated hourly power dispatch schedule in the NCG for the Water Scarcity Eradication scenario during four different years. 76

Figure 3-10 Cumulative net renewable fresh water resources available per capita by region, including existing supply weighted over monthly precipitation averages, and desalination supply DESEC results for the Water Scarcity Eradication scenario. The red dotted line represents the absolute water scarcity threshold, defined by the United Nations at 500 m^3/capita/year or 0.057 m^3/capita/hour. 77

Figure 3-11 Deferrable desalination construction, operation and transportation costs In NCG. 80

Figure 4-1 Possession of private passenger vehicles in China’s six regions: North (Beijing Tianjin Hebei Shanxi Inner Mongolia), Northeast (Liaoning Jilin Heilongjiang), East (Shanghai Jiangsu Zhejiang Anhui Fujian Jiangxi Shandong), South (Henan Hubei Hunan Guangdong Guangxi

Hainan), Southwest (Chongqing Sichuan Guizhou Yunnan Tibet), and Northwest (Shaanxi Gansu Qinghai Ningxia Xinjiang).. 84

Figure 4-2 Net present cost per vehicle for NEVs and ICEVs using an annual discount rate of 5% and assuming that the average vehicle useful lifetime is 10 years. 92

Figure 4-3 Probability of parking at each time of the day for private vehicles in Shanghai................ 92

Figure 4-4 Daily national load in 2045 under the four NEV deployment scenarios and without electric vehicles, assuming that NEV charging load is smoothed out across the day but temporally constrained by probabilities of parking time and of charging. 93

Figure 4-5 Average urban population share per province over the 2010-2015 period (colored areas) and number of private passenger cars on the road in urban areas per province in years 2030 and 2050 calculated with a Gompertz function (bar diagrams)... 94

Figure 4-6 Projections of annual CO_2 emissions from urban private passenger vehicles in China under four NEV deployment scenarios (model results)... 95

Figure 4-7 Modeled projections of circulating NEVs in China in the four scenarios. 96

Figure 4-8 Net present cost of urban passenger vehicles (consumer and infrastructure levels) in China in the four scenarios using an annual discount rate of 5%... 97

LIST OF TABLES

Table 2-1 Existing bottom-up models of China's electricity mix........ 17

Table 2-2 Technology-specific national targets for China's power sector, as of 2015........ 21

Table 2-3 Elements of the QP........ 32

Table 2-4 Change in electricity supply costs and relative standard deviations for the efficient portfolios P_1 and P_2 compared to the least-cost portfolio P_S in 2030 (QP results)........ 37

Table 3-1 Average SEC, specific electricity loss, and gain output ratio of MED and MSF desalination technologies for a modeled 500,000 m^3/day nuclear desalination plant (DEEP results)........ 44

Table 3-2 Characteristics, including maximum desalinated water production capacity, of the fleet of nuclear reactors suitable to desalination in 2030........ 47

Table 3-3 Inputs used in the four scenarios explored by the DESEC optimization model........ 73

Table 4-1 Description of NEV deployment scenarios........ 90

ACRONYMS

ACPR1000 — Advanced China Power Reactor, Generation III Chinese nuclear reactor design of 1100 MWe [1]

AP1000 — Advanced Passive, Generation III Westinghouse Electric Company nuclear reactor design of 1200 MWe [2]

BAU — Business-as-usual

CAES — Compressed air energy storage

CAP1400 — Generation III Chinese nuclear reactor design of 1400 MWe [1].

CAS — Chinese Academy of Sciences, China

CCS — Carbon capture and storage

CNP-600 — China Nuclear Power, Generation II Chinese nuclear reactor design of 600 MWe [3]

CPR1000 — Generation II+ Chinese nuclear reactor design of 1080 MWe [4]

DEEP — Desalination Economic Evaluation Program

DR — Demand-response

EPR — European Pressurized Reactor, French nuclear reactor design of 1770 MWe [2]

ERI — Energy Research Institute, China

ESMAP — Energy Sector Management Assistance Program, U.S.A.

FYP — Five-year plan

Gt — Gigaton

GUCAS — Graduate University of the Chinese Academy of Sciences, China

GWe — Gigawatt electric

HTR-PM — High Temperature gas-cooled Reactor - Pebble-bed Module, Generation IV Chinese nuclear reactor of 250 MWth [5].

Hualong One — Flagship Generation III Chinese nuclear reactor design of 1070 MWe, main Chinese export design [1]

IAEA — International Atomic Energy Agency, Austria

ICEV — Internal combustion engine vehicle

IEA — International Energy Agency, France

IIASA — International Institute for Applied Systems Analysis, Austria

IPCC — Intergovernmental Panel on Climate Change

LBNL — Lawrence Berkeley National Laboratory, U.S.A.

LCOE — Levelized cost of electricity

LP — Linear program

MED — Multi-effect distillation

MSF — Multi-stage flashing

MSRP — Manufacturer's suggested retail price

MWe — Megawatt electric

MWth — Megawatt thermal

NCEPU — North China Electric Power University, China

NCG — North China grid

NDRC — National Development and Reform Commission

NEA — National Energy Administration

NEV — New energy vehicle

NHR-200 — Nuclear Heating Reactor, Generation IV Chinese nuclear reactor of 200 MW thermal [6]

NDRC — National Development and Reform Commission, China

O&M — Operation and maintenance

PHS — Pumped-storage hydroelectricity

PV — Photovoltaics

PWR — Pressurized water (nuclear) reactors

QP — Quadratic program

RAEL — Renewable and Appropriate Energy Laboratory, U.S.A.

RO — Reverse osmosis

SEC — Specific energy consumption

SNWTP — South to North Water Transfer Project

SOW — Safe operating window

TMP — Transmembrane pressure

TOU — Time-of-use

TU — Tsinghua University, China

UCB — University of California, Berkeley, U.S.A.

UHV — Ultra-high voltage

VRE — Variable renewable energy

VVER-1000 — Voda Voda Energo Reactor, Generation III Russian nuclear reactor design of 1060 MWe [2]

WEETP — West to East Electricity Transfer Project

CHAPITRE 1 INTRODUCTION

Starting in 1978, under the impulsion of Deng Xiaoping, the Chinese government has concentrated its efforts on economic development by introducing market principles. The particularities of the reform in its nature—inspired from Western countries but conserving political attributes, hence called "socialism with Chinese characteristics"—and its implementation—gradually and by experimenting, not through rapid standardization—have led to profound economic and social changes in the country. Over the last forty years, more than 800 million people have been lifted out of poverty [7] and the Chinese middle class has grown significantly [8]. As far as energy is concerned, this fast development has resulted in massive addition of electricity generation capacity installed in record time. Because of its abundance and relative low cost, coal has been an essential engine of China's industrial and economic development. Electricity production from coal has more than doubled in the last ten years, from 1,700 TWh in 2004 to 4,400 TWh in 2014, and is still the country's main source of power today—representing 66% of its total electricity production in 2016 [9].

This fast and massive coal-powered economic development encouraged migration from rural Western regions to economic centers in the East, especially in the 1990s and early 2000s [10]. For example, the 2000 census in China documented 24.4 million permanent migrants and 86.3 million temporary migrants [11]. The rapid and disorganized urbanization that has followed [12] has been performed at the expense of the environment, in particular the climate, air quality, water supply, and overall public health [13]–[17]. At the global scale, this development has resulted in China becoming the global largest emitter of carbon dioxide in 2006, seconded by the United States (Figure 1-1 (left)). In 2017, the country released 10.5 gigatons (Gt) of CO_2 to the atmosphere, half of them from the power sector [18]. CO_2-emission equivalent per capita in China has reached a globally significant level as well, but remains about 50% lower than in the United States (Figure 1-1 (right)). At the local scale, high concentration of fossil-fuel-based power plants near cities, intense economic activity and gasoline vehicles have led to health-threatening air pollution levels in urban areas [19].

Yet, the urban transportation sector in China, currently demonstrating low vehicle ownership levels compared to Western countries, is poised for massive expansion in the next decade. Through its "corner overtaking" (弯道超车) strategy [20], the Chinese government has communicated its desire for the country to become a global leader in new energy vehicles[1] (NEV).

[1] Here, new energy vehicles designate plug-in hybrid and battery electric vehicles. Depending on the context, hydrogen electric fuel cell vehicles are sometimes included in the NEV label, however it is not considered in the present analysis, given the very low market for such technology in China today compared to plug-in hybrid and battery electric vehicles.

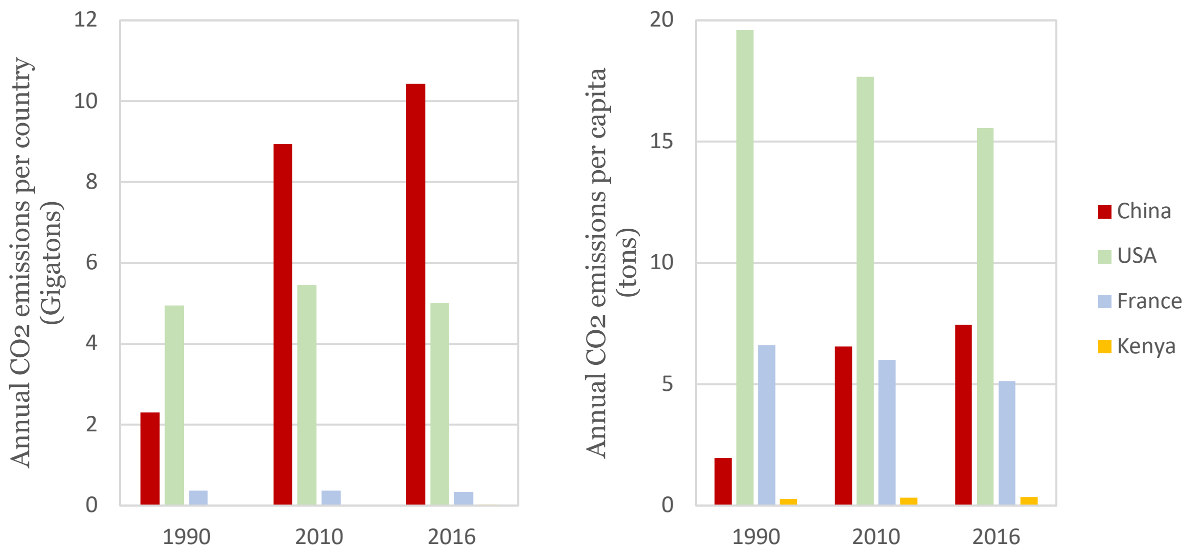

Source: Emissions Database for Global Atmospheric Research (EDGAR), European Commission [21].

Figure 1-1 Annual CO_2 emissions in China, the United States, France and Kenya at the national level (left) and per capita (right) in years 1990, 2010 and 2016.

Despite China being the largest market for NEVs, their relative share in the country's total vehicle sales remains low, especially for passenger cars, and negative externalities from the gasoline-dominated urban transportation sector keep intensifying. As an example, air pollution cost Beijing ¥583.02 million in 2012 [22], as a result of expenses in cardiovascular diseases treatment (18.3% of economic losses), respiratory diseases treatment (12.6% of losses) and depreciation of human capital due to premature death (69.1% of losses). The potential of transportation electrification to alleviate these challenges depends on the characteristics of China's future power sector, especially its emission intensity and its ability to accommodate additional load.

China's economic development has also increased water demand, impacted by population growth, income growth and industrial development, as the country hosts 22% of the world's population but only 6% of its fresh water resources [23]. Water scarcity is further exacerbated by pollution. Nationwide, 61.5% of groundwater reserves and 31.4% of surface water have a quality of class IV or lower, characterized as "poor" or "very poor" by China's Environmental Quality Standards classification, therefore unsuitable for human consumption and for some industries [24]. 21% of the country's surface water is not even suitable for agricultural use [25]. Water supply is also closely related to power supply for two main reasons. First, water is used for cooling purposes in thermoelectric plants. In 2010, thermoelectric water withdrawals added up to 60 km^3 in China [26], or 10% of global thermoelectric water withdrawals that year [27] and 11% of China's annual water demand [28]. Second, electricity and thermal energy are used to power a small but rapidly increasing fleet of water treatment plants in China [29]. In particular, encouraged by the official "13th Five-Year Seawater Utilization Plan" [30], the national desalination capacity is expected to grow from 1.2 million m^3/day in 2017 [31]—meeting 0.8% of the national water demand—to 2.5-3.1 million m^3/day in 2020 [29].

Desalination is powered, in majority, by China's coal-dominated grid or by coal plants directly. Given the small size of today's desalination capacity in the country, this industry is only responsible for nearly one megaton of CO_2 emissions per year [32] or 0.008% of national CO_2 emissions annually [18]. Today, water scarcity primarily hits some of China's most developed provinces, in the North-Eastern part of the country, while Southern and far Western provinces are water-rich. The Chinese government's response to the geographic mismatch between water demand and supply has been the construction of a massive project, the South-North Water Transfer Project (SNWTP), to divert water from resource-rich to scarce provinces, with tremendous direct and indirect costs, such as people resettlement [33], and the long-term risk of drying out Southern provinces [34]. Despite this project, the national water gap between demand and supply is expected to reach 130-230 km^3 in 2030 [35], resulting in an economic loss of $35 billion annually [36]. Deploying a desalination capacity sufficient enough to alleviate China's tremendous water needs would, under the current electricity mix, significantly increase CO_2 emissions. As a mean of comparison, filling the water demand-supply expected gap by means of desalination, with its current footprint, would increase the country's annual CO_2 emissions by 0.3 to 0.6 Gtons, or between 3% and 6% of national CO_2 emissions in 2016. To summarize, concerns around the ability to achieve emission reductions despite increasing number of vehicles on the road and increasing fresh water needs, and the electrification opportunity, suggest that the transportation and water sectors will become key players in China's clean energy transition.

People's increasing awareness of the negative impacts of environmental challenges has fueled social unrest throughout China. Increasing pressure is put on the government by the growing middle class, empowered by its recently acquired wealth, urging it to solve these challenges. Such social pressure, in addition to the evident need to deal with the country's socio-economic disparities and environmental problems to ensure a functional economy and society, might be the reason behind the creation of a new slogan, the "China Dream" (中国梦), first mentioned by President Xi Jinping during the 18th Congress of the National Communist Party of China in 2012 [37]. This slogan sketches the medium-term achievement of moderate prosperity and the long-term rejuvenation of the nation. It is the continuation of a previous concept, the "harmonious society," first coined by Confucius around 500 BC [38] and, in the mid 2000s, put at the center of Hu Jintao's Scientific Outlook on Development [39]. The China Dream embeds two key objectives. The first one is for China to develop a functional middle-class by improving living conditions to increase "people's happiness" (人民幸福), becoming a *xiaokang shehui* or "moderately prosperous society" (小康社会) around 2025. The second objective is to "reshape the country" (国家重塑) to create a fully-developed and globally leading nation (國家富強 "national rejuvenation") by 2050 [37]. These two objectives are sometimes called the "material" and "modernization" goals, respectively, and realization dates approximately match the "Two 100s": the 100th anniversary of the Chinese Communist Party in 2021, and the 100th anniversary of the People's Republic of China in 2049 [40]. The term "material" refers to the goal of completing the middle-class transition to reach living conditions similar to those of today's most developed nations. The term "modernization" refers to the Chinese society getting ahead of most developed nations, seizing the opportunity of its much-needed infrastructure transition to develop and implement advanced technologies. Be it a mere propaganda tool or a true roadmap for governmental funding and action, the radical rethinking of resource management and infrastructure reflected in the China Dream will be a necessity for the country to ensure its long-term sustainability. In fact, China's transition toward sustainability is not an active choice but a reactive and logical response to the environmental issues mentioned above [41].

The China Dream relies on the idea that there exists a successful path for China's development, similar to Western countries in goal but not in methods, relying on "socialism with Chinese characteristics" and large-scale technology deployment. Such idea is even more interesting when put into the perspective that current high pollution levels do not only result from an increase in fossil fuel burning to accommodate industrial and other needs. They also result from technological inefficiencies of old thermal plants and electricity transmission congestion, as well as institutional and organizational inefficiencies of a predominantly state-owned power sector. In the context of very large power demand created by a market-based economic development, the transition toward clean power supply has become a necessity. In practice, the transition is two-fold. First, the power sector actors themselves—power generation firms, transmission companies, regulators and, eventually, consumers—and interactions between them, as well as sector-wide practices, must be rethought for the power industry overall structure to be functional and efficient under the new economic paradigm. Second, the unbearable negative externalities of inefficient fossil-fuel burning warrant the deployment of clean energy technologies, as well as the infrastructure allowing for their reliable operation, transmission and distribution, coupled with energy efficiency measures.

Before 1985, administration, planning and operation of the power sector were fully controlled by the central government. Electricity prices were used for accounting purposes rather than real resource allocation and were kept low to support economic growth [42]. China terminated the state monopoly of "exclusive investment in power generation" in 1985 to gradually open its power generation market [43]. Since then, the power industry restructuring of the last three decades can be broadly divided into three stages: economic reform to fund the deployment of power infrastructure through open capital investment (1985-1996), market-oriented institutional reforms of state-owned companies to introduce competition (1997-2001) and, more recently, unbundling of generation firms from grid companies with the creation of five generation entities and two grid entities (2002-present) [44], [45]. Since the issuance of the "Provisional Regulation on Encouraging Fund-Raising for Power Construction" document by the State Council in 1985, the power sector has successfully raised investment from both domestic and foreign entities [45]. In 1997, the State Power Corporation was created with the mandate to take over electricity assets from the Ministry of Electricity Power and manage operation of the power sector [46]. The same year, the Energy Conservation Law was passed, requiring local governments to collect and communicate energy statistics, and companies to report energy usage [47]. A few years later, encouraged by worsening acid rains and SO_2 pollution levels, the Law for Prevention and Control of Air Pollution was revised and enhanced [48]. The Chinese government has gradually implemented reforms, national and regional targets, and monetary and non-monetary incentives to build a more economically and environmentally efficient power sector. The first round of power industry reform was carried out in 2002 under the guidance of Mandate No. 5, issued by the central government. This Mandate acted the separation of electricity generation and grid operating companies, the establishment of the State Electricity Regulatory Commission in 2003, and enhanced overall efficiency of the power industry while fulfilling power demand needs across the country [49]. The Renewable Energy Law, which includes hydroelectricity, wind power, solar energy, geothermal energy and marine energy, was passed in 2005 and updated in 2010 to reflect technological and policy progresses. It offered a series of policy and financial instruments to promote the deployment of renewable energies in the country [50]. Unlike VREs, nuclear power usually demonstrates a baseload generation pattern similar to other thermal plants, such as coal, around which the legislation was initially developed. Therefore, no major change in grid-level legislation solely focused on nuclear energy. Yet, the 2003 "Law on Prevention and Control of Radioactive Pollution" [51] and the 2017 nuclear safety law [52], [53] provide a structure to enable the safe, large-scale use of this energy. Given the fast socio-economic development of the country, some pricing and planning mechanisms prescribed by Mandate No. 5 rapidly became outdated. This has led to irrational and inefficient deployment and use of energy systems, jeopardizing meaningful development of clean power [49]. While, in the early 2000s, China's reliance on international support to attract foreign investment forced the country to consider the World Bank's recommendation of full-scale privatization of the power sector [54], strengthened and diversified funding streams in later years—as well as the risks of broken deregulation, illustrated by the 2000 California electricity crisis [55]—encouraged China to progress with caution on the vertical restructuring path. In recent years, we even observed a backward trend where state-owned enterprises increased their monopoly in power generation and transmission, a phenomenon sometimes coined 国进民退 ("the state advances, the private sector retreats") [42], while the share of private investment in the power industry has decreased [56]. Document No. 9, "Deepening the Reform of the Electric Power System," was issued in 2015 to update the central government's power industry development guidance to China's new socio-economic context. Document No. 9 highlights the industry's most pressing issues and most needed reforms: promoting electricity power pricing mechanisms; reforming power trading systems; reforming power generation, power utilization and the current market mechanisms; establishing independent electricity trading institutions and a fair and regulated trading platform; steadily reforming power sales and distribution; enhancing fair access to power grid and transmission; reinforcing electricity safety, scientific supervision and an integrated power planning system [56]. While this series of guidance documents was primarily destined to a local audience, the central government has also set increasingly ambitious objectives, largely communicated on the international stage, through its Five-Year Plans (FYPs), National Action Plan on Climate Change[2], Energy Development Strategy Action Plan, Nationally Determined Contributions and several carbon targets, to encourage the development of a clean power sector. Reforms toward a retail electricity market relying on real-time electricity pricing and the implementation of a national trading scheme for carbon dioxide emissions are illustrations of how, despite an industrial re-organization that is still in its infancy, China has started implementing reforms that are ahead of most Western countries. Given China's unique size and socio-economic

[2] At the time of its creation in 2007, China was the first developing country to publish a national strategy addressing climate change.

heterogeneity, addressing the energy transition challenge is both a tremendously complex task and an incredible opportunity for the country to position itself at the forefront of low-carbon technology development worldwide. China's status as a global leader in the fight against climate change, demonstrated through colossal investments in renewable energies that are equal to none [57], is reinforced by antagonistic decisions from the second global largest CO_2 emitter, the United States, which withdrew from the Paris Agreement in 2017 [58]. Yet, despite numerous guidelines and targets to encourage the energy transition, China remains a polluting and polluted country. The power generated in China per energy source, dominate by coal, is presented in Figure 1-2.

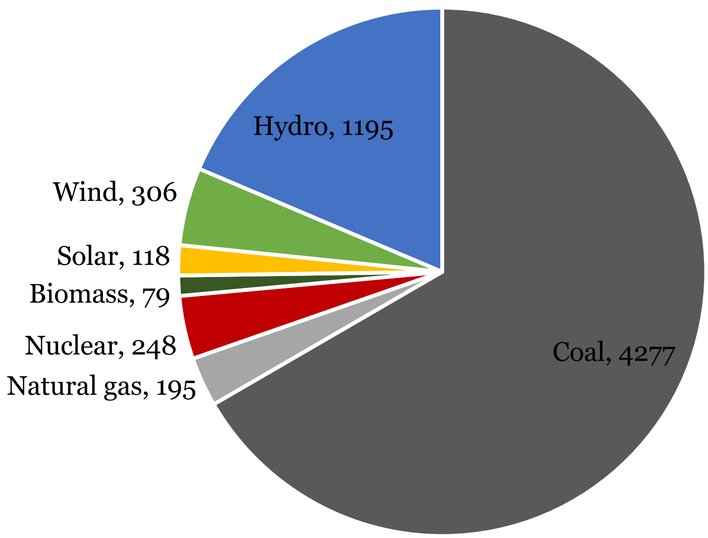

Source: China Energy Portal [59].

Figure 1-2 Power generation share by source in China, end 2017. Total power generation in 2017: 6418 TWh.

The current difficulties to achieve the energy transition can be explained by the existence, besides structural and reorganization challenges mentioned above, of intrinsic energy challenges related to China's large and diverse territory. The geographic mismatch between largest power demand centers, located on the Eastern and South-Eastern coastal regions, and energy resources is, today, one of China's most serious problems [60]. 80% of national coal reserves are located in North and Northwestern areas and 82% of hydro resources are located in South and Southwestern regions [43]. As an example, in 2016, Eastern China accounted for 35% of the country's electricity consumption [61] but only has 8% of the country's total coal reserves and 4% of its exploitable hydro power resources [62]. As far as variable renewable energies (VREs) are concerned, Northern China concentrates 90% of the national wind power potential [63] and low-populated Western China is the most affluent region with regards to solar resources [64]. Additionally, the variability of wind and solar energies creates temporal mismatch between power generation and demand [63]. In fact, only nuclear power, with its high energy density, has proved to be an efficient, low-carbon source of electricity that can be located in or near high-demand coastal centers [42]. As a consequence, with its recent constructions, China has become the country with the largest new nuclear development worldwide. Nuclear energy is expected to represent 8-10% of China's total power generation by 2030 and 15% by 2050, with installed capacities of 120 GWe and 240 GWe, respectively [65]. Longer-term plans have mentioned a potential six-fold increase in installed nuclear capacity between 2050 and 2100. However, at only 35 GWe of installed capacity in 2018 [65], or 2.1% of China's total power capacity [66], site selection, uranium supply, safety, environmental and economic issues, intensified by the difficult task of developing an indigenous reactor technology, challenge the large-scale development of nuclear power in the country. In addition, as economic centers appear and grow in non-coastal regions, building inland nuclear reactors becomes a challenge. In fact, following the Fukushima accident, the State Council cancelled inland nuclear power construction projects that had been arranged in the 12th FYP [67]. One example of the favorable environment provided by coastal areas for nuclear operation is the fact that offshore winds, prevailing around the coast, reduce the direct consequences of accidents. Yet, operation of inland nuclear reactors has been performed safely around the world, and preparatory work for inland nuclear development was included in the 13th FYP [68]. Advanced reactor technology, with increased intrinsic safety, may further enable a large inland expansion.

Besides the need for restructuring the power sector and significant energy geographic mismatch, a third set of challenges has emerged in China in the absence of a coordinated, inter-regional and inter-sectoral strategy. The country's ability to successfully enforce public policies and deploy the necessary infrastructure to operate a clean power grid still remains to be proved. The uncoordinated application of the central government's guidelines at the local level has resulted in large but inefficient investments. The existing balance between coal transportation and power transmission has been disrupted by the large-scale deployment of VREs in remote locations, far from demand centers. As an example, the recent construction of wind turbines in Inner Mongolia, which concentrates 62% of the country's technically exploitable wind capacity [69], has led to the congestion of long-distance transmission lines resulting in power curtailment. In addition, the recent erratic investment in new coal-fired power plants, despite low power demand growth and despite clean energy commitments at the central level, has led to power generation overcapacity at the national level and has increased CO_2 emissions [70]. Excess power capacity could reach 200 GWe by 2020 [71] or 10% of the projected national capacity in that year [72]. This over-investment in coal-fired plants, resulting from a lack of foresight and coordinated planning from local governments, continued until the central government, through its National Energy Administration (NEA) and National Development and Reform Commission (NDRC), imposed restrictions on further plant construction approvals [73]. In countries operating under economic dispatch, which determines the optimal short-time output of generation systems to meet power load at minimum operating costs, VREs are said to be "self-scheduled" and their power output is always used, when needed, since their operating costs are close to zero [74]. On the contrary, in China, the majority of thermal plants operate under equal-share dispatch: plants are allocated utilization hours as a function of their vintage, independent of the real-time output from other, non-dispatchable units [56]. In the Chinese context, the equal-share—or proportional—dispatch is environmentally inefficient since it entitles coal-dominated thermal capacity to a minimum output level, and economically inefficient since it increases the risk of curtailment and since VREs usually have lower operation and maintenance (O&M) costs than thermal plants. While pilot projects have been implemented to explore economic dispatch in China [56], the nationwide transition toward economic or energy-efficient dispatch is challenged by various political, economic, and technological challenges [75]. The combination of VRE installation in remote locations, transmission line congestion, coal overcapacity, and a dispatch largely relying on equal shares has resulted in China exhibiting the world's highest curtailment level: 17% of wind- and 10% of solar-generated electricity were curtailed in 2016, or 56 TWh of electricity in total [76]. This has created a climate of distrust among VRE system owners and investors, who have experienced lost earnings estimated between $4.2 billion and $4.95 billion annually [77], [78]. This situation has made investors more reluctant to further engage in VRE systems, and has forced the NEA to slow down wind development in six of the country's provinces with highest wind resource potential [69], [79]. As a consequence, newly installed capacity in wind power in China has decreased between 2016 and 2017 [80].

The current initiative undertaken by the Chinese government to solve this situation is the West to East Electricity Transfer Project (WEETP), initiated in the 10th FYP and expected to grow by 130 GW during the 13th FYP, from 140 GW in 2015 to 270 GW in 2020 [81], [82], with the long-term objective to build a nationally interconnected power grid. This project, which will likely face logistical and policy constraints [83], should help decrease high curtailment levels by decongesting transmission lines between regions with large power capacity and power demand centers, especially via its Northern corridor [84]. With these additional lines and provided that VRE capacity growth will be slower than transmission capacity growth, one can hope that current curtailment levels will diminish to the point that they will potentially disappear. Making the optimistic assumption that, by 2020, VRE and transmission deployment targets of the 13th FYP will be met, and provided that all VRE-generated power can be used, their maximum generation share in the national electricity mix will still only be 15% [82]. Fossil-based generation capacity will therefore remain dominant and much larger low-carbon system integration will still be needed to achieve meaningful decarbonization. In fact, the difference is striking between the scale of VRE generation at which grid operation is already currently challenged—173 GW of installed capacity [82] corresponding to less than 5% of total electricity generation [76]—and the needed scale of VRE generation to achieve deep decarbonization by 2050—around 50% of total electricity generation [85]. This is because China's VRE grid integration challenges do not only result from limited transmission capacity, but from limited flexibility of the power system [77], although solutions exist, as described later in this study. The ability to smooth out and maintain a reliable electricity grid despite increasing shares of wind and solar energies remains a key challenge.

More generally, an important gap remains between exemplary, ambitious announcements from the central government, and poor success rates of policy implementation by local governments and environmental protection bureaus. One of the cited reasons behind China's decentralized environmental governance failure is a blame-shifting game from central to local governments [86]. The real issue is probably more profound: the forward-looking central government makes environmental announcements that are essential goals to create a sustainable future for the country.

However, practical techno-economic challenges faced by local governments, in addition to their limited access to information and network, lack of adequate training in power sector planning [49], and local resistance against inter-regional power sector coordination which jeopardizes utilization hours entitlement [87], prevent them from being able to efficiently implement such ambitious targets. A recent example of the mismatch between policy goal and implementation is the coal production capacity cut introduced in 2016. The policy, decided at the national level by the NDRC, aimed to cut inefficient, old coal capacity and unsafe mines, and replace it with more efficient and profitable capacity [88], [89]. This resulted in a significant gap between supply and demand, resulting in coal price surges. To stabilize prices, the NDRC implemented a response mechanism relying on a single national price benchmark, which did not take into account the heterogeneity of China's resource markets across regions. As this mechanism failed to limit price surge, suggesting that implementation of the policy was technically infeasible, the NDRC was forced to soften and even reverse its coal capacity cut policy [90]. More generally, the combination of extremely ambitious but not contextualized targets imposed by the central government to local governments, and the resulting implementation failure, warrant a profound rethinking of China's decarbonization planning approach, exploring new options that are compliant with both central-level environmental goals and local-level feasibility constraints. Unfortunately, persisting reliance on traditional, sector-specific, standardized approaches currently makes the problem unsolvable.

The development of novel energy technologies, such as advanced nuclear reactors—using innovative fuel forms, coolants, and manufacturing process to achieve better operation performance under various conditions and better economics at smaller scales—, coal with carbon capture and storage (CCS), more efficient flexibility options including utility-scale batteries, other forms of energy storage, ultra-high-voltage long-distance transmission lines, smart grids and demand-response (DR) practices including smart electric vehicle charging, coordination of power supply with fresh water production, to only cite a few, can offer practical solutions that would be well aligned with the technological focus of the China Dream. However, large and relatively risky investments needed to fund R&D programs and pilot projects stress the necessity of carefully designing an optimal roadmap to inform energy system deployment planning.

China's unconventional challenges and opportunities suggest that a novel energy infrastructure, combined with non-traditional deployment and operation strategies, might be the optimal solution. Identifying and planning such unconventional solutions requires to refine current modeling approaches and adapt them to the Chinese context to provide meaningful information to policy-making, resilient against uncertainty. The motivation behind this study is to bridge the gap between decarbonization objectives set by the central government and techno-economic and operational constraints faced by local governments. This objective is achieved by developing an integrated planning approach that identifies and designs viable energy technology deployment and resource management pathways in space and time, and compares them according to their decarbonization potential, technical efficiency, operational feasibility and cost effectiveness, both at the individual level and in their synergies with other technologies, through the use of innovative modeling approaches.

In Chapter 2, this study investigates the resource-related challenges that China's electricity mix will be facing over the 2050 horizon. Relying on more than 200 types of data at the province level for each year, including projected hourly power demand, capacity factors from wind turbines, solar photovoltaics (PV) and concentrated solar power, technical performance as well as capital and O&M costs of various energy generation systems, we propose and use a high-resolution capacity expansion model for China's power sector, SWITCH-China, to explore optimal expansion pathways for the electricity mix under various assumptions. Improving this optimization model by integrating uncertainty, this study then looks at the future risks of both VRE output intermittency and cost projections on optimal electricity mix pathways. Recommendations are derived for setting meaningful targets at the central level while accounting for province-level specific constraints.

In Chapter 3, the scope of the study is broadened to integrate linkages between power and water supply into the optimization framework. The hypothesis that seawater desalination is a viable and sustainable source of water supply for the decades to come is tested. First, nuclear and coal thermal desalination are compared to the mega SNWTP, partially under construction, in terms of environmental and social impact, costs, and water supply quantity. Second, recognizing that China's main barrier to further VRE deployment today is power curtailment, the feasibility and implications of using desalination as a controllable load to balance VRE power generation and electricity demand is analyzed.

In Chapter 4, province-level projections for passenger cars until 2050 are built through a combination of census and economic data. We model the deployment of NEVs under different scenarios, including the future impact of current pro-NEV policies, the recent announcement of future gasoline vehicle sales ban, and the minimum NEV deployment level needed to cap CO_2 emissions after 2030. These scenarios are compared in terms of decarbonization potential, costs, and impact on power demand, and evaluate their potential alignment with the country's overall environmental commitments.

At the time of writing, parts of this dissertation were published in academic peer-reviewed journals as research articles ([85], [91]–[93]), which Anne-Perrine Avrin authored or co-authored.

CHAPITRE 2 SYSTEM-LEVEL ANALYSIS OF CHINA'S ELECTRICITY MIX DECARBONIZATION

2.1 INTRODUCTION

Designing cost-efficient strategies for planning the deployment of an electricity mix, including generation, transmission and storage systems, requires accounting for their interactions with one another, environmental constraints and projected electricity needs in space and time. This is a complex challenge that a vast majority of nations around the world currently face.

Given the large numbers of parameters involved, the use of optimization models for capacity expansion planning has become a necessity. Multiple modeling tools, demonstrating various levels of performance and result accuracy, have been developed and used to help governments, planning agencies, policy makers, utilities, and private investors plan long-term evolution of the power sector. Those models vary in scope, in their objective function, in data resolution, in the assumptions they make to translate energy systems and actors—consumers, utilities, investors—into model parameters, in their ability and approach to deal with input and structural uncertainty. The validity and usefulness of their results depend mainly on two factors. The first factor is access to data, including for electricity demand projections, technical performance and economic factors of future energy systems and infrastructure, new technologies and new operation practices. With the increasing share of VRE sources in electricity mixes across the globe, weather-related predictions are also becoming essential. The second factor is the ability to build computable optimization algorithms that include adequate constraints to design a realistic and viable electricity mix, adequate objective functions to account for divergent or convergent interest across shareholders, adequate representation of the impacts and opportunity costs over time of making a choice versus another.

Despite the many differences that exist among them, energy capacity expansion planning models can be broadly classified into two categories. Bottom-up models use disaggregated data while top-down models rely on high-level, aggregated information to design strategies [94], [95]. Modeling the power sector as one interconnected component of a region's economy is performed by top-down models, often computable general equilibrium models, which use macro-economic indicators to assess how an economy might react to changes in energy supply and demand, and inversely. These models, usually based on linear equilibrium, use simplifications to reduce modeling complexity and mainly employ regression equations [96], [97]. In contrast, bottom-up models focus on the micro level. Their scope is often limited to the power sector, with the common simplification that it is largely independent from other sectors. They plan and simulate the operation of the electricity grid at the individual energy system-level and often include associated investment options [98]. The complexity of top-down tools lies in the vast number of factors and relationships between them that influence, in reality, the value of macro-economic parameters, and which, today, cannot be represented in a single model. In bottom-up models, while the number of parameters and interactions between them are usually much smaller, the complexity lies in the large quantity of data needed to accurately represent all possible states and pathways of the future electricity mix [96]. Both approaches have been used to build decarbonization scenarios for the power sector, and each of them has its own strengths and limitations [99]. While bottom-up models lack the ability to grasp economy-wide interactions and characteristics of the imperfect real-world, such as initial tax distortions or market failures, they are better suited than top-down approaches to analyze specific energy system behaviors and their techno-economic characteristics, and to respect physical energy conservation constraints [95].

In China, top-down models are key to quantifying the impact of fossil-fuel burning on the overall economy, including public health, through metrics that can be compared to future investment options. Yet, China's principal challenge with regards to capacity expansion planning is the ability to find viable decarbonization configurations while solving the country's mismatch between power demand and supply in a cost-efficient manner. Such technology-level analysis is performed by bottom-up models. Therefore, in this study, China's power sector decarbonization planning is addressed using bottom-up approaches that allow to assess and design technical, environmental and cost constraints and opportunities at a high degree of granularity.

In traditional electricity mixes, primarily composed of dispatchable energy sources, unit commitment is performed relatively easily using screening curves with merit-dispatch order. Yet, since the information about dynamic load variation is lost in load duration curves, screening curves cannot account for startup costs, ramping constraints, minimum turndown, and other system considerations [100]. As a consequence, more detailed models have been developed for capacity expansion planning, identifying optimal options by performing a cost-benefit analysis across feasible solutions. Low spatial and temporal data resolutions have forced these models to make approximations, which were acceptable in the case of dispatchable units. In light of the increasing share of VREs, which are non-dispatchable, a new generation of energy models is needed. These models must be able to plan the co-deployment of ancillary services to increase overall grid flexibility and accommodate short-term power fluctuations from VREs.

Electricity grid services needed to maintain system stability and variability can be classified roughly in two groups: services needed for expected events such as load variation (including load following and frequency regulation), and services needed for unexpected events such as blackouts (including black start capacity and contingency reserves) [101]. Today, five main options exist to increase flexibility of the electricity grid. Two of them—load following and transmission—are widely used today. Two others—grid-scale storage and demand response—are still in their infancy. Co-generation has been used for decades, but its utilization to accommodate VRE intermittency is not widespread. These five approaches, and the current challenges they face in China, are presented below.

Load following—sometimes called load maneuvering—is the practice of modifying the output of a power plant, usually a thermal plant, as a function of demand fluctuation. In electricity mixes that include VREs, load following plants tend to operate as a function of the net load, i.e. load minus electricity generation from wind and solar systems. From an economic point of view, load following practices favor plants with low capital costs since their utilization rate is low. From a technical standpoint, plants must be able to follow variations from the net demand, ideally in real time. Technical factors, resource accessibility, and regulations limit the range of options available to perform load following. With their relatively higher operation cost than construction cost and their ability to quickly ramp up and down, natural gas power plants, sometimes coined "peaking plants," are widely used as a mean to accommodate VRE fluctuation. While national resources remain uncertain [102], the Chinese government has enacted a series of market-oriented policies since the early 2000s to accelerate the development of the natural gas industry. The national consumption of natural gas across sectors increased more than seven-fold between 2000 and 2014 [103], and has slowed down since then. In the power sector, despite central and local governments advocating for a "coal-to-gas" approach, the share of natural gas remains low [104]. In 2017, only 3% of the total electricity generated in the country was produced by natural gas (see graph in Chapter 1), unable to accommodate the 6.6% generation share of VREs. A series of challenges hinders the development of natural gas infrastructure. First, the high dependency on foreign imports—in 2016, the country consumed 50% more natural gas than it produced [105]— results in high energy security risks [106]. Second, inefficient pricing mechanisms favor low city-gate prices, discouraging investment in infrastructure, and high-end use prices, discouraging coal-to-gas end-use applications in the industry [107], [108]. Finally, because of its carbon intensity, natural gas is perceived as a transitional fuel rather than a sustainable, long-term solution in coping with pollution in China. In fact, it has been found that, if all coal consumed to produce electricity was replaced by natural gas, CO_2 emissions would indeed diminish but total greenhouse gas emitted from the power sector would remain the same over the 2030 horizon if the methane leakage rate from natural gas systems is 10% or lower [108]. Another study, applied to the United States, found that natural gas plants had net climate benefits compared to efficient new coal plants only if leakage is less than 3.2% [109]. As a consequence, power companies are reluctant to invest in this energy source [104]. Nuclear and coal power have less very-short-term agility in modifying their output, and they are less economically attractive for load-maneuvering than natural gas plants, yet they have proved their viable operation in load following mode across the world. The French nuclear fleet, for example, provides 650 MWe of primary reserve, with variations less than 15 to 30 seconds. It is also extensively used for daily load following [110]. The minimal power level of a nuclear reactor is about 30% of nominal power, sometimes 20% [111] (Figure 2-1). In addition, China's climate change mitigation objectives favor nuclear power over coal and natural gas as a sustainable option to increase power grid flexibility.

Yet, in China, guaranteed annual utilization hours for thermal plants, allocated by the provincial government, and the lack of a spot market for electricity do not provide an incentive for load following [56]. These regulation issues can be overcome. However, the share of nuclear power capacity in China's power mix in the long run—which could reach up to 500 GWe according to the World Nuclear Association [65], or 20% of the installed power capacity in 2050 [112]—will not be sufficient, alone, to back up the projected large fluctuations from future VRE capacity.

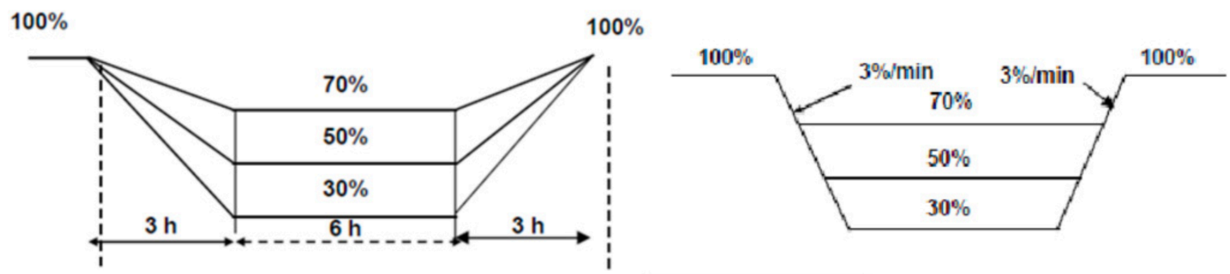

Source: C. Cany, C. Mansilla, G. Mathonnière, and P. da Costa, "Nuclear power supply: Going against the misconceptions. Evidence of nuclear flexibility from the French experience" [110].

Figure 2-1 Theoretical ramping profiles of Pressurized Water nuclear Reactors (PWR).

The transmission network enables to transport electricity from places where it is produced—in particular, in regions with high resources in wind, solar, or hydropower—to places where it is needed. Given China's large territory and diverse energy resource landscape across provinces, ultra-high voltage (UHV) AC and DC lines present technical, economic, and resource conservation advantages compared to other technologies [113]. As described in Chapter 1, a number of new UHV transmission routes have been planned by the central government, referred to as the WEETP, with the ultimate goal of creating a quasi-national power grid. While, traditionally, coal was transported over long distances in China from mines to demand centers, this large-scale project aims at transporting non-dispatchable resources, such as solar power from the West and wind power from the North of the country, to coastal demand centers. Yet, it remains unclear whether the planned transmission capacity will be sufficient to not only reduce current high curtailment levels, but also accommodate larger planned VRE shares, and what the impact of transmission upgrade on overall electricity costs will be [114].

Storage allows to shift the timing of electricity supply. It can be broadly divided into grid-scale—sometimes called central, or bulk—storage systems and distributed, often off-grid, systems in homes and commercial sites. Grid-scale storage can be further separated according to the level at which it connects to the grid: transmission, primary distribution, and secondary distribution. The U.S. Department of Energy's Global energy storage database provides information about existing storage systems, including the type of services they provide. The specific services provided by storage systems tend to be correlated with the level at which they connect to the grid (Figure 2-2). Among a sample of 243 utility-owned energy storage systems currently in operation globally, we find that storage systems are mainly used for electric energy time shift, electric supply capacity, voltage support and frequency regulation.

In 2018, the global operating capacity of utility-owned energy storage is 94.7 GW [115]. Many technologies such as flywheels, capacitors, hydrogen and magnetic fields, are not ready for utility-scale deployment, because of economic, technical and environmental limitations [116], [117]. In particular, the number of charge and discharge cycles is larger for large- than small-scale usage [117]. It has been argued that CAES and battery energy storage could potentially be deployed at large scale in a near future [116]. Yet, despite an important and growing need for storage system able to accommodate grid-level VRE fluctuations, only PHS has proved its scalability. Its total installed capacity of 93.5 GW represents close to 99% of the global storage capacity. The average size of pumped-storage hydroelectricity (PHS) projects is 250 times, 140 times, and 50 times larger than the average size of thermal, electro-chemical and electro-mechanical storage projects in operation today, respectively. The largest non-hydro individual system is the McIntosh compressed air energy storage (CAES) plant in Alabama, U.S.A., which has a capacity of 110 MW.

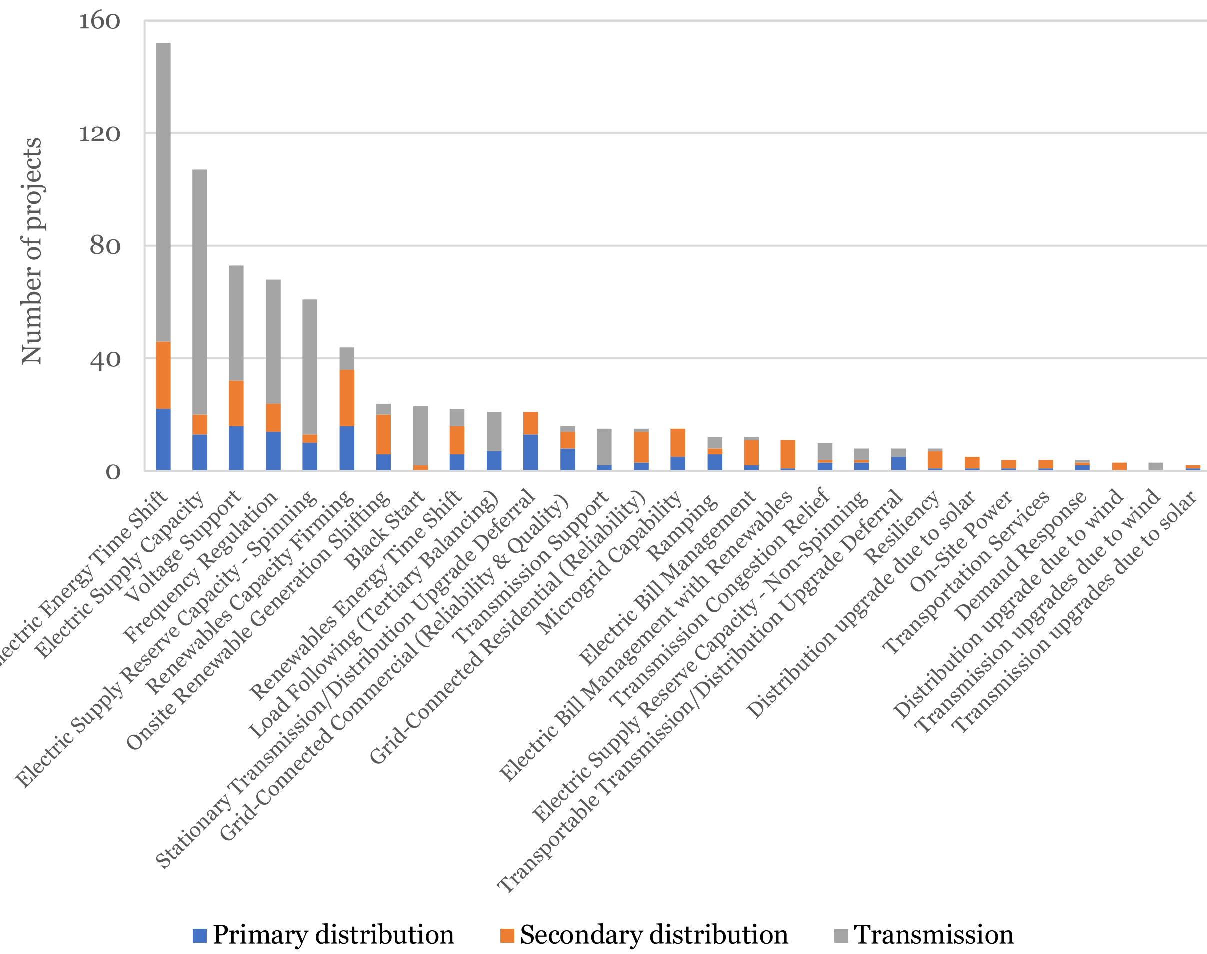

Source: U.S. Department of Energy's Global Energy Storage Database [115].

Figure 2-2 Count of operational storage systems per type of energy service provided worldwide in 2018. The color code indicates the level at which the storage system connects to the grid.

PHS is the only operating utility-owned storage technology in China today, with an installed capacity of 12.6 GW, expected to grow by 17 GW during the 13th FYP. One of the country's major PHS projects under construction is the 3.6-GW Fengning plant in Hebei province [118]. Geographic constraints in China limit the maximum deployment potential of PHS to below 100 GW [119]. As described later in this chapter, the flexibility scale needed to accommodate large shares of VREs in 2050 in a deep decarbonization scenario is considerably higher. Electric vehicles can constitute a form of distributed storage for grid purposes, provided that their number increases considerably and that DR-related limitations are overcome.

DR programs allow to shift the timing of electricity demand by end-users generally by adjusting it to the price of electricity [120]. It requires the installation of new technologies, mainly advanced metering infrastructure. It also requires the implementation of new social practices, either through the active involvement of power consumers through price-based programs ("non-dispatchable DR") such as time-of-use (TOU) pricing, or through incentive-based programs such as direct load control and interruptible or curtailable load by appliance control from the grid operator ("dispatchable DR") as agreed by the consumer [120], [121]. While first demand-side management programs were implemented in the 1990s in China, TOU measures really rose after the NDRC announced its "Electricity Demand-side Management Measures" in 2010 [122], [123]. In 2013, 70% of Chinese households had a smart meter, and in 2016, 66% of commercial and industrial consumers had access to TOU [124]. Yet, several barriers currently limit the efficient large-scale deployment of DR programs in China. These barriers include the current power overcapacity across the country; no adequate economic incentive for grid operators—their profits are directly related to the quantity of electricity sold— nor consumers; incomplete market reform and lack of a mature wholesale electricity market where DR aggregators could sell their capacity, as done in the United States for example; costs of smart infrastructure deployment and adoption; low priority of DR program development in the central government's policy agenda, which mostly focuses on supply-side management [114], [120]–[122]. In addition, apart from a few pilot cities, no mechanism has been established in China today to recover DR participant costs.

Finally, cogeneration relates to the use of the energy produced in a power plant for other purposes than power generation. Traditionally, cogeneration refers to the direct use of waste heat to produce useful heating or to power thermal desalination plants in order to produce fresh water [125]. It can also be used to generate useful cooling. In the current context, grid operation is mainly challenged by intermittent power generation from wind and solar PV, which directly produce electricity. In this context, cogeneration can also consist in the deployment of a controllable infrastructure, powered intermittently when electricity from VREs is generated in excess. Cogeneration of power and desalinated water is the focus of Chapter 3.

China's power sector shows a crucial need for more flexibility. Multiple factors—technical, economic, social, institutional, and organizational—should be accounted to optimize flexibility infrastructure development. This highlights the need to account for individual system-level constraints when planning future capacity expansion at the grid level. Such grid-wide scope is also essential to grasp the true cost of deploying energy technologies, beyond limited metrics such as Levelized Cost of Electricity (LCOE), which do not accurately account for the cost and technical constraints of ancillary systems dedicated to increasing flexibility.

Several models exist to assess and explore the evolution of China's power sector. A list of existing bottom-up capacity expansion planning models is given in Table 2-1. While this list is not exhaustive, it shows that a large majority of these tools have a similar structure: they allow for an explicit representation of generation technologies, they simulate their capacity deployment and operation over a medium- to long-term horizon—here, between 2020 and 2100—, they rely on either cost-minimization optimization or scenario-based simulation to assess strategies. What varies significantly between them is their data resolution. Most models average power demand and generation data, including from non-dispatchable variable energies, over one year and in a single location—i.e. with a spatial dimension of zero. Yet the spatiotemporal disparity of resources is the single largest challenge that countries are facing today in enabling its clean energy transition (see Chapter 1). Only LomLog from Tsinghua University and CREAM-EDO from the NDRC's Energy Research Institute combine both sub-national and hourly data resolution. Yet, to the best of the author's knowledge, neither of these models, nor their datasets, are accessible to the public. The need remains for an accessible high-resolution tool that combines long-term optimization of energy systems and infrastructure with simulation of grid operation subject to short-term intermittency of renewable energies, as well as spatial mismatch between supply and demand. This is what motivated the creation of the SWITCH-China model at the University of California, Berkeley. The development of SWITCH-China, its uncertainty module, SWITCH-MVO, and their application to China's power sector decarbonization over the 2050 horizon are the focuses of Chapter 2. It should be noted that several of the models presented in Table 2-1 improve on SWITCH regarding their geographic and sectoral scopes. Models that consider power systems across countries can identify cross-frontier coordination opportunities and compare decarbonization options across contexts. Models that include other sectors of the economy beyond the electric grid are able to grasp holistic factors of decarbonization. Increasing the scope of a model enables to account for additional suitable configurations that a China-focused, power sector-focused model might miss. Yet, high data resolution is probably the most essential feature to account for practical intra-sectoral and intra-regional constraints in order to design viable, realistic solutions, and truly inform energy policy-making.

Table 2-1 Existing bottom-up models of China's electricity mix.

Model (institution)	**Explicit technology representation**	**Optimization problem**	**Horizon**	**Spatial resolution of data**	**Temporal resolution of electricity generation/supply data**	**Source**
BOMCES-MESEIC (TU)	Yes	Cost minimization	2050	Six regions	Yearly	[126]
CREAM-EDO (ERI)	Yes	Cost minimization	2050	Province-level	Hourly	[127]

CRESP-EEM (ESMAP & ERI)*	Yes*	None*	2020	Province-level	Yearly	[128] [129] [130]
DREAM (LBNL)	Yes	None (scenario-based)	2050	Three climate zones	Yearly	[131] [132] [133]
EPS (Energy Innovation)	Yes	None (scenario-based)	2050	None (country-wide)	Yearly	[134] [135]
ETP-TIMES (IEA)	Yes	Cost minimization	2060	None (country-wide)	Hourly	[136]
IPAC-AIM (ERI)	Yes	Cost minimization	2100	Province-level	Yearly	[137] [138] [139]
LCPGE (TU)	Yes	Cost minimization	2030	None (country-wide)	Yearly	[97] [140]
LEAP (NCEPU)	Yes	None (scenario-based)	2030	None (country-wide)	Yearly	[141]
LEAP-China-Electricity (TU)	Yes	None (scenario-based)	2030	None (country-wide)	Yearly	[142] [143] Several version exist [144]
LoMLoG (TU)	Yes	Cost minimization	2035	17 load areas	Hourly	[145]
MARKAL (TU)	Yes	Cost minimization	2050	None (country-wide)	5 years	[146]
MESSAGE (IIASA)	Yes	Cost minimization	2050	None (country-wide)	Yearly	[147]
MESSAGE (GUCAS)	Yes	Cost minimization	2050	None (country-wide)	Yearly*	[148]

Model (CAS)	Yes	Cost minimization	2030	12 regions	Yearly	[149]
Model (TU)	Yes	Cost minimization	2050	None (country-wide)*	Yearly	[150] [151] [152]
SWITCH-China (RAEL, UCB)	Yes	Cost minimization	2050	Province-level	Hourly	[85]
TIMES (TU)	Yes	Cost minimization	2050	None (country-wide)*	Yearly*	[153] [154] Several versions exist

Data is obtained from [155], [144] *and references cited in the table. Host institutions are mentioned within brackets. Asterisks highlight model information that the author had to infer as it was not clearly provided in the publicly-available references cited in the table.*

The first section of this chapter presents the SWITCH-China model developed in the Renewable and Appropriate Energy Laboratory at the University of California, Berkeley. This model is used to analyze cost-efficient, reliable pathways for China's power sector under various decarbonization objectives.

The second section explores how modeling results from linear programs (LP) such as SWITCH-China can be refined in order to account for non-linear uncertainty of future costs. A modeling uncertainty module is developed and applied to configurations presented in the previous section. The impacts on optimization results of this two-step approach are analyzed.

2.2 Capacity Expansion Planning Modeling

2.2.1 Methodology and Model Description

The SWITCH model was developed to provide a consistent, automated method for choosing optimal energy system portfolios by accounting for synergies between systems in space and time. The first version, with a California power sector focus, was created at the University of California, Berkeley by Dr. Matthias Fripp [156], [157]. Several versions were subsequently developed by graduate students of the Renewable and Appropriate Energy Laboratory at the University of California, Berkeley, including about the North American Western Electricity Coordinating Council [158] and Nicaragua [159]. The SWITCH-China model, presented in this study, was initially created by Dr. Gang He and its development was continued by Anne-Perrine Avrin.

SWITCH-China is a linear programming optimization model whose objective function is to minimize the cost of producing and delivering electricity through the construction and retirement of various power generation, storage, and transmission options between present day and future target dates according to projected demand and under various policy and cost scenarios. In particular, SWITCH improves on other cost-minimizing models with similar objectives thanks to its combination of high spatial and temporal resolution, and its capacity to optimize long-term capacity expansion and hourly generation dispatch simultaneously to ensure the reliability of grid electricity supply on small and large time-scales. Investment decisions are divided into four ten-year-long periods: 2015-2024, 2025-2034, 2035-2044 and 2045-2054. SWITCH-China calculates optimal power capacity and generation configurations at the province level. However, costs are minimized at the national level, thus exploring potential synergistic opportunities between diverse areas. More information about the model structure and data can be found in the Supporting Document of [85].

The objective function of the SWITCH-China model includes the following system costs: capital costs of existing and new power plants and storage projects; fixed O&M costs incurred by all active power plants and storage projects; variable costs incurred by each plant, including variable O&M costs, fuel costs to produce electricity and provide spinning reserves, and any carbon emission costs; capital costs of new and existing transmission lines and distribution infrastructure; annual O&M costs of new and existing transmission lines and distribution infrastructure. All economic data are exogenous. Cost assumptions vary with the scenario considered, as detailed in section 2.2.2.

The model includes five main sets of constraints: power demand, capacity reserve margin, operating reserves, technology-specific targets—for example, VRE and nuclear development plans—and carbon caps.

China has existing technology-specific capacity deployment targets, presented in Table 2-2. In addition, the central government has implemented objectives to reduce national carbon intensity—defined here as the amount of CO_2 produced per unit of GDP—by 40 to 45% below 2005 levels by 2020. It has announced an extension of the efforts to achieve a 60 to 65% reduction by 2030 [160]. It also aims for a national CO_2 emission peak by 2030. While CO_2 emissions in China decreased between 2014 and 2016, creating speculation around the fact that the peak might have been reached ahead of schedule, national emissions rose again in 2017 [161]. 2017 also saw coal consumption grow for the first time in three years. This highlights the need not to rely on year-by-year comparison to assess the success of an emission reduction objective, but to design an electricity system able to maintain these targets on the long run.

2.2.2 SCENARIOS

Four scenarios are designed to explore options for China's electricity mix expansion: a Business-as-Usual (**BAU**) scenario for which no carbon constraints are applied, a Business-as-Usual with Carbon Cap (**BAU with Carbon Cap**) scenario which differs from the first scenario by the inclusion of carbon constraints, a **Low Cost Renewables** scenario, and an **IPCC Target** scenario.

Table 2-2 Technology-specific national targets for China's power sector, as of 2015.

	Resource type	Target 2015	Target 2020	
Sources	*12th FYP* [162]	*13th FYP* [82]	*China Energy Development Strategy Action Plan 2014-2020* [160], [163]–[166]	
Wind turbines	Onshore wind (GW)	99	205	200
	Offshore wind (GW)	5	5	
Solar PVs	Central PV (GW)	10	45	100
	Concentrated Solar Power (GW)	1	5	
	Residential PV Commercial PV(GW)	10	60	
Nuclear reactors	Nuclear (GW)	40	58	

Future availability and cost assumptions in the **BAU**, **BAU with Carbon Cap**, and **IPCC Target** scenarios are consistent with current projections for future technology costs. The **BAU with Carbon Cap** scenario reflects the application of China's current CO_2 emission reduction policies: the 2020 carbon intensity target and 2030 peak carbon commitment. This scenario is used as a baseline for China's electricity mix evolution in Chapters 3 and 4. In the **Low Cost Renewables** scenario, wind and solar system costs are assumed to decrease significantly in the next decade, following technological improvements as well as cost declines enabled by large-scale deployment, in line with the government-supported growth of solar and wind manufacturing and deployment in China [167]. In this scenario, the capital cost of wind turbines linearly decreases to half of its 2010 costs by 2020. Solar photovoltaics overnight costs decrease until they reach the value provided by the Solar Shot initiative in 2020 [168]. Both cost components are assumed to remain fixed after 2020, assuming that these two technologies reach commercial maturity by then. The cost of storage is consistent with projections from the U.S. ARPA-E program [169]. This scenario does not include any carbon constraints. The **IPCC Target** scenario relies on the same assumptions as the **BAU with Carbon Cap** scenario, but adds a CO_2 emission limitation constraint in 2050 of 80% below the 1990 level baseline, in line with the global 2°C scenario of the Intergovernmental Panel on Climate Change (IPCC), applied to China [170].

2.2.3 RESULTS

China has implemented cap-and-trade pilot programs in five cities and two provinces since 2011 [171], [172]. Since the implementation, carbon allowances have traded between \$3 and \$20 per ton of CO_2 [173]–[175]. The central government extended this program to power plants nationwide in December 2017 [176]. As of 2018, this countrywide program is the world's largest emission trading scheme, representing almost twice the European Union's and ten times California's cap-and-trade systems [173], [177]. The SWITCH-China model calculates that a carbon price of at least \$30/tCO_2 is needed to achieve 45% of carbon intensity reduction in 2020, as it would boost the deployment of wind and solar as well as the transition from coal to nuclear and natural gas power. We also calculate that a price of \$40/tCO_2 is needed to peak CO_2 emissions in 2030. Liu et al. find a uniform equilibrium trading price of 214 RMB (\$33.5) per ton of CO_2 [178]. The Guangzhou China Emission Exchange director communicated that he was expecting the national carbon price to gradually rise up to 300 RMB (\$45) per ton of CO_2 [176]. Therefore, achieving carbon prices between \$30 and \$40 per ton of CO_2, as calculated by SWITCH, seems realistic.

Results show that China's carbon targets in 2020 and 2030 significantly impact power sector emissions and the corresponding electricity mix to be deployed (Figure 2-3). In order to meet its 2030 target, China's power sector emissions will have to decrease by 1.5 Bton CO_2 compared to the **BAU** scenario. Implementing low-cost renewable energies falls short of this number by 0.5 Bton CO_2 in 2030.

The **Low Cost Renewables** scenario shows that aggressive VRE cost reductions alone can displace about 300 GW of coal power by 2050 (Figure 2-4). Such large-scale deployment requires to rethink the grid infrastructure in order to accommodate energy generation fluctuations. The ability of natural gas to quickly ramp up and down to accommodate such short-term variations is favored in this context, especially since no carbon constraints are applied. 40 GW of additional natural gas capacity are deployed in this context. The high cost of natural gas in China is offset by the low cost of VRE systems in this scenario.

Yet, a VRE technology-oriented policy does not provide sufficient economic incentive to significantly reduce the growth in CO_2 emissions. Coal and coal with CCS would still dominate the energy mix in 2050, representing 62% of total electricity generation in the **Low Cost Renewables** scenario, and 70% in the **BAU** scenario.

In the absence of carbon constraints, the least-cost electricity mix in the **Low Cost Renewables** scenario emits about eight times more than what is mandated by the IPCC. Yet, an 80% CO_2 emission reduction by 2050 is technically achievable through a combination of nuclear, wind and solar power with large-scale storage, and coal with CCS.

Nuclear power costs and operation patterns make it an essential component of the clean energy transition. Given its large capital cost, the development of nuclear power in a majority of countries, including China, depends on policy, and policy-making is influenced by political, economic and social factors, among others [67]. On the fuel supply side, domestic uranium production growth is much slower than capacity expansion, increasing the country's dependence on foreign imports, which appears risky as international sources of uranium ore are concentrated and their exploitation is largely dominated by only four foreign companies [179]. Solutions might come from on-going discussions around the construction of a nuclear fuel reprocessing facility in China, and the development of fast neutron reactors. The lack of organization between nuclear power actors, including fights over the design of the flagship Hualong One indigenous design, the willingness of giant Chinese energy generation companies to enter the nuclear construction and operation arena, and the competition between nuclear equipment manufacturers, challenge cost-efficient development, resource optimization and efficient operation feedback sharing.

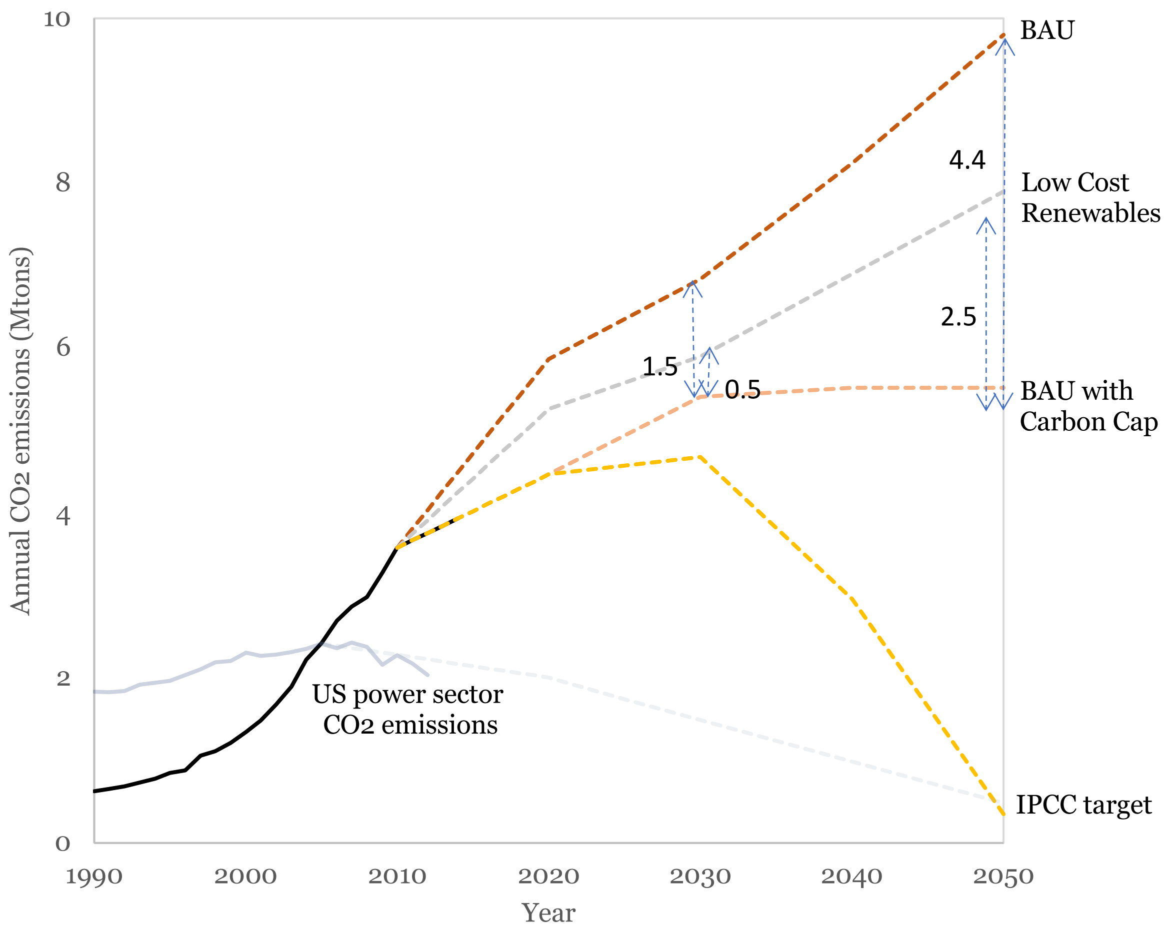

Figure 2-3 Carbon dioxide emission trajectory for China's power sector under the four scenarios (SWITCH-China results), as well as historical emissions in China and the United States until 2015.

Yet, China has been operating nuclear reactors and has maintained a good record of safety for more than 50 years [180], [181]. The main law that dictates nuclear power safety, and covers various aspects such as siting, operation and decommissioning, is the "Law on Prevention and Control of Radioactive Pollution" which was passed in 2003 [51]. A nuclear safety law was passed in 2017 to include inter-agency coordination mechanisms, a national committee in charge of emergency response, a set of protocols for nuclear safety operators and most importantly, more independent power to the National Nuclear Safety Administration [52], [53], [182]. Main safety challenges in China's nuclear industry appear to be the lack of well-developed safety culture in nuclear facilities and poor construction quality resulting from insufficient controls, unqualified workers, and corruption. The multiple reactor designs that coexist in the country add a layer of complexity to the operation of the nuclear fleet. Although the Chinese nuclear industry has followed French and American standards since the 1990s, translation and other appropriation issues challenge the practical application of these standards [67]. For these reasons, nuclear power capacity is capped at 300 GW in the SWITCH-China model, or about five times the government's target for the year 2020.

Given the relatively flat and concentrated power demand in Eastern China, nuclear power is a competitive low-carbon baseload energy source for the country. As a consequence, the model deploys nuclear capacity up to its upper limit of 300 GW in 2050 in the **IPCC** scenario. Although existing reactors in China are all located on the coast, new construction in the model occurs both on the coast and in inland provinces, especially in the Central and Eastern grids, where the economy is growing and which are less affected by the current power overcapacity [72]. As mentioned in the Introduction chapter of this dissertation, the State Council cancelled inland nuclear power construction projects that had been arranged in the 12th FYP, following the Fukushima accident [67]. Since operation of inland nuclear reactors has been performed safely around the world, preparatory work for inland nuclear development was later included in the 13th FYP [68]. Advanced reactor technology, with increased intrinsic safety, may offer additional guarantees and thus enable increased inland expansion. More generally, nuclear power in China could play a much more important role, provided that the challenges mentioned above are overcome.

In the **IPCC** scenario, 80% of the 1000 GW coal capacity is coupled with CCS systems in 2050 despite their significant costs. About 60% of the power demand is met by VREs. Several provinces present high potential for solar and wind power, especially in Northern and Western areas, far from demand centers. Large-scale storage systems and long-distance transmission lines must be deployed in order to accommodate the variable electricity supply from more than 1500 GW of wind and solar systems. The system dispatch shows seasonal patterns of VRE generation (Figure 2-5). Hydropower and wind power productivity are highest in the Summer and Fall, and the Winter and Spring, respectively. Hydropower resources are largest in South China, while wind power capacity factors are highest in North and North-East China. These different patterns can present an advantage in operation of the grid, provided that an interregional grid is developed. The daily variability of solar power requires that short-term flexibility be added to the overall system, even though solar energy matches peak demand fairly well. Such short-term variation cannot realistically be accommodated by baseload energy sources, such as coal, nuclear and hydropower. On average, storage charges 8% and discharges 9% of the system load. On a storage incentive day, it can charge up to 26%, and discharge down to 9% at night when thousand GW-scale solar is offline. Using existing projections for future storage system costs, and given the significant CO_2 emission constraint in the IPCC target, natural gas has a limited role in this scenario despite its ability for fast ramping.

The deployment of storage and CCS systems, which do not produce electricity but are added to smooth out VRE intermittency and to maintain CO_2 emissions below the IPCC target, increases costs by more than a third compared to the **BAU** scenario, from \$64/MWh to \$88/MWh.

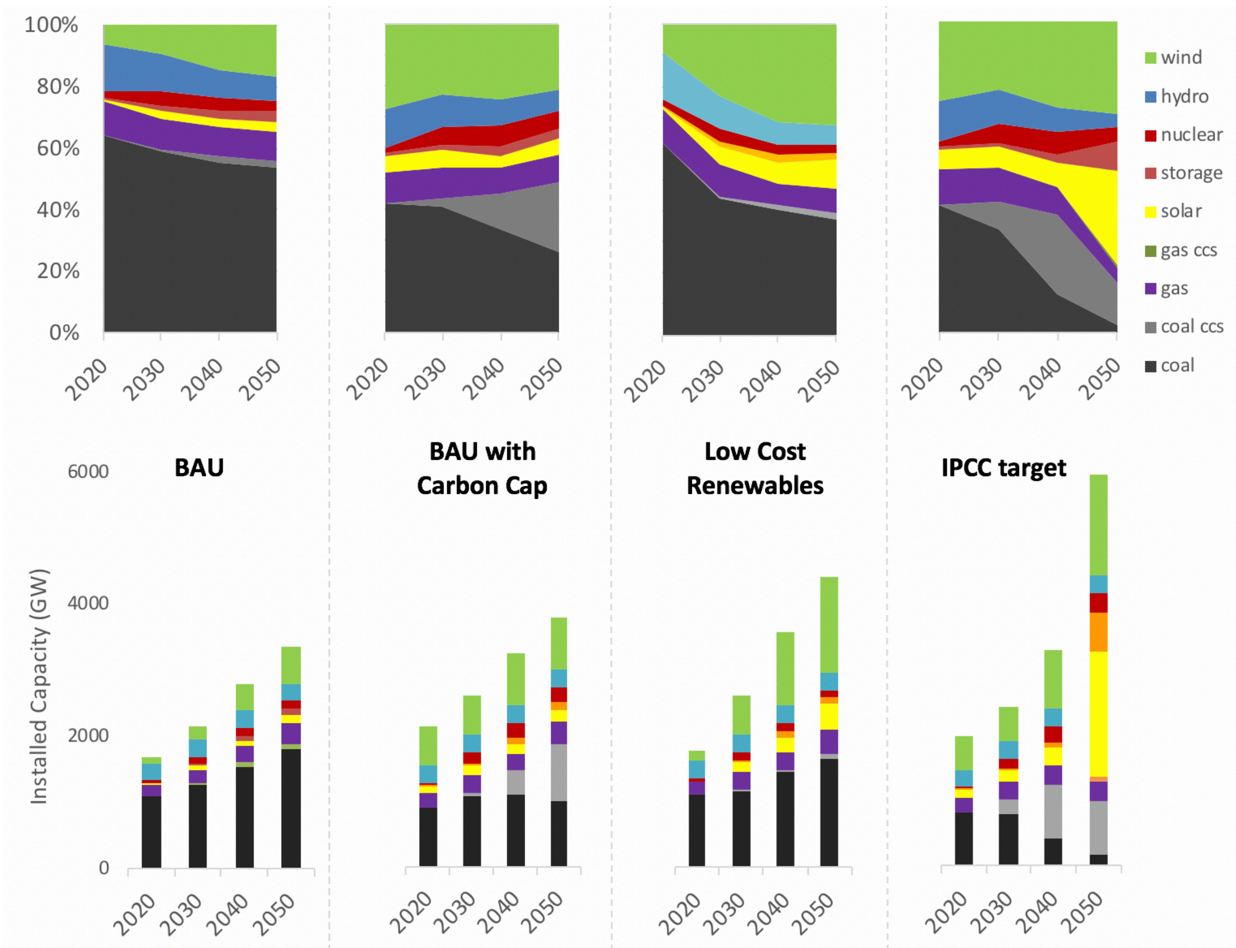

Figure 2-4 Evolution of China's installed power generation capacity mix over time for the four scenarios (SWITCH-China results).

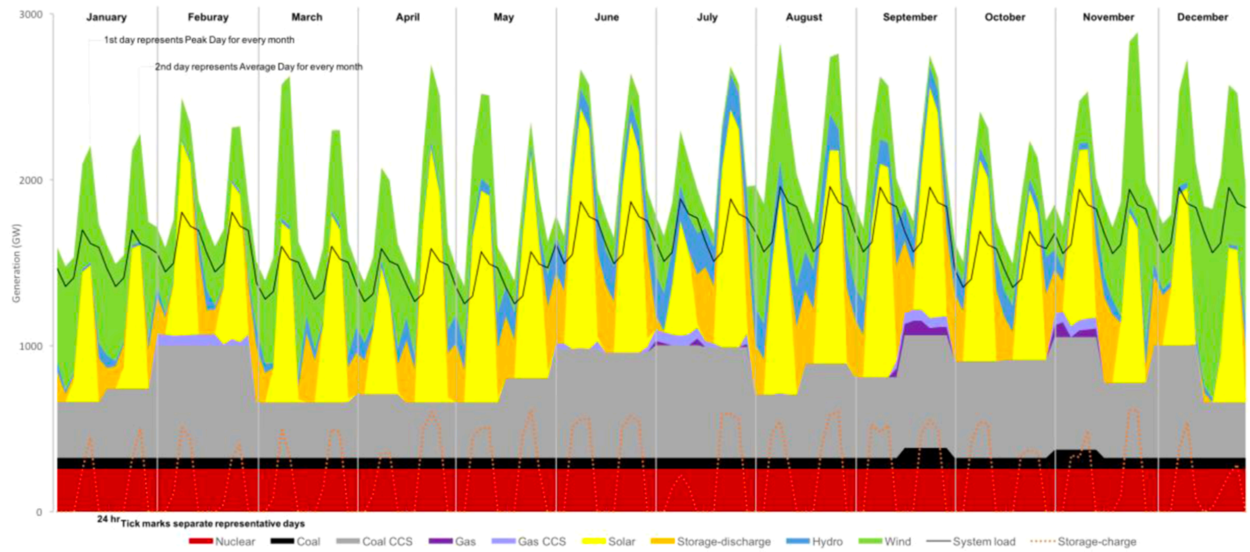

Figure 2-5 2050 dispatch schedule for the least-cost electricity mix in the IPCC Target Scenario (SWITCH-China results).

The combination of the 2020 carbon intensity target and the 2050 IPCC target favors a least-cost electricity mix where coal is largely phased out by 2050, and replaced by a combination of coal with CCS, nuclear and VREs. Coal plants with CCS are built in regions with low coal prices, including Xinjiang, Inner Mongolia, Shaanxi, and Jilin.

An 80% CO_2 emission reduction requires a large deployment of storage capacity to provide operational flexibility. We find that the country will need 600 GW of energy storage by 2050 to accommodate its 50% share of wind and solar resources. As mentioned in introduction, PHS potential in China is estimated below 100 GW. To reach a capacity of 600 GW, and to provide sub-daily and even sub-hourly storage, other storage sources will be needed which, today, have not been developed at such a large scale anywhere in the world.

Storage deployment calculated by SWITCH is eight times higher than the modeled storage capacity in 2050 of the International Energy Agency's 2DS scenario analyzed in 2014, which assumes that 33% of China's electricity generation will come from VREs [183]. This can be explained by the lower resolution of the IEA's 2014 model, which uses 32 time points per year and does not account for intranational spatial dimension, while SWITCH-China uses a sample of 144 data points per year and optimizes electricity mixes at the province-level [184]. In particular, the IEA assumes infinite electricity transmission capacity while SWITCH-China accounts for practical infeasibilities and economic trade-offs between transmission and other flexibility options, such as storage. Indeed, SWITCH finds that decarbonizing China's power sector also requires the inter-regional deployment of the electricity transmission network to connect regions with high electricity generation potential to demand centers, as shown on Figure 2-6.

Additional transmission corridors are built in SWITCH to transport power from inland regions such as Xinjiang, Qinghai, Inner Mongolia, Shaanxi, and Shanxi to coastal demand centers including Beijing, Tianjin, Shanghai, Zhejiang, and Guangdong. Inner Mongolia becomes a major hub of clean energy generation thanks to its convenient location—close to coastal demand centers—and high-quality renewable energies, especially wind. Yet, connecting this region with populated provinces such as the Jing-Jin-Ji region is already an important challenge today, also addressed in Chapter 3. Transmission capacity makes coal in Xinjiang available at a competitive cost, although the province has high-quality VRE resources. Such unintended consequences must be addressed in the planning process. Tibet has high wind and solar capacity factors, however, transmission infrastructure will not be built to connect this province because of its remote location and very low population density, unless capital and operation costs of very-long-distance transmission lines decrease significantly over the 2050 horizon.

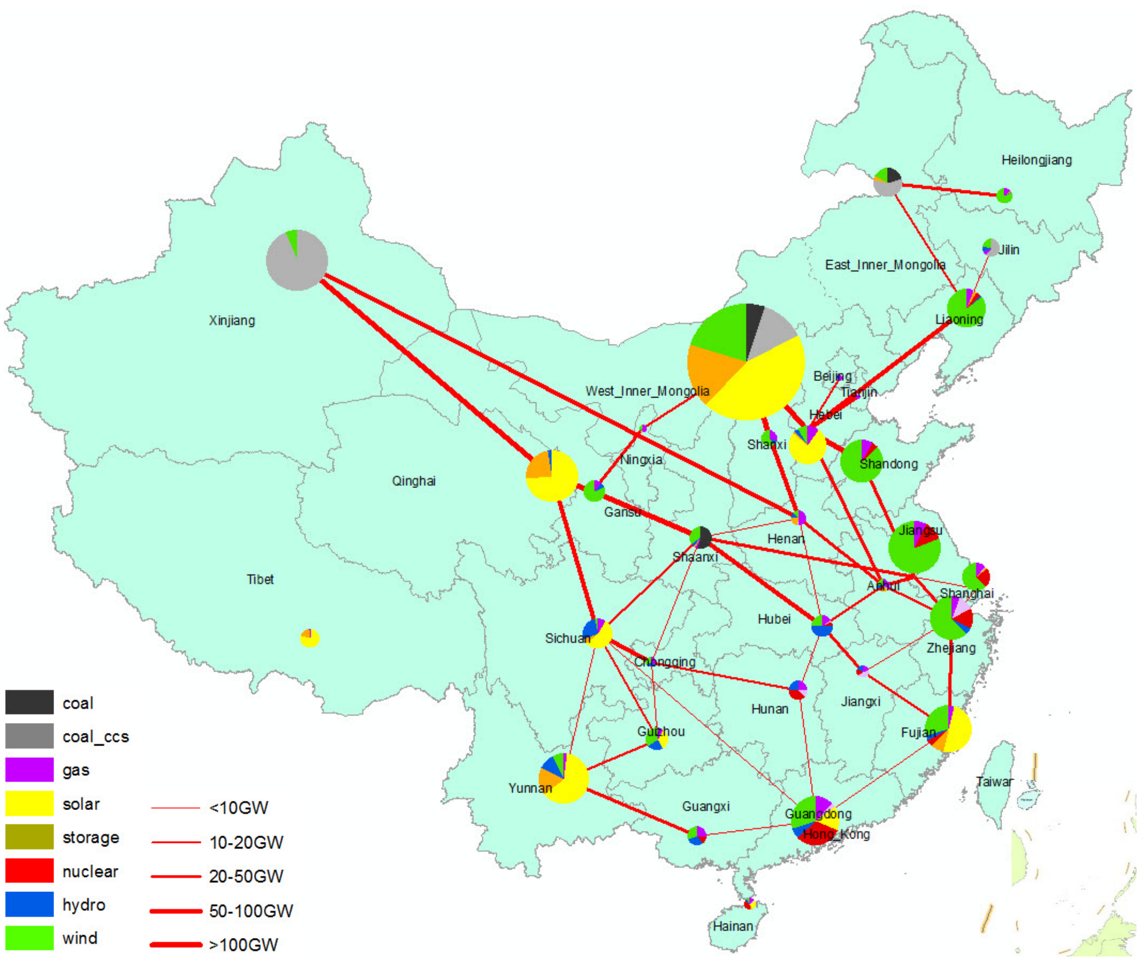

Figure 2-6 Infrastructure, generation and transmission capacity needed to achieve the IPCC target (SWITCH-China results). All represented lines are new transmission expansion.

While the 80% reduction in CO_2 emissions warranted by the IPCC is not an official target in China, results show that such national policy actions can have a high impact on fuel cost saving, air pollution reduction, inter-regional connectivity and asset diversification to increase resilience, and other co-benefits. The resulting optimal generation capacity mix to reach this target includes, in 2050, 14% of nuclear, 23% of wind, 27% of solar, 6% of hydro, 1% of natural gas, 3% of coal and 26% of coal with CCS. As mentioned, a deep decarbonization target would result in a 37% increase in total power cost compared to the **BAU** scenario. Increased costs would be partially offset by lower environmental pollution, as well as public health and climate benefits—all externalities that are not currently taken into account in power pricing. Given the significant reliance of this strategy on coal with CCS and grid-level battery storage, which have not been deployed at large scale today, technological and economic innovation as well as novel financial mechanisms will be necessary to enable deep decarbonization in the country.

2.2.4 CONCLUSION

By optimizing province-level capacity expansion and hourly generation dispatch simultaneously, SWITCH-China is uniquely suited to identify and compare viable, cost-efficient decarbonization pathways across power system infrastructure and technology options. SWITCH-China helps identify the least-expensive viable pathway to achieving national energy and climate targets.

China is on track to achieve its short-term energy goals, with more wind and solar capacity installed each year than what is needed to achieve those targets. However, long-term carbon mitigation and technology pathways are more uncertain. Because investment strategies have a waterfall effect, decisions taken today will determine the country's ability to achieve its future environmental targets and, in particular, its role into the global 2DS target. SWITCH-China is a tool that combines technologies, policies, and investment decisions to enable strategic thinking on the future of China's low-carbon power transition. Concerted action is needed to develop such a system.

Yet, power demand projections are driven by economic growth, efficiency measures, general technological innovation, and the large-scale deployment of grid flexibility options, which all embed uncertainties [185]. Cost and performance assumptions have uncertainties that will appear in the learning curve of new technologies, and could impact their competitive advantage over time. Fuel price fluctuation and new fuel availabilities could also change optimal strategies. Other social and political changes, not directly related to economics—such as training, safety, public perception and acceptance of large projects—could add uncertainty to the deployment of some technologies.

The next section proposes a module to be added to the SWITCH-China model to account for uncertainty on cost projections and VRE capacity factors. The resulting trade-off between risk minimization and cost minimization can be balanced as a function of policy-makers' degree of risk aversion. Chapters 3 and 4 tackle power-related challenges that are not explicitly addressed in this section, including the fresh water co-generation opportunity for decarbonization, wind power curtailment in North China, and the role of transport electrification in China.

2.3 TWO-STEP UNCERTAINTY MINIMIZATION APPROACH

Traditional linear-programming cost-minimization tools, including the SWITCH-China model presented above, provide valuable information to compare energy sources within a given context. However, among a set of possible electricity mix expansion trajectories with similar yet not identical costs, LPs invariably favor least-cost options without accounting for the probability that projected costs might not match actual future costs. As a result of the inherent uncertainty of exogenous cost projections, the stability of costs—i.e., affordability of the mix—is not ensured in cost-minimizing optimizations. Yet, in reality, policy makers seek to include in their decision-making the likelihood that future costs or revenues would remain close to projections should the modeled scenario be implemented. In fact, it has been suggested that planning authorities, whether public or private, are more concerned by worst-case scenarios than best estimates of performance of selected configurations, suggesting a high degree of risk aversion among decision makers [186], [187]. As the share of VREs grows in electricity mixes around the globe, resulting in higher curtailment levels, operational and, ultimately, economic risks increase. Whether those risks are borne by consumers—for example through the use of feed-in tariffs that guarantee payment to power generation system owners in France, Germany and Australia—or directly by VRE project owners, as it is the case in China, they call into question the accuracy of traditional planning optimization efforts such as the SWITCH-China model [188]. In reality, optimizing an electricity portfolio should be seen as a trade-off between the minimization of expected costs, and the minimization of uncertainty—or "risk"—on costs.

State-of-the-art LPs currently used by policy makers are complex, joint optimization efforts where, often, the variables of interest—power supply reliability, costs, carbon emissions, etc.—operate at cross purposes. Not only planning authorities must have access to capacity expansion planning model results to inform their decisions, but they also need to understand the underlying reasoning and implications of those recommendations. Given the myriad of existing models presenting various approaches—sometimes very similar—for planning the future electricity mix, and the adaptation time that is required to transition the new modeling tool from a research-based to a policy-making usage, decision makers tend to favor time-tested tools. In fact, there exists a trade-off between the accuracy of model results and the complexity of using and understanding the model. Tools are needed that can simultaneously minimize *costs* and *risks on costs* for long-term planning of the energy mix. Unfortunately, the majority of those time-tested tools do not account for risks. In this study, we propose a new approach to account for risk aversion while allowing decision makers to use cost minimization tools they are familiar with.

A common way to address uncertainty in energy planning models is the use of scenarios [189], as does the SWITCH model [158], [190], [191], or sensitivity analysis, as performed in the HOMER model [192]. The set of possibilities spanned by these approaches is limited as it relies on human imagination, often qualitative rather than quantitative— e.g., "high gas price" and "low gas price" scenarios. There exist two main methods to account for risks in "static" or "perfect forecast" programming tools used by policy makers: repeated random sampling—e.g., Monte Carlo simulations—and mean-variance analysis—also called modern portfolio theory. The former is based on simulations while the latter is an optimization technique solved by a quadratic program (QP). The main caveat of random sampling is the impossibility to ensure that all possible, rare but high-consequence events have been simulated. This is related to the well-known problem of induction, illustrated by the phrase in Nassim N. Taleb's book: *Every swan that I have ever seen is white, therefore there is no black swan* [193]. Another related issue is the large number of outcomes resulting from the multiple simulations, leaving policy makers with a range of options and possible futures almost as broad as the initial set of options.

Mean-variance optimization poses some reliability challenges too, as it often assumes no uncertainty on the uncertainty: the standard deviation, including its future values, is assumed to be known. While this can be problematic in branches of finance subject to a selection bias [194], centralized long-term expansion planning of a national electricity mix is usually less subject to this bias. Values that energy planners rely on to create cost projections are usually based on existing data such as historical market prices for fuel and past construction and operation costs for energy systems. While average values of past data cannot be considered as an accurate prediction of future costs, the typical scope embraced is usually old and large enough to represent a more accurate landscape of the range of future possibilities. For these reasons, we choose mean-variance optimization over random sampling in the present study.

Policy makers could comprehensively plan expansion of the electricity mix through two successive steps. The first step, well-known in the sphere of energy planning, involves the identification of least-cost installed capacity scenarios for various power infrastructure systems, via a thorough linear cost-minimization. An example of high-resolution capacity expansion planning was proposed in the first section of this chapter, with the SWITCH-China model. The second step, detailed in this second section, consists in refining least-cost electricity mix results obtained in the first step. By setting a sufficiently narrow limit for allowed deviations around those results—proposing a "reliability net"—this second step supplements findings from complex cost-minimizing modeling tools by confronting them against a simpler risk-minimization model, while preserving the grid reliability ensured by the LP. By switching from LP to QP, policy makers have the opportunity to abandon the "individual technology" focus in favor of the "alternative resource portfolio" analysis [195].

China's power system is an ideal laboratory as its centrally-coordinated planning facilitates the identification of configurations that are optimal across regions. Moreover, as concluded in the first section, the extent of the country's future power demand is such that its future electricity supply system will require novel, unconventional technologies, for which taking risk on costs into account is crucial. This section presents the methodology developed for risk calculation, the QP formulated to perform mean-variance optimization, and its application to refine cost-minimization results for China's future electricity mix obtained from the SWITCH-China model.

From its creation and first application to the field of finance in 1952 [196], modern portfolio theory has been extended to other contexts. Its application to energy portfolio management can be traced back to 1976 [197], however it has only significantly expanded in recent years [198]–[201], together with increasing environmental awareness and subsequent regulations, as well as democratization of innovation in technology and information. While including risk consideration in energy planning is crucial, models' own assumptions and structure considerably impact results and can lead to discrepancies between Pareto optima modeled with different beliefs. Compared to the existing literature, the contributions of this study are three-fold. First, as our study focuses on improving energy planning practices, we propose an original, versatile two-step process ensuring easy adoption of the tool by policy makers. Second, we ensure the high-fidelity of the method by constraining the risk-minimization analysis within the vicinity of the LP results, hence preserving potential grid reliability ensured by the high-resolution cost-minimization. Third, we use datasets of several hundred thousand data points for technology costs as well as hourly capacity factors for central PV and wind turbines across China in order to assess the magnitude of the uncertainty.

2.3.1 METHODOLOGY AND MODEL DESCRIPTION

2.3.1.1 Risk Factors

Mean-variance portfolio analysis uses the variance of cost projections, or economic return, as a metric to account for uncertainty in meeting a desired objective. Variances are either obtained from the literature or calculated based on available datasets. Given the nature of the optimization approach, it is assumed, when needed, that cost probabilities are normally distributed, although it is not a necessary condition [202].

The following uncertainty factors are taken into account: overnight costs ($\sigma_{overnight}$), including potential future regulation around emissions from fossil-fuel power plants and nuclear safety, increasing construction costs; uncertainty as to fuel price volatility and future carbon tax (σ_{fuel}); fixed O&M costs ($\sigma_{O\&M}$); variability in wind and solar power output ($\sigma_{intermittent}$). In particular, the variance on costs resulting from short-term intermittency of VREs appears not to have been covered in the existing literature. Here, a simple methodology is presented to calculate standard deviations resulting from this phenomenon. Standard deviations from variable power output are calculated using province-level hourly capacity factors for solar PV and wind turbines from historical data. In order to translate these into risk on costs, we make the assumption that intermittency must be backed by peaking plants, typically gas combustion turbines. This is a first-level approximation. Costs of storage systems could also be used, depending on the dominant source of flexibility in the considered electricity mix. Given the limited potential for further PHS capacity development in China, the absence of other storage technologies at utility-scale, and the wide use of natural gas to back up VREs in other countries, natural gas is used as a proxy for grid flexibility cost.

Standard deviations from uncertainty factors mentioned above—overnight costs, fuel costs, fixed O&M costs, intermittency costs—are aggregated. LCOE per technology per year is calculated using the same cost projections [203]. A standard deviation of LCOE per technology per year, expressed in $/MWh, is calculated. These are the components of the Hessian matrix of the program presented below.

2.3.1.2 Quadratic-Programming Model Description

The program formulated in this study is a QP with linear constraints. It is designed as a versatile module to be applied, as a second step, to results from cost-minimization models and, as such, must avoid redundancy. Following the example of the SWITCH-China model, the LP used in the first step is assumed to optimize transmission lines, storage capacity, and hourly dispatch of the electricity grid in order to ensure reliability of the grid operation. Therefore, these components are not taken into account in the QP.

The QP is constrained to minimize risks within +/- 15% around the generation levels of each energy technology in the least-cost portfolio calculated by the LP, defining a "reliability net." It is assumed that a maximum change of 15% in new capacity can be allowed without resulting in major constraints related to siting and transmission, thus eliminating the need to account for additional infrastructure and transmission development beyond LP results. The objective function of the model is to minimize the total variance on costs of the electricity mix. A mathematical formulation of the QP is presented in Equations 2-1 to 2-9 and in Table 2-3. The subscript $_{-LP}$ designates outputs of the cost-minimizing LP (first step), used as inputs in the risk-minimizing QP (second step).

$$\min \frac{1}{2} x^T Q x \qquad 2\text{-}1$$

With:

- $x = (x_i) \in \mathbb{R}^{n\times 1}$ 2-2
- $Q = \left(\sigma_i \times \sigma_j \times \rho_{ij}\right) \in \mathbb{R}^{n\times n}$ 2-3

Subject to:

- $\forall i, x_i \geq 0$ 2-4
- Reliability net: $\forall i, 0.85 x_{i-LP} \leq x_i \leq 1.15 x_{i-LP}$ 2-5
- Preserving intermittency back-up (gas plants here): $\frac{x_{wind}+x_{solar}}{x_{gas}} \leq \frac{x_{wind-S}+x_{solar-LP}}{x_{gas-LP}}$ 2-6
- Preserving annual electricity production to meet demand: $\sum_{i=1}^{n} x_i = \sum_{i=1}^{n} x_{i-LP}$ 2-7
- Total cost: $\sum_{i=1}^{n} c_i \times x_i = TC$ 2-8
- Carbon emissions are capped at levels of LP outputs: $\sum_{i=1}^{n} e_i \times x_i \leq \sum_{i=1}^{n} e_i \times x_{i-LP}$ 2-9

Table 2-3 Elements of the QP

Symbol	Definition
Q	Covariance (or Hessian) matrix: Q = 2*[$\varrho_{ij}\times\sigma_i\times\sigma_j$]
x_i	Power generation from technology i (MWh/y)

x	Vector of x_i
n	Number of power production technologies
σ_i	Standard deviation of LCOE for technology i ($/MWh)
ϱ_{ij}	Correlation coefficient between technologies i and j
c_i	LCOE of technology i ($/MWh)
TC	Total power production cost ($/y)
e_i	Intensity of CO_2 emissions from technology i (tCO_2/MWh)

In practice, the majority of correlation coefficients are equal to zero, except for fuel prices.

2.3.2 Application to China's Power Sector and Results

The SWITCH-China model is used as a proxy for cost-minimization models used by policy makers. We apply the two-step methodology to the **BAU with Carbon Cap** scenario, explored by SWITCH and presented in the previous section. The corresponding SWITCH results—the least-cost electricity mix expansion pathways—are used here as inputs to the QP to illustrate the risk-refining approach over the 2015-2050 period.

The analysis focuses on new power capacity, installed by SWITCH beyond capacity already existing and operating in the country in 2015. Generation technologies to be deployed according to results of the **BAU with Carbon Cap** scenario are coal steam turbine, gas combustion turbine, wind turbine, solar PV, nuclear PWR and, from 2035 on, coal steam turbine with CCS. For limited availability reasons, SWITCH does not enable further deployment of hydropower besides currently existing capacity. Therefore, this energy source is not explored in the risk minimization approach. For each of the six technologies, the corresponding installed capacity in the **BAU with Carbon Cap** scenario is presented in Figure 2-4.

Expected future costs are assumed to be the same as for the SWITCH-China model, presented in the previous section. Values for standard deviations of technology cost components are found in [198], [201], [204]–[207]. These values are updated and adapted to the Chinese context. Standard deviations of wind and solar intermittency are calculated based on capacity factor datasets from [208], [209] with 3TIER wind hourly wind speeds and solar irradiation data. We assume that risks across technologies are independent, except for fuel costs where covariance values are non-null, consistently with the literature. Projections for future carbon price trajectories range from $0 to $115/t-$CO_2$ in 2050 [210].

Hereafter, the term "portfolio" refers to a set of specific annual power generation levels from 2015 to 2050 for the six technologies mentioned above. As mentioned, the QP does not include technologies that are not deployed, besides existing capacity, after 2015. The terms "SWITCH," "LP" and "cost minimization" refer to the first step of the methodology, while "QP" and "risk minimization" indicate the second step.

2.3.2.1 Risk Minimization in the Year 2030

First, risk-minimization, performed by the QP, is applied to the year 2030 only. The projected portion of electricity demand to be met in 2030 by the six technologies considered in the QP is 4,300 TWh.

The SWITCH least-cost portfolio, P_s, presents an average electricity production cost of $72.60/MWh and a risk on cost of $15.80/MWh. Its CO_2 emissions for the year 2030 add up to 2.24×10^9 tons. By allowing annual power generation from each technology to vary within plus and minus 15% around their SWITCH least-cost generation levels, the QP identifies least-risk portfolios, subject to the set of constraints presented above, as a function of LCOE. For a given LCOE, the electricity mix with lowest risks is called the Pareto efficient portfolio, or *efficient portfolio*. In Figure 2-7, portfolios on the Pareto efficient frontier (left branch of the black curve) have costs ranging between $72.63/MWh and $73.47/MWh.

Two factors explain that QP solutions depart from the SWITCH results within the allowed boundaries. First, energy systems that have high LCOE, relatively to other technologies, are penalized in the SWITCH optimization, while they might be favored in the QP if they demonstrate low standard deviations. Second, diversification has an absolute positive impact on decreasing risks: even the addition of a risky technology in the energy mix can, under some conditions, lower the overall risk of the portfolio. This diversification phenomenon is not accounted for in the SWITCH optimization.

Among the Pareto-optimal portfolios, P_1 is the least-cost solution, presenting slightly higher costs than the "non-Pareto efficient" least-cost portfolio P_S calculated by SWITCH. In this particular case, P_1 is also a solution of the problem defined in Equation 2-10:

$$\min_{P_i} \left(Risk(P_i) - Risk(P_S)\right) + \left(Cost(P_i) - Cost(P_S)\right) \qquad \text{2-10}$$

P_2 presents the lowest risks among feasible portfolios. P_2 is the efficient portfolio with the largest differences in power generation levels from the SWITCH least-cost portfolio. Yet, differences across portfolios do not considerably vary, as the QP optimization is bounded between +/- 15% of SWITCH generation levels.

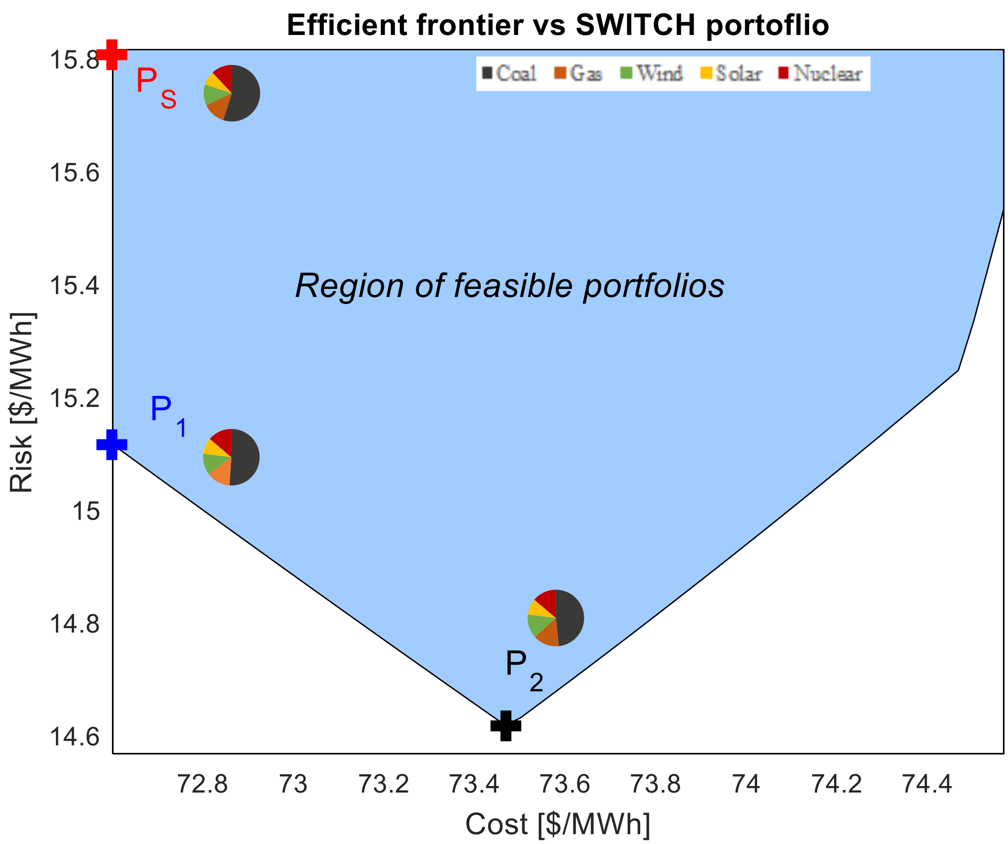

Figure 2-7 Feasible portfolios—including the Pareto efficient frontier from P_1 to P_2—characterized by expected LCOE and standard deviation of LCOE in the year 2030 (QP optimization results). P_S represents the least-cost electricity mix (SWITCH-China results from the BAU with Carbon Cap scenario). Pie charts represent generation shares for the five energy sources considered in portfolios P_S, P_1 and P_2.

As a result of the QP optimization, 8% and 13% of the annual power demand in P_1 and P_2, respectively, are met by a different energy source from what was prescribed in the SWITCH-China model. Resource-specific changes compared to P_S include: -169.6 TWh of coal and +77.2 TWh of nuclear for P_1, -288.8 TWh of coal and +83.4 TWh of natural gas for P_2 (Figure 2-8). In practice, these power generation changes result in a higher change in installed capacity for VREs than for thermal plants, because of the limited capacity factors for wind and solar systems, which have national averages of 0.18 [208] and 0.19 [209], respectively.

Coal steam turbines have low average LCOE in China compared to other technologies and are, for this reason, favored by cost-minimization models unless constraints, such as the CO_2 emission reduction targets presented in the previous section, prevent their expansion. Even when CO_2 emissions are capped after 2030, coal remains the dominant source of power in the SWITCH results of the **BAU with Carbon Cap** scenario. Yet, uncertainties on future coal prices and CO_2 emission regulations impact the variance of coal steam turbine costs. For this reason, and because of the effect of diversification on portfolio-wide risks, the share of coal in all efficient portfolios is lower than in P_s. P_1, the Pareto-optimal portfolio with lowest costs, generates more electricity from coal than the other Pareto-optimal portfolios. The diversification effect also results in an increase in the share of natural gas compared to P_s. While natural gas is significantly increased in P_2, its relatively high LCOE in China does not make it a good candidate when costs are limited, therefore its share is only slightly increased in P_1. The larger the reduction in coal and the increase in natural gas, the lower the total variance of the corresponding efficient portfolio under the 15% maximum change constraint. For the same reason, the small share of solar PV is increased up to its maximum (+15%) compared to the SWITCH results in all efficient portfolios. On the other hand, the relatively high LCOE variance of wind, and its large share compared to solar in P_S, do not make wind energy a favored option in a risk-minimization approach when total costs are limited. Finally, in all portfolios on the efficient frontier, the share of conventional nuclear systems is increased up to its maximum limit with the QP optimization, as a result of its low LCOE and low share, and despite its relatively high cost uncertainty.

In all efficient portfolios, the total increase in VRE generation from risk optimization is higher than the increase in fossil-fuel generation, despite the additional constraint between renewable energy share and natural gas share to maintain grid operability. One important finding is that the cap on CO_2 emissions is not an active constraint in any of the Pareto-optimal portfolios. Therefore, accounting for risk on costs leads, in this specific case, to a reduction in CO_2 emissions compared to a simple cost-minimization.

Figure 2-8 Change in annual electricity generation per energy source for the two efficient portfolios P_1 (top) and P_2 (bottom) compared to the SWITCH-China least-cost portfolio in the year 2030 (QP results).

P_1 demonstrates smaller changes in costs and risks than P_2 (Table 2-4). Any portfolios on the efficient frontier between P_1 and P_2 would yield a decrease in risks on costs of between \$3.04 billion/year and \$5.10 billion/year. An infinite number of portfolios between P_1 and P_2 could be favored over P_s by policy makers, depending on their level of risk-aversion, that is the expected cost premium they are willing to accept in order to reduce cost uncertainty.

Table 2-4 Change in electricity supply costs and relative standard deviations for the efficient portfolios P_1 and P_2 compared to the least-cost portfolio P_S in 2030 (QP results).

	Total change in costs in $/year (%total cost)	**Total change in risks in $/year (%total risk)**	**ΔCost + ΔRisk in $/year**
P_1	$+1.43\text{x}10^8$ (0.46%)	$-3.04\text{x}10^9$ (-4.49%)	$-2.90\text{x}10^9$
P_2	$+3.72\text{x}10^9$ (1.19%)	$-5.10\text{x}10^9$ (-7.52%)	$-1.38\text{x}10^9$

2.3.2.2 Risk Minimization over the Entire Horizon and under the Introduction of a New Technology

While the previous section was focused on risk minimization in a single year—year 2030—, this section explores the evolution of risk-minimizing portfolios across each of the four periods of the SWITCH-China model, until 2050. In this study, the efficient frontier of an electricity mix can evolve over time for two reasons. First, the overnight costs of a few technologies—here, wind turbines, solar PV and coal with CCS—are assumed to decrease in the future, following R&D and large-scale deployment programs. These learning curves impact both future expected LCOEs and their standard deviations. Second, the introduction of a new technology—coal with CCS—from 2035 on impacts the SWITCH optimization, the Hessian matrix and the constraints in risk optimization.

The QP is run over the four ten-year-long periods of the **BAU with Carbon Cap** scenario. In all years, changes induced by minimizing risks lead to lower CO_2 emissions. Figure 2-9 shows that the magnitude of this change varies according to the initial least-cost mix in each year. In period 1, maximum allowed deviations for all technologies are limited for wind, solar and nuclear given their relatively small shares in 2015, further limiting the potential for emission reduction. In periods 2 and 3, decarbonization is favored by the uncertainty of carbon price, leading to a sharp decrease in CO_2 emissions between P_s and Pareto efficient portfolios. In period 4, the expected implementation of new carbon regulations forces SWITCH to choose a portfolio that is cleaner than in previous periods. Therefore, the impact of a subsequent risk minimization on emission reduction is relatively lower.

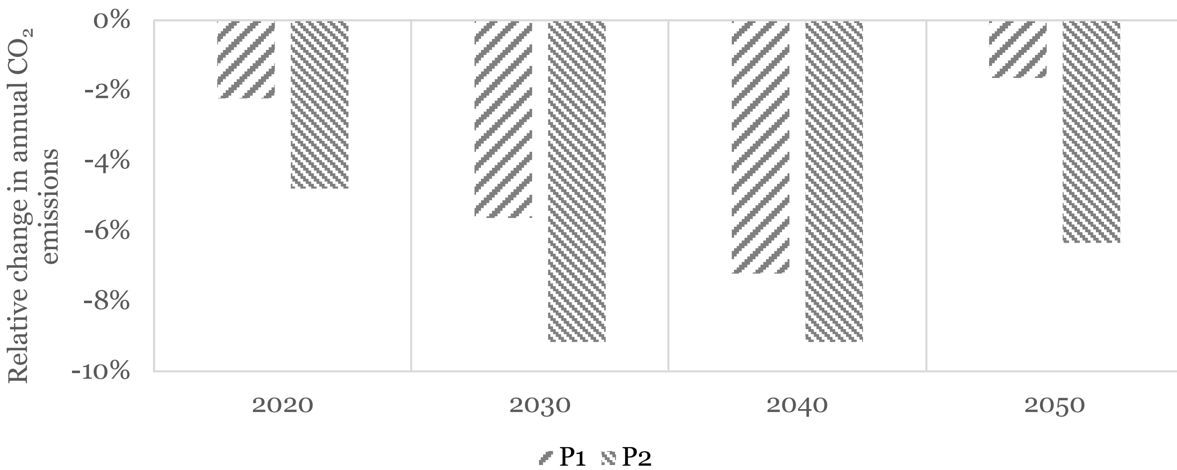

Figure 2-9 Change in annual CO_2 emissions for the two efficient portfolios P_1 and P_2 compared to the SWITCH portfolio in the four periods (QP results).

At the time of its first implementation, in 2035, the optimal generation share of coal with CCS in P_s equals 4.5%, and the share of coal is 30%. A hypothetical situation where these 4.5% would instead be conventional coal leads to an increase in total portfolio risk on costs of 1.75% or $0.92 billion per year. Although coal with CCS shows significantly higher variance on technology cost than conventional coal, the advantage of coal CCS against carbon price uncertainty makes it a valuable asset to decrease overall risk on costs in the mix.

The addition of coal with CCS in the electricity mix does not lead to a positive diversification effect. As mentioned before, a majority of the literature assumes that risks across technologies are independent except for fuel costs. Therefore, the addition of novel low-carbon energy technologies whose costs are less impacted by fuel than the overall system, such as advanced nuclear reactor designs, would have a higher impact on decreasing portfolio risks than coal with CCS.

2.3.3 Conclusion

In all four periods from 2015 to 2054, we find that it is possible to create portfolios that can be maintained close to cost-minimization results, and without a significant increase in costs, while showing lower risks on costs.

While the ultimate portfolio choice depends on policy makers' aversion to risks, an infinite number of efficient portfolios could be favored by policy makers willing to accept a cost premium, from the least-cost portfolios found from conventional LPs, provided that it yields a reduction in risks.

Despite the economic impact of safety regulations and uncertainty of its construction lead-time, low costs and relatively low share of nuclear power in China give this technology a key role in reducing risks on electricity supply costs over the 2050 horizon. Wind turbines and solar PV are favored from 2035 to 2055, while the share of natural gas is increased in the near term, despite its carbon intensity, high costs, and high variance. In all periods, risk minimization leads to a decrease in coal and subsequent decrease in CO_2 emissions, although capping emissions at the least-cost portfolio level is never a binding constraint in the QP optimization. Uncertainty on future carbon regulations can significantly increase the share of renewable energies, and reduce CO_2 emissions, of an electricity mix even without the actual implementation of these regulations. As a consequence, when the risk of a future carbon tax is accounted for, the optimal transition to a clean power sector occurs earlier than in a simple cost minimization. The "fear of regulation" can be seen as a first step towards a cleaner electricity industry.

This analysis shows that, while cost-minimization provides valuable insight into least-cost technology deployment directions to help decision makers, it should only constitute the first step of a thorough energy planning approach. Reliable sources from which policy makers obtain cost projection data usually provide standard deviations, error bars, or other metrics to represent the uncertainty of their calculations. While cost-minimization models only use half of the available information—the projected or expected value—the other half—uncertainty quantification—can also be used, without much additional effort, thanks to the two-step methodology presented in this study.

This two-step module makes the transition easier for policy makers, since it integrates well with existing, "legacy" linear tools. Compared to simple cost-minimization, it provides, at low costs, a more accurate picture of future consequences of energy planning decisions and on levers to strengthen electricity access and affordability. Yet, there exists a trade-off between low computing time and versatility on the one hand, and solution accuracy on the other hand.

First, other measures than standard deviation could be used to quantify exposure and uncertainty, for example by focusing on downward risk. However, such approach would complexify the risk minimization process and result in larger computing time.

Second, the proposed approach, which allows policy makers to use the cost-optimization tool they are familiar with by using the risk-minimization module as a second step, is suboptimal compared to a high-resolution model that would optimize costs and risks in a single step. In particular, the 15% maximum deviation constraint, which limits the set of feasible solutions, would no longer be needed. Such integrated cost-risk approach might prove to be a better tool, should policy-makers find it appropriate to transition to a new model.

Finally, future improvements should focus on integrating other sectors in the optimization scope, such as transportation and water, while maintaining reasonable computing times, and on accounting for factors—technical, social, institutional, geopolitical— that create uncertainty, beyond costs and renewable energy variability.

CHAPITRE 3 DECARBONIZED, REGIONAL-SCALE ALTERNATIVES FOR FRESH WATER SUPPLY IN CHINA

3.1 INTRODUCTION

China contains 20% of the world's population but only 7% of its water resources [211]. Water scarcity in the country has been described as a challenge as serious as air pollution but more difficult to solve [212]. Similar to the mismatch between energy resource and demand mentioned earlier in this dissertation, water resources are unevenly distributed across the country, larger in regions with low population density. Scarcity primarily hits most developed regions, in the North-Eastern part of China, while Southern and far Western provinces are water-rich. Today, renewable fresh water resources per capita are a third of the global average [213]. Moderate to severe water shortages affect municipal, industrial, and agricultural sectors alike, representing 16%, 32% and 51% of the demand, respectively [214]. This phenomenon has been exacerbated in the last decades by increasing water consumption as a result of economic and population growth. The possible negative impact of climate change on water resources has also been recognized by the Chinese government [215]. Moreover, at RMB 3.5/m^3 on average in Chinese cities, the water residential price represents only 28% of the global average price [216]. Artificially low water prices across the country lead to overuse and inefficiencies, increasing pressure on resources. For example, in 2007, China was using three times more water than the global average for the production of a given worth of industrial good [217]. Efficiency, recycling and conservation programs have been implemented to save water, but they have not addressed the shortage issue in its totality. Scarcity is exacerbated by pollution. Nationwide, 61.5% of groundwater reserves and 31.4% of surface water have a quality of class IV or lower, unsuitable for human needs and even for some industries [24]. 21% of the surface water is not suitable for agricultural use [25]. Finally, scarcity challenges the operation of the power sector, which requires large quantities of water for hydropower and thermal power plant cooling. In 2010, thermoelectric water withdrawals added up to 60 km^3 in China [26], or 10% of the world's total thermoelectric water withdrawals that year [27] and 11% of China's annual water demand [28], although a large share of it is sent back to reservoirs and can be used for other purposes. The national water gap between demand and supply is expected to reach 130-230 km^3 in 2030 [35], representing 25% of the total demand [214]. It will result in an economic loss of $35 billion annually in reduced economic and industrial output and lost lives [36] [218].

The Chinese government's response to the geographic mismatch between water demand and supply has been the construction of cross-region water diversion projects. In particular, the SNWTP, presented in Figure 3-1, aims at diverting water from resource-rich to scarce provinces. The Eastern route and the Central route will transport 24-25 billion m^3 of water annually from the Yangtze river and the Danjiangkou reservoir to water-scarce Eastern provinces [219]. This project, the cost of which has already reached $81 billion, will not increase the total quantity of water available in the country. It also has tremendous indirect costs, such as people resettlement [33] and the long-term risk of drying out Southern provinces [34]. The Western route, planned by the central government for several decades, is even more controversial.

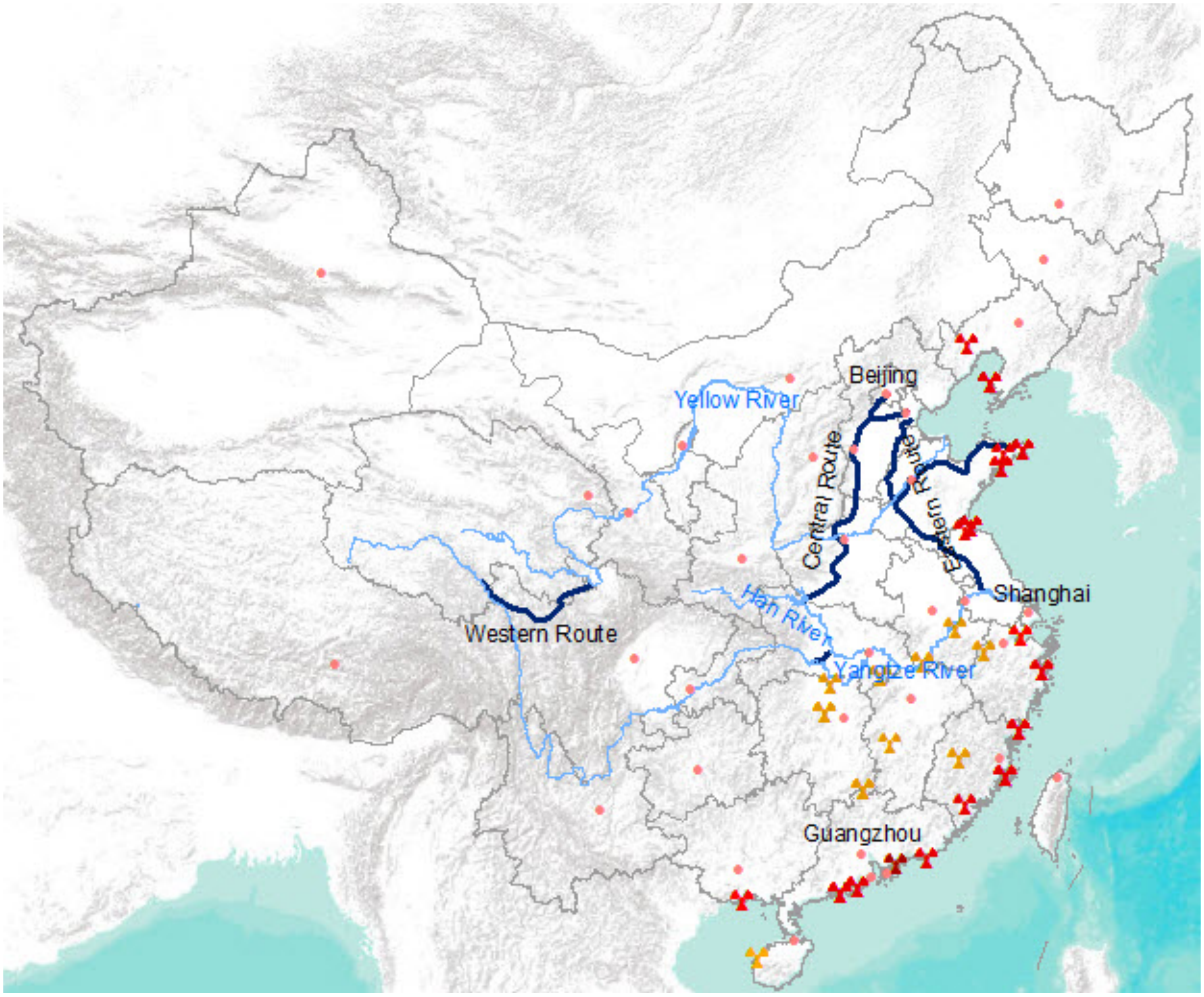

Sources: [4] [220] [221]

Figure 3-1 China's projected nuclear fleet in 2030 and Eastern, Central and Western routes of the SNWTP, as of 2015. The three routes are drawn in dark blue. Red crosses represent nuclear plants hosting reactors found appropriate to nuclear desalination in 2030, while yellow crosses indicate nuclear plants that, for geographic or age-related reasons, are considered not appropriate.

Costs, scale, and impacts of the SNWTP warrant the exploration of alternative approaches for non-disruptive water supply, beyond existing recycling and conservation programs. Today, electricity and thermal energy are used to power a small but increasing fleet of water treatment plants in China [29]. Encouraged by the official "13th Five-Year Seawater Utilization Plan" [30], the national desalination capacity is expected to grow from 1.2 million m^3/day in 2017 [31]—meeting 0.8% of the national water demand—to 2.5-3.1 million m^3/day in 2020 [29]. Desalination is powered, in majority, by China's coal-dominated electricity grid or directly by coal plants. Given its limited deployment today, current desalination practices are responsible for nearly one megaton of CO_2 emissions per year [32] or 0.008% of the country's annual CO_2 emissions [18]. However, deploying a national desalination capacity large enough to alleviate China's tremendous water needs would, under the current electricity mix, emit a significant amount of carbon dioxide and other polluting emissions. The location of water demand centers, on the coast, suggests that there exists a nexus opportunity for co-development of clean energy systems and water desalination plants to solve the country's clean power and fresh water challenges simultaneously.

This chapter proposes two frameworks to explore the interrelation between water and power supply, and how their synergies can be used to design public policies and plan infrastructure expansion aligned with the climate change mitigation goal. In particular, it evaluates the relevance of regional desalinated water supply as an alternative to national-scale water diversion.

First, given the important role given by the Chinese government to nuclear power for the country's climate and air pollution strategy, and plans for additional nuclear reactor deployment in water-scarce North-Eastern provinces, we develop a methodology to assess the technical, economic and environmental relevance of nuclear desalination for fresh water supply, and compare it to the SNWTP and existing coal desalination practices.

While the first section of this chapter compares desalination and diversion options at the technology level, the second section explores the opportunity for clean power-water treatment coordination at the grid level. Power curtailment is one of China's main barriers to further large-scale deployment of VRE systems. The current solution undertaken by the central government is the construction of a national-scale electricity transmission network, the power counterpart of the SNWTP. Recognizing that the risks and challenges of nationwide projects, including the inability to offer diversified and tailored solutions to regional disparities, apply to both power and electricity, this second section proposes a new approach to create independent regional grids, self-sufficient in both clean power and water supply. More specifically, we develop a framework to evaluate if and at what costs the use of desalination as a deferrable load can help integrate large shares of intermittent energies while maintaining reliable electricity supply at affordable costs.

3.2 Relevance of Nuclear Desalination as an Alternative to Water Transfer Geoengineering

China's electricity mix in 2030 is expected to remain dominated by fossil fuels [222], making grid-powered desalination technologies, such as membrane-based processes, polluting. Unlike these, hot steam from nuclear reactors can be extracted to directly power low-carbon desalination. China is deploying nuclear power reactors at large scale [4]. The purpose of this study is to determine if and under what assumptions, in the long term, nuclear thermal desalination can become an appropriate option to meeting China's water needs and to compare it to water diversion and coal desalination alternatives on economic and environmental levels. The choice of a 2030 horizon results from a trade-off between the need of a period of time long enough to expect substantial evolution in the Chinese nuclear fleet, and the uncertainty of long-term planning.

The literature addressing water scarcity in China is extensive but not comprehensive; several studies have been conducted on water desalination in China but with no detail on nuclear desalination [223]–[226], on nuclear desalination but not from a Chinese perspective [227]–[232], and on novel reactor technologies to perform desalination in China but not on its industry-scale potential to address water shortage across the country [233]–[237]. Zhang et al. [223] and Zhou and Tol [224] described the technical and economic characteristics of different desalination processes and their implementation in China. However, the relationship between thermal water desalination and electricity production in China was not evaluated. The present study focuses on one type of desalination process—steam extraction from nuclear reactors. Projections for China's water shortage and nuclear fleet in 2030 allow for a meaningful evaluation of the maximal production capacity of desalinated water, the distance between future water-scarce provinces and desalination plants, and the resulting costs and affordability of desalinated water for domestic and industrial needs in the 2030 Chinese context. This study provides a framework to assess nuclear desalination impact: the affordability of fresh water supply in water-scarce provinces through the use of the five-percent rule, as defined later. Finally, previous studies mentioned other solutions than nuclear desalination to water shortage in China, particularly the SNWTP, but no research was executed prior to the present study on the development of an interdisciplinary framework to evaluate and quantify nuclear desalination assets and drawbacks compared to its two main alternatives: SNWTP and coal desalination.

3.2.1 METHODOLOGY

3.2.1.1 Data Sources

In this study, the technical configuration, performance and economic assessments of building a desalination plant and coupling it to a nuclear reactor have been performed with the Desalination Economic Evaluation Program (DEEP) model developed by the International Atomic Energy Agency (IAEA) [238]–[240]. DEEP's calculation methods and inputs have been modified and adapted to the characteristics of the present study. Data come from the World Nuclear Association, DEEP, IAEA's Power Reactor Information System [241] and Advanced Reactors Information System [2] for the nuclear and desalination technical and economic sections; from Zhou and Tol [242], Gleick [228], IAEA [243] and DEEP for the water transportation section; from the World Nuclear Association, Nicobar Group, University of South China (USC) and Google Maps for the nuclear facility location section; from China Water Risk [244] regarding China's current and future water situation; and from the Chinese Bureau of South-to-North Water Transfer Planning and Designing for the SNWTP. Costs and prices are given in 2017 US dollars, and the conversion rate between Chinese RMB and US dollars is 0.16.

3.2.1.2 Selection of the appropriate desalination technology

Desalination technologies differ by energy consumption intensity, form of energy required, flexibility in plant siting options, and quality of water produced. Existing technologies for large-scale desalination are usually divided into two broad categories: membrane separation and thermal processes [245]. The three predominant commercial seawater desalination processes, as identified by the IAEA, which are proven and reliable for large-scale production of fresh water, are multi-stage flashing (MSF) and multi-effect distillation (MED) for distillation (thermal) processes; reverse osmosis (RO) for membrane processes [246].

Because RO uses electricity from the grid, it is only as clean as the electric grid it is powered from. MSF and MED can be coupled to a nuclear reactor to perform water desalination through steam extracted from the nuclear facility, therefore free of air pollutants during normal operation. Nuclear desalination relies on on-site coupling of a nuclear reactor with a desalination plant in order to produce fresh water through a thermal process. The coupling point is the cogeneration steam turbine, used to produce electrical energy and bleeding steam for process heat. The electrical energy required by the desalination plant for ancillary services, although low compared to the amount of heat needed, can also be supplied by the nuclear reactor [247].

In order to identify the most attractive technology among MSF and MED for nuclear desalination purposes, a 500,000 m^3/day water plant powered by nuclear energy was modeled under the two thermal process options using the DEEP model. The resulting specific energy consumption (SEC) is presented in Table 3-1. The model shows that, to desalinate one cubic meter of water, MED requires 28% less heat and 37% less electricity than MSF. In addition, the nominal gain output ratio, common measure of the efficiency of a thermal desalination plant representing the quantity of pure product produced per unit of driving steam, is slightly higher in the case of MED than MSF [245].

Table 3-1 Average SEC, specific electricity loss, and gain output ratio of MED and MSF desalination technologies for a modeled 500,000 m^3/day nuclear desalination plant (DEEP results).

	MED	**MSF**
Heat from nuclear to water plant (kWh/m^3)	42.65	59.28
Electricity consumption for desalination (kWh/m^3)	2.02	3.19
Loss of electricity due to steam extraction (kWh/m^3)	4.08	10.9
Gain output ratio	15	12

The MED process is more attractive as it demonstrates lower energy consumption than other thermal processes because the vapor produced in each stage is used to heat up feed water in the next stage. Compared to MSF, this not only reduces the energy required for distillation but also the overall electric power consumption [245], as well as investment costs [248]. MED is more cost-efficient and energy-efficient than MSF, thus it is the technology selected in the rest of this study.

3.2.1.3 Technical Characteristics and Production Capacity of a Nuclear Desalination Fleet in China in 2030

In this study, we explore the deployment of a desalination capacity in 2030 to be powered by nuclear reactors in China. We use data for operating, under construction, and planned reactors from the IAEA PRIS database [241] and from the World Nuclear Association [4]. We do not include reactor sites where construction has been considered but not confirmed. The Chinese nuclear fleet in 2017 consists of 36 reactors in operation on 11 different sites, for a total net electricity generation of 32.4 GWe. By 2030, the total nuclear net capacity could reach 91.5 GWe with 94 reactors—excluding non-PWR reactors and reactors smaller than 100 MWe (Figure 3-2). The 58 additional reactors to be built by 2030 will be spread over 21 sites.

Inland and island-based nuclear plants, as well as plants scheduled to be decommissioned before 2045, have not been considered for desalination purposes as calculations show that this would not be economically attractive. According to these criteria, 19 nuclear power plants[3] have been identified as appropriate sources of energy for nuclear desalination by 2030. These 19 plants host 69 reactors in total, for a net total capacity of 71.9 GWe.

This study evaluates the desalination capacity as well as construction and operation costs of 69 desalination plants. It is assumed that each desalination plant will be built as close as possible to one of the 69 nuclear reactors and coupled with it. A desalination plant can be built either during or after the construction of a nuclear plant [249]. To provide a meaningful framework for comparison purposes, all desalination plants considered in this study are assumed to be built in 2030.

The main parameters that influence maximum desalination production capacity are the power capacity and thermal efficiency of nuclear reactors, which vary according to the nuclear technology considered. The 69 reactors identified above cover eight different nuclear technologies listed in Table 3-2.

To determine the size of each desalination plant to be powered by one of the 69 nuclear reactors, the corresponding available heat, depending on the nuclear reactor technology, is calculated. It is assumed that maximum available heat does not vary across reactors of a same technology. The theoretical quantity of water that can be produced by the maximum quantity of heat available is de-rated by 15%—rounded down to meet standard capacities of water plants. The 15% margin is in line with the average reserve margin advocated by institutions' standards for power generation systems [250], as the primary purpose of future nuclear reactor construction planned by the central government is electricity supply.

[3] Bailong, Fangchenggang, Fangjiashan, Fuqing, Haixing, Haiyang, Hongyanhe, Huizhou, Ling Ao, Lufeng, Ningde, Putian, Qinshan, Sanmen, Shidaowan, Taishan, Tianwan, Xudabao, Yangjiang and Zhangzhou.

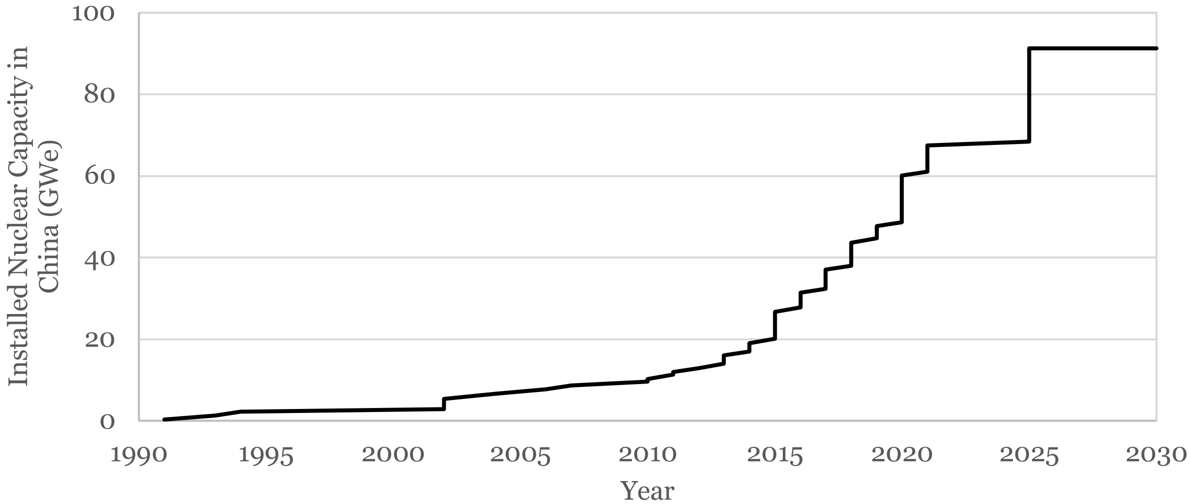

Source: World Nuclear Association [4]

Figure 3-2 Nuclear capacity expansion in China until 2030. For nuclear reactors whose starting year is not known yet but that are planned to be built before 2030, first grid connection is assumed to be 2025.

The nominal water production capacity of each reactor technology per unit of time, W_y, is calculated using:

$$\boldsymbol{W_y} = \frac{P_{th} \times (1-\eta)}{L} \times GOR \times (1-M) \times CF_{nuclear} \times CF_{desalination} \qquad 3\text{-}1$$

Where P_{th} is the thermal power specific to the nuclear reactor technology considered, η is the thermal efficiency. Although thermal efficiency varies across nuclear reactor technologies, they remain in the 30%-40% range for conventional pressurizes water reactors considered in this study. L (*2334 kJ/kg* [251]) is the latent heat of vaporization of water at 70ºC, GOR is the gain output ratio (assumed to be *15* for MED [245]). M (*15%* [250]) is the percentage of maximum heat available that is used as electricity reserve margin, therefore not used for desalination purposes. A nine percent forced outage rate is assumed for both desalination and nuclear plants—$CF_{desalination}$ and $CF_{nuclear}$ —assuming that scheduled outage for maintenance will be performed along with scheduled outages of nuclear reactors.

The number of reactors and maximum total desalinated water production, classified by reactor technology, is provided in Table 3-2. Water production capacity from the 69 MED desalination plants, to be built near the 19 nuclear sites, adds up to 20.7 billion m^3 per year.

Table 3-2 Characteristics, including maximum desalinated water production capacity, of the fleet of nuclear reactors suitable to desalination in 2030.

Nuclear reactor technology	Number of reactors suitable for desalination in 2030	Maximum annual water production (billion m^3/y)
ACPR1000	6	2.0
AP1000	18	5.7
CAP1400	2	0.7
CNP-600	2	0.4
CPR-1000	22	6.2
EPR	4	1.6
Hualong One	13	3.5
VVER-1000	2	0.6
Total	*69*	*20.7*

Source : Calculations based on ARIS database, International Atomic Energy Agency [2]. It is probable that some of the planned AP1000 reactors will in fact be Hualong One. In this case, the total maximum water production could decrease by up to 3.5%, to reach 19.98 billion m^3.

The change in temperature of a nuclear reactor's secondary loop induced by the desalination process—i.e. the extraction of energy from steam—leads to a reduction in the reactor power output. The resulting loss in electricity generation per unit of time is calculated as follows:

$$\boldsymbol{E_{reduc-y}} = \frac{W_y \times L}{GOR} \times \left(1 - \frac{T_c}{T_{cm}}\right) \times \eta_{is} \times \eta_{turbine} \times \eta_{generator} \qquad 3\text{-}2$$

where T_c (*40°C*) is the average condensing temperature, or lowest available temperature point and T_{cm} (*75°C*) is the modified condensing temperature of the dual-purpose power-water plant. η_{is} (*85%*) is the isentropic efficiency of the low pressure turbine, $\eta_{turbine}$ (*98.8%*) is the mechanical efficiency of the turbine, $\eta_{generator}$ (*97%*) is the generator efficiency. Data come from the DEEP model [251] and are considered typical values across desalination systems.

Over the entire nuclear fleet, the reduction in power production induced by desalination is 8.2 GW, assuming round-the-clock operating modes for both nuclear reactors and desalination plants.

3.2.1.4 Economics of Nuclear Desalination in China in 2030

Calculations of nuclear desalination economics are based on the DEEP model [251]. Values of exogenous parameters are given in the same units as provided in the initial data source. To avoid overloading formula and to ensure their clarity, unit conversions of spatiotemporal values are not made explicit.

Capital and production costs of desalination plants:

The capital cost of a desalination plant is calculated as follows:

$$\boldsymbol{I_{desal} = SC_{base} \times W_y \times (F_{ow} + F_{contin} + F_{adj}) \times (1 + I)^{LT}} \tag{3-3}$$

Where SC_{base} is the addition of specific base cost for in and outfall systems (*\$77*/m³/*day* [251]) and plant base unit cost (*\$900*/m³/*day* [234], [239], [252]). F_{ow} (*1* [251]), F_{contin} (*0.05* [251]) and F_{adj} (*0.105* [251]) are the water plant's adjusted base cost factor, owner's cost factor and contingency cost factor, respectively. LT (*12 months* [251]) is the lead-time of the desalination plants. The choice of the discount rate I depends on the context of the study. A prescriptive approach, also known as social perspective, which is what the analysis aims at, usually uses lower discount rate than a descriptive or "decision-maker's" perspective [253]. Here, discount rate I is *4%* [254].

The total capital cost of the 69 desalination plants is \$66 billion. This corresponds to a net fixed charge per year, FC_y, of \$4.3 billion over the 25-year lifetime [249] of the water plants.

The resulting cost per unit of time of the construction and operation of a desalination plant over its 25-year lifetime is the sum of its annual fixed charges and annual variable charges:

$$\boldsymbol{FC_y = IC \times CRF_{desal}} \tag{3-4}$$

where CRF_{desal} is the capital recovery factor for the water plant with a 4% discount rate.

Total O&M costs, including human resources and equipment, represent \$7.7 billion per year:

$$\boldsymbol{OMC_y = (S_{lab} \times P_{lab} + S_{man} \times P_{man}) \times W_y + \left(SC_{OM-spare} + SC_{replace} + SC_{OM-pre} + SC_{OM-post}\right) \times W_y} \tag{3-5}$$

where S_{lab} (*\$23,190/year* [255]) and S_{man} (*\$43,481/year* [255]) are the annual salary of production engineers and product manager, respectively. P_{lab} and P_{man} are the labor personnel and management personnel, respectively (calculation based on data from the Carlsbad desalination facility [256] in the United States and the Victorian desalination plant [257] in Australia, and assuming that the shares of labor and management personnel are 80% and 20%, respectively). $SC_{OM-spare}$ (*\$0.03*/m³ [251]), $SC_{replace}$ (*\$0.01*/m³ [251]), SC_{OM-pre} (*\$0.03*/m³ [251]) and $SC_{OM-post}$ (*\$0.02*/m³ [251]) are the specific O&M spare parts cost, tubing replacement cost, specific O&M chemicals cost for pre-treatment, and specific O&M chemicals cost for post-treatment, respectively.

The resulting cost per unit of time of the construction and operation of a desalination plant over its lifetime is the sum of its fixed and variable charges:

$$\boldsymbol{C_y = FC_y + OMC_y} \tag{3-6}$$

For the 69 desalination plants, C_y adds up to $12 billion/year.

The additional opportunity cost resulting from the reduction in electricity sales from the nuclear plants, due to lost shaft work from steam extraction and water desalination plant electricity use, must be added to the total. Here, we make the conservative assumption that the totality of the electricity loss induced by desalination would have otherwise be sold.

Total electricity costs, adding up to $0.4 billion per year in this study, are calculated as follows:

$$\boldsymbol{EC_y = (E_{sale} - E_{transm}) \times (W_y \times SE_{use} + E_{reduc-y})} \tag{3-7}$$

Where E_{sale} is the average electricity sale price in China (*$0.085*/kWh [258]–[260]), E_{transm} is the average electricity transmission cost (*$0.010*/kWh [261]), and SE_{use} (*2.02kWh*/m^3 [251]) is the specific electrical power use of the MED technology considered in this study.

Finally, the following formula is used to calculate the production cost of one cubic meter of desalinated water:

$$\boldsymbol{SC_{desal} = \frac{C_y + EC_y}{W_y}} \tag{3-8}$$

The resulting specific water production cost from nuclear desalination is $0.72/m^3. This cost is divided as follows: 29% ($0.21/m^3) of fixed charge, 14% ($0.10/m^3) of O&M costs, and 58% ($0.41/m^3) resulting from electricity generation loss following steam extraction and desalination ancillary services.

Economics of water transportation from desalination plants to demand centers:

The cost of transporting water from production plants to demand centers depends on the quantitative and geographical distribution of water needs, more specifically on three parameters: transport length, altitude difference and water flow per unit of time. Applying the law of conservation of energy, and making the assumption that velocity stays constant as water flows along the pipe (assuming constant area piping), the pumping energy to transport water on a given path is computable.

The average electric power cost per unit of time of transporting Wy of water in a pipeline is:

$$\boldsymbol{EC_{transp-y} = (E_{flat} \times l + E_{lift} \times h) \times \eta_{pump} \times W_y \times E_{sale} \times (1 + \frac{L}{2})} \tag{3-9}$$

Where E_{flat} (*0.018kJ*/m^3/*m* [262]) is the energy required by a pump to transport one cubic meter of water over 1 meter on a flat path, E_{lift} (*13.986kJ* m^3/*m* [262]) is the energy required by a pump to lift one cubic meter of water one meter. l is the pipeline length and h the pipeline total elevation, varying with the path considered (starting point: desalination plant; ending point: demand center). η_{pump} (89% including energy recovery device [263]) is the efficiency of the seawater pump. L (30% [264]) is the percentage of water lost through leakage.

The corresponding fixed charge cost per unit of time is calculated by:

$$\boldsymbol{FP_{transp-y} = l \times SC_{pipe} \times D \times N \times (1 + I)^{LT_p} \times CRF_{pipe}} \quad \text{3-10}$$

With $\boldsymbol{D = 2 \times \sqrt{\frac{W_y}{\pi \times FS}}}$ 3-11

and $\boldsymbol{N = \lfloor \frac{D}{D_{max}} \rfloor}$ 3-12

D is the economically-optimized diameter of the pipelines, and N is the number of pipelines needed to transport water to the considered province from the closest desalination site.

SC_{pipe} (*\$160/m* [243]) is the cost of building one meter of a one-meter diameter pipeline. FS (*1m/s* [265]) is the average water speed. LT_p (*48 months*) is the pipeline construction lead time. CRF_{pipe} is the capital recovery factor for the pipeline with a discount rate of 8% and the pipeline's lifetime—set at 25 years, equal to the desalination plant lifetime plants, although in reality pipeline lifetime ranges between 30-100 years [266], [267]. D_{max} (*150 inches* [268], [269]) is the average maximum diameter of water transmission mains designed by manufacturing companies.

O&M cost per unit of time:

$$\boldsymbol{OM_{transp-y} = FP_{transp-y} \times F_{OMp}} \quad \text{3-13}$$

where F_{OMp} (0.07 [251]) is the O&M cost factor for pipelines.

Water transport specific cost (\$/m^3):

$$\boldsymbol{SC_{transp} = \frac{FY_{transp-y} + OM_{transp-y} + EC_{transp-y}}{W_y}} \quad \text{3-14}$$

For l and h fixed—i.e. for a given desalination plant and demand center—SC_{transp} varies inversely with the square root of plant-level water production. As a consequence, the larger the desalination capacity per plant, the lower the specific water transportation cost.

3.2.2 Results

3.2.2.1 Relevance of Nuclear Desalination in 2030

Identification of a metric:

The average inflation rate in China over the past ten years equals 2.83% [270]. Logic suggests that desalination costs be compared with water prices to assess the affordability of nuclear desalination by

2030. However, state control of water prices prevent them from being determined by the market in China, leading to artificially low values and utilities not being able to recover their costs [271], [272]. In line with the nationwide economic transformation, market reforms have been implemented for water, increasing prices beyond the sole effect of inflation [273]. For example, urban water prices experienced a 50-fold increase between 1991 and 2014 in Beijing, as a result of tariff increase, as well as the implementation of resource and water treatment fees [274], while the inflation raised prices by only a factor of two. During the year 2005 alone, water price increased by 20% [275]. Since government contributions are still too low to fill the gap between the true cost of service and the revenue from users [276], the current unsustainable situation suggests that additional reforms will be enforced in the near future, making the water price landscape even less predictable. Because of the preponderance of political reforms over market laws to set water prices in China, it is almost impossible to forecast 2030 water tariffs [271].

High uncertainty on future water prices and unpredictable governmental reforms suggest that nuclear desalination be evaluated on the basis of its relative cost and benefits to population. The "five-percent rule" [277] advocates that water purchase must be equal to or lower than five percent of households' income in order to be affordable. Here, we evaluate the affordability of fresh water from nuclear desalination for households with minimum monthly wages, including both production and supply costs, according to the five-percent rule. This metric is more stable than 2030 water tariff projections as historical wage changes in China have shown to be more correlated to overall economic context than historical water price changes.

Using data for renewable water resources per capita at the provincial level from China Water Risk [244] and natural growth rate per province from China Statistical Yearbook [278], we calculate that, in 2030, eleven provinces—Beijing, Tianjin, Shanghai, Shandong, Hebei, Jiangsu, Henan, Anhui, Shanxi, Gansu, and Ningxia—will have less than 500 m^3 of renewable water resources per capita per annum, which is the threshold for absolute scarcity [279], [280].

Below, we evaluate the quantity of water that can be produced and supplied from nuclear desalination plants to the capital cities of the eleven water-scarce provinces identified above while meeting the five-percent rule in 2030. The calculation method is detailed in the case of Beijing below; same formulas and contextualized parameters are used for other cities.

Desalinated water supply quantity within the five-percent rule threshold:

The minimum monthly wage in Beijing in 2013 was $275 [281], that is $3,302 per year. Wages in China are expected to be multiplied by 2 between 2013 and 2030 [282]. Therefore, according to the five-percent rule, supply of fresh water from desalination plants to Beijing in 2030 will be affordable if the production and supply costs to Beijing is below $165 per person per year.

The cost of water production and supply from Chinese desalination plants to Beijing in 2030 (Figure 3-3) depends on the quantity supplied per person per day and the location and costs of the specific desalination plants to supply the city.

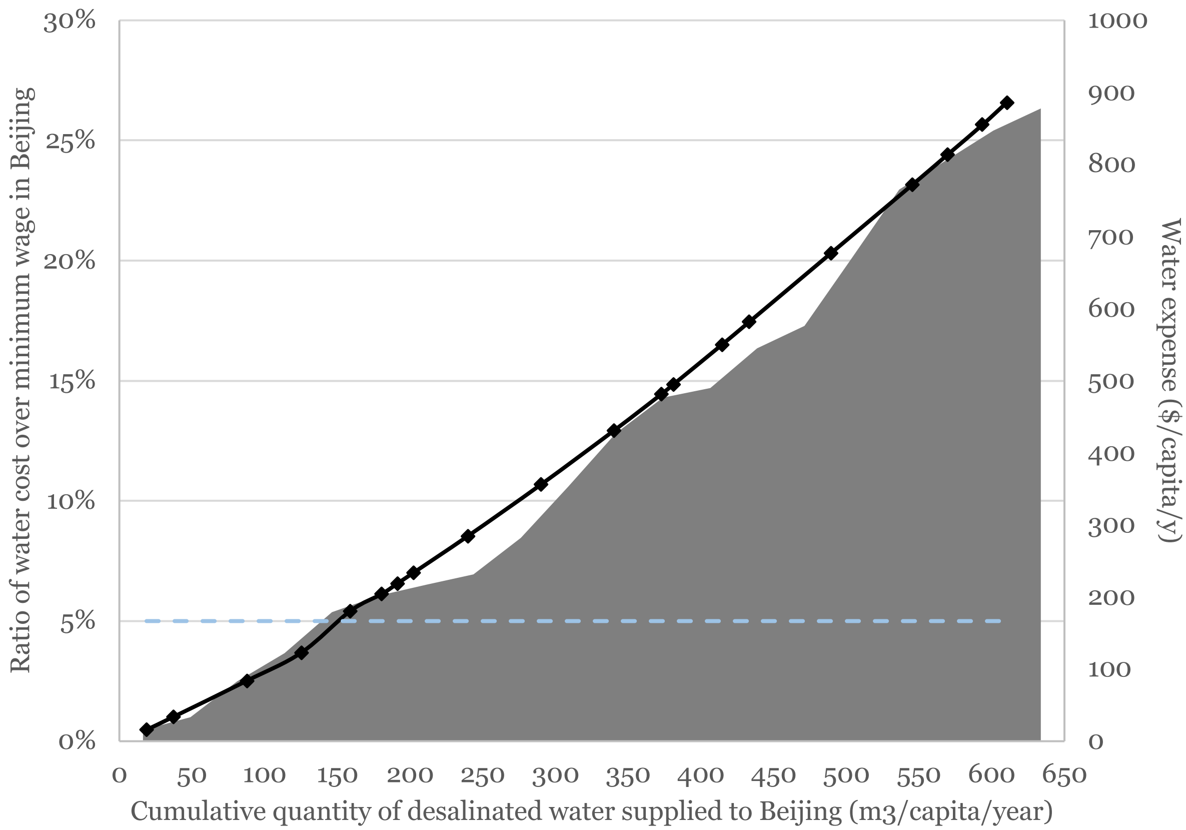

Figure 3-3 Desalinated water supply cost in 2030 as a function of the quantity of water supplied per person per year in Beijing (model results). The blue dashed line indicates the threshold for the five-percent rule. Squared black markers represent quantities of water for which the capacity of an additional water plant is required (small quantities are supplied by nearby plants and cost increases as production from additional plants, farther from demand centers, is needed).

The maximum quantity of water that can be supplied from desalination plants to Beijing's 33.6 million inhabitants, for a cost lower than or equal to five percent of minimum wage, is 159 m^3 per capita per year. According to data from China Water Risk, renewable water resources in Beijing in 2030 will be 79 m^3 per capita per year. Nuclear desalination therefore offers the possibility to double the projected renewable water resources at affordable costs. The closest plant to Beijing is Haixing, 230 kilometers from Beijing, and the furthest plant that still meets the five-percent rule is Tianwan, 670 kilometers from the capital.

The same cost-supply simulation was performed on the capitals of the ten other water-scarce provinces; results are presented in Figure 3-4.

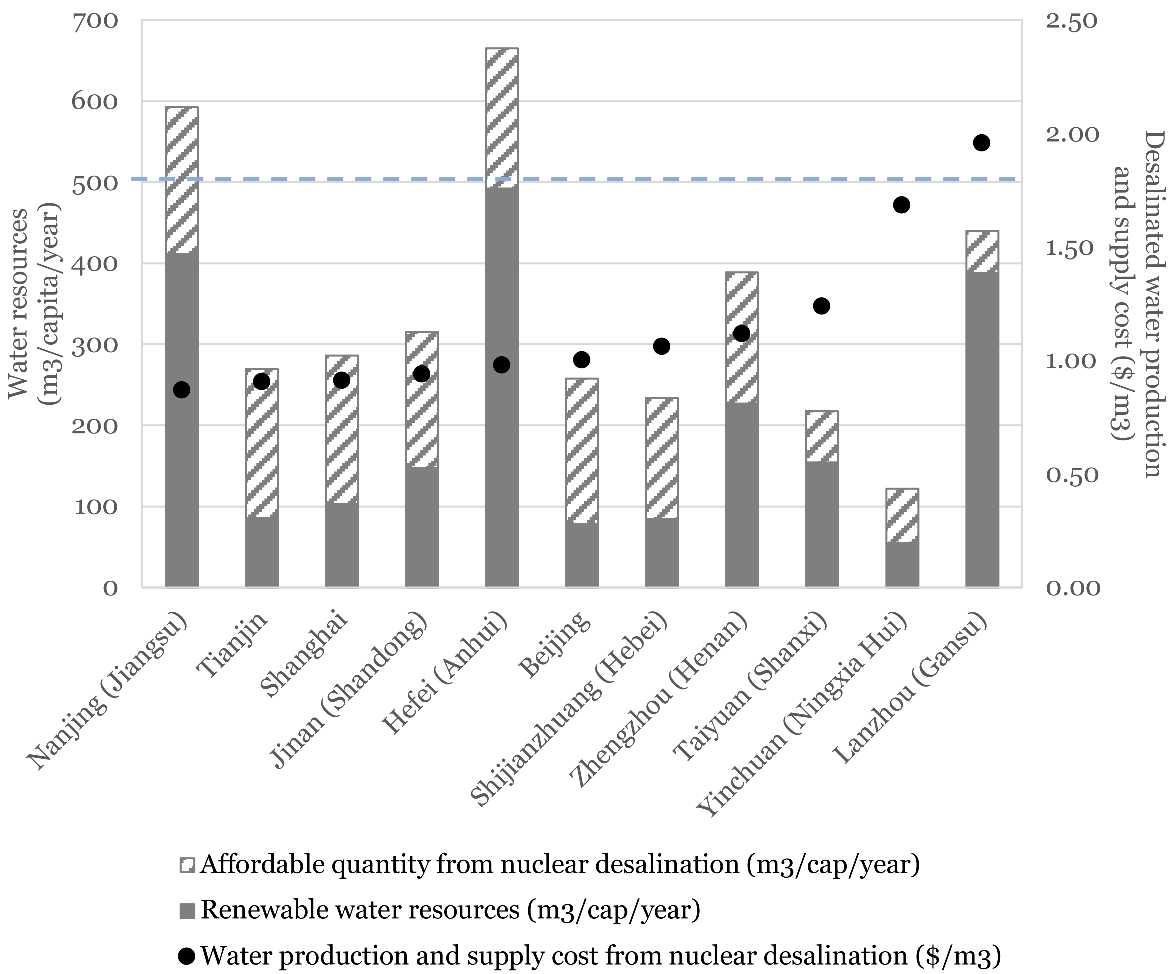

Figure 3-4 Annual renewable water resources (current: gray bars; model results for desalination: dashed bars) as well as total cost (production and transportation) from modeled nuclear desalination plants to the capitals of the eleven water-scarce provinces in 2030. The dashed blue line represents the threshold for absolute water scarcity.

Calculations show that, while water production costs remain around $0.72/m^3$ across the country, supply costs vary significantly across regions, between $0.87/m^3$ and $1.96/m^3$. In cities located relatively near to the coast such as Nanjing, Tianjin, Shanghai, Jinan, Hefei, Beijing and Shijiazhuang, this cost is equal to or below $1/m^3$. It significantly increases for inland cities such as Yinchuan and Lanzhou, which consequently limits the maximum quantity of affordable water that can be supplied according to the five-percent rule. However, in cities such as Shijiazhuang, Hebei province, and Yinchuan, Ningxia region, where water resources are projected to be extremely limited in 2030, supplying fresh water from desalination plants enables to multiply the total amount of water resources by a factor of 2.76 and 2.22, respectively. On the contrary, despite its low supply cost in Nanjing, affordable desalinated water can only multiply the total quantity of projected water resources by a factor of 1.44. While nuclear desalination can significantly increase resources in water-scarce provinces, limiting supply to quantities meeting five-percent rule does not enable provinces to reach the absolute scarcity threshold, except in Jiangsu and Anhui. Moreover, since the total nuclear desalination capacity is limited to current plans for 2030, there exists a trade-off in water supply allocation between those eleven places.

Results from the five-percent rule also show that water tariffs by 2030 in all water-scarce capitals could be increased well above inflation's sole effect without jeopardizing households' ability to pay for fresh water. In case of pure water needs - for special industries for example - water production cost in 2013 will be around $5/m^3 due to treatment. Because MED purifies water to such standard, nuclear desalination costs are already below water market price in China [243].

3.2.2.2 Comparison Between Nuclear Desalination and Two Other Approaches with Similar Objectives: Coal Desalination and SNWTP

As of 2018, although China General Nuclear Power has commissioned a small 10,080 m^3/day desalination plant and China Nuclear Engineering & Construction Group has signed a cooperation agreement for "developing desalination projects using high-temperature gas-cooled nuclear reactors" [283], there is no desalination plant thermally coupled with nuclear reactors in China. To address its water shortage, the country has invested in two main initiatives, in addition to improving water use efficiency: the SNWTP, and water desalination using energy from coal-fired plants. Beijiang's desalination and power plant in Tianjin, with state-of-the-art MED and coal-fired technologies, is the most advanced and largest plant of its kind in China, with a water production capacity aiming to reach 400,000 m^3/day [284].

In this section, CO_2 emissions and water production specific costs are calculated for nuclear desalination, SNWTP, and coal thermal desalination. In order to enable meaningful comparison, we make three additional hypotheses. First, water production capacity from coal desalination is assumed to be the same as production capacity from nuclear desalination (20.7 billion m^3/year). Second, the operation of the currently planned Western route of the SNWTP is not included in calculations because no accurate cost estimates are available and no commitment has been made with regards to its construction[4]. As a consequence, the annual quantity of water diverted through the SNWTP, W_{SNWTP}, is 25 billion m^3 [219]. Third, coal plants powering desalination are assumed to use state-of-the-art technology, reflecting the characteristics of Beijiang's ultra-supercritical coal-fired plant, with a thermal efficiency of 46% and a carbon intensity of 700 g/kWh.

The specific water production cost of the SNWTP is $0.51/m^3, calculated as follows:

$$\boldsymbol{SC_{SNWTP}} = \frac{I_{SNWTP} \times CRF_{SNWTP} + OM_{SNWTP-y} + SP_{SNWTP-use} \times E_{csale}}{W_{SNWTP}} \qquad 3\text{-}15$$

[4] First official economic evaluation for the Western route shows that costs will likely be higher than for the two other routes as this route transfers water from far-West remote locations.

Where I_{SNWTP} (*$81 billion* [285]) is the capital cost of the Eastern and Central routes of the SNWTP. CRF_{SNWTP} is the capital recovery factor using a discount rate of 4% and assuming that the SNWTP lifetime is 50 years—twice the lifetime of a desalination plant. $SP_{SNWTP\text{-}use}$—which includes electricity used for pumping (0.11 kWh/m^3, calculation based on [286]–[288]) and water treatment (1.15 kWh/m^3 [289])—is the specific power consumption per cubic meter of water transferred.

The water diversion project is less energy intensive per cubic meter supplied than desalination. Coal and nuclear desalination use 2 kWh/m^3 with an additional 2 kWh/m^3 for water transportation on average, and negatively impact power plant output by 4 kWh per m^3 produced, while the SNWTP uses only 1.16 kWh/m^3 for water supply and treatment.

However, construction of the SNWTP requires 15 million m^3 of cement and 0.7 million tons of steel [32], while the construction of the 69 desalination plants, powered by coal or nuclear, would require 0.3 million m^3 of cement and 0.02 million tons of steel [290].

Carbon dioxide emissions from construction and operation in the three alternative cases, over their respective lifetimes, add up to 3 million tons per year for nuclear desalination, 18 million tons per year for the SNWTP, and 182 million per year for coal desalination. Data for carbon intensity for power plants come from the IPCC [291] and carbon intensity projection for China's 2030 power grid from [142].

As mentioned in the previous chapter, China's national emission trading scheme, announced by President Xi in September 2015, started in December 2017 [176]. While national carbon price ranges are not known yet, some sources have mentioned expected prices between $33 and $45 per ton of CO_2 [178], [176]. The country had previously implemented cap-and-trade pilot projects with prices between $3 and $12 per ton of CO_2 [292], [293]. Water production and supply costs of the three alternatives are shown in Figure 3-5 for three different hypothetical carbon prices.

Water production and supply costs from the SNWTP range from $0.51/m^3 when no carbon price is implemented to $0.58/m^3 when one ton of carbon costs $100/m^3. This is not a significant variation, unlike coal desalination, whose costs varies between $1.62/m^3 and $2.50/m^3 across the same carbon price range. The price of carbon has no significant impact on the cost of nuclear desalination, which stays around $1.62/m^3.

The SNWTP therefore has lower energy requirements but larger carbon emissions than nuclear desalination, however a carbon price does not challenge its economic attractiveness compared to nuclear and coal desalination.

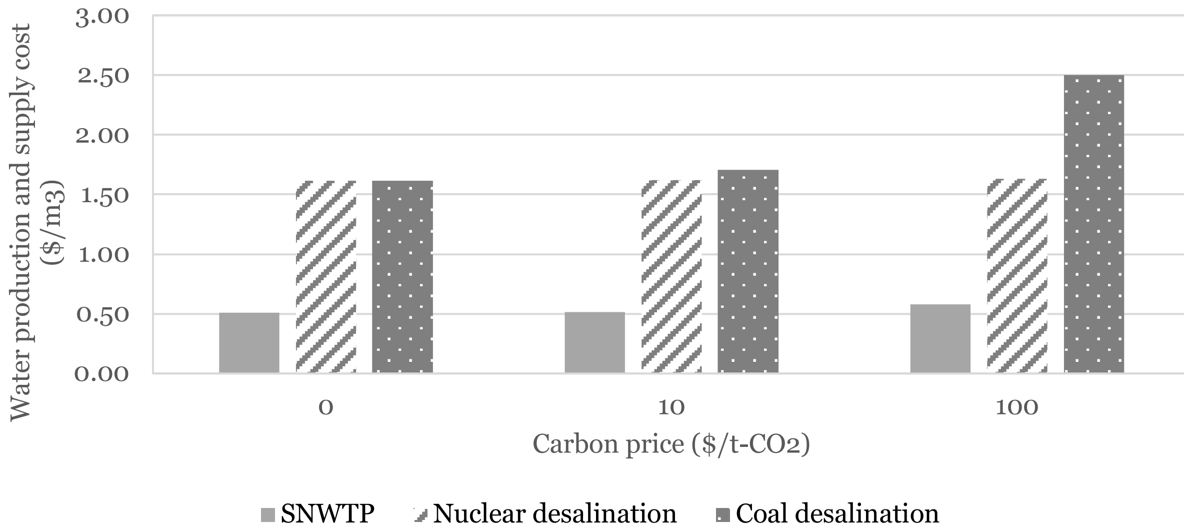

Figure 3-5 Average specific desalinated water cost—including production and supply—for the SNWTP, nuclear desalination, and coal desalination in 2030, as a function of hypothetical carbon prices (model results).

The SNWTP presents several other challenges that are not quantified in this analysis. In its current version, it is not able to supply several water-scarce places, including Taiyuan (Shanxi) and Yinchuan (Ningxia), accounting in total for more than 19 million people who will experience water scarcity by 2030. As a seasonal supply mean, water availability of the SNWTP will also be substantially reduced during some periods of the year. Water quality is high enough in the three water supply alternatives to be considered as potable and therefore meet domestic needs but, in the case of SNWTP, it is not pure enough to meet the needs of special industries. Therefore, in the latter case, a cost to purify water must be added to meet higher-quality water needs.

Beyond air pollution from coal burning, the social and environmental impacts of nuclear and coal desalination mostly lie in their potential effects on coastal marine life. SNWTP, on the other hand, will have a substantial impact on fluvial life, but the high social consequences of this project reside in the resettlement of 300,000 people [33], and the potential drying-out of South China, which has already endured searing droughts in 2000, 2007 and 2009 [34] that could be accentuated because of water transfer toward Northern provinces.

3.2.3 Conclusion

Through the use of an interdisciplinary framework, the affordability of nuclear desalination in China by 2030 to significantly increase projected water resources is confirmed through the use of a proxy: the capitals of China's eleven most-scarce provinces. The SNWTP has lower costs than nuclear desalination, however its implementation is significantly more challenging than nuclear desalination from environmental—including CO_2 emissions—and social perspectives. While calculations show that coal desalination should not be part of the solution to China's water shortages, as it is economically unattractive and not consistent with the country's commitments towards sustainability, water diversion projects can play an important role, yet different from the one currently planned by the central government. Rather than providing water to coastal cities, the SNWTP, rooted in river springs in the middle of the country, could instead be dedicated to supplying remote provinces like Ningxia and Gansu, which are too far from the coast to receive significant amounts of affordable fresh water from desalination plants.

In the longer term, desalination could be performed using high-temperature nuclear reactors like the HTR-PM (High Temperature Reactor Pebble bed Module), whose efficiency will be higher than conventional reactors. The use of nuclear heating reactors like the NHR-200 (200-MWt Nuclear Heating Reactor) could enable more performant desalination production at lower costs than dual-purpose reactors. On the other hand, the costs induced by building an advanced reactor technology and adapt its fuel cycle consequently may be higher than well-known PWR technologies that will still compose most of the Chinese nuclear fleet in 2030, at least in the short term. Finally, desalination through wind and solar energies, although at its early days, may be significantly deployed in the next years, as explored in the second part of this chapter.

International working groups such as the Global Water Desalination Alliance [294] launched in Paris during the COP21 should be pushed further in order to favor the pooling of technical knowledge and efficient use of available funds. Several countries, including China, India, the Republic of Korea and Pakistan, demonstrate both a lack of water and the ability to use nuclear power [295], and represent potential long-term markets for nuclear desalination. To achieve this, the public must be informed and investors must be convinced. This requires the systematic and publicly-available evaluation of assets and drawbacks presented by nuclear desalination and other types of energy, as well as geoengineering diversion projects—including risk assessment and cautious cost evaluation of each option in each country's particular context—as presented in this study.

3.3 From Power Generation to Value Creation: De-Risking Clean Energy Investment via the Untapped Power-Water Coordination Opportunity in the North China Grid

As detailed in Chapter 1, the share of clean energy systems in electricity mixes across the globe has increased as a result of countries' environmental commitments and improvements in systems manufacturing and installation costs. While baseload operation is favored in the case of nuclear reactors, mainly for economics and reliability reasons, intermittent wind and solar energy penetration challenges traditional practices to operate the electric grid by increasing the temporal and geographic mismatch between electricity supply and demand. In times when VRE supply is lower than demand, flexibility options such as thermal backup plants and inter-regional transmission lines have proved to be effective alternative supply means to ensure the operational viability of the grid, as illustrated by Germany and Denmark [296], [297]. On the other hand, times when power supply exceeds demand result almost inevitably in electricity curtailment in the absence of scalable storage or DR mechanisms. As a result, curtailed electricity and under-utilized thermal plants reduce the total value generated by the power system and have, in recent years, discouraged several investments in new VRE systems. As a consequence, despite continuously decreasing system costs, the main challenge of VRE deployment today remains, indirectly, its economics.

In China, this challenge is exacerbated by the fact that renewable energy resources are of highest quality in remote inland regions while major demand centers are located in coastal areas. As a consequence, China exhibits the world's worst curtailment level: 17% of wind and 10% of solar generated electricity were curtailed in 2016, representing a total of 56.2 TWh [76], further exacerbated by an oversupply in coal power. Around half of the country's total curtailment happens in Northwestern China [77]. Increasing VRE penetration in China has led to transmission line congestion. In Inner Mongolia, which hosts 26 GW of wind power capacity [298] and 6 GW of solar power capacity [299], 14% of wind power was curtailed in the third quarter of 2017 [300]. More importantly, this situation has created a climate of distrust among VRE system owners and investors, who have experienced annual lost earnings estimated between $4.2 billion and $4.95 billion [77], [78]. This revenue loss significantly reduces return-on-investment to the point where it makes VRE investment unattractive. Not only has this situation created financial risks for investors, but it has impacted the country's political ambitions regarding clean energy. China's NEA has slowed down wind development in six of the country's provinces with highest wind potential [79], [69]. As a consequence, newly installed wind power capacity in China has decreased between 2016 and 2017 [80].

The current initiative undertaken by the Chinese government to solve this situation is the construction of an interregional transmission network, the WEETP, with the long-term objective to build a national power grid. From a governance standpoint, the establishment of a national operator to supervise the WEETP is not consistent with the central government's successive reforms to break down monopolies and decentralize the resource management corporate sector [83]. The WEETP, prone to logistical and policy challenges [83], aims to decrease high curtailment levels by decongesting transmission lines between regions with large installed VRE capacity and power demand centers, especially via its Northern corridor [84]. Assuming that VRE and transmission deployment targets of the 13th FYP will be met, and provided that all VRE-generated power can be used thanks to new transmission lines, VRE's maximum share in the country's power generation will be 15% in 2020 [82]. Fossil-based generation capacity, mainly coal, will remain dominant. Much larger VRE penetration will still be needed to achieve true decarbonization. The difference is striking between the scale of VRE generation at which grid operation is currently challenged—173 GW of installed capacity for less than 5% of total electricity generation [82], [76]—, and the needed scale of VRE generation in order to reach deep decarbonization by 2050, in line with the 2°C target—5,500 GW of installed capacity, representing around 50% of total electricity generation, as presented in Chapter 2. China's VRE grid integration challenge does not only result from limited transmission capacity, but from limited flexibility of the power system [77].

The WEETP and the SNWTP both rely on large-scale connectivity and central coordination, requiring large investment, with increasing dependency between regions but no guarantee of success. In addition, they both become unsustainable at the limit: while trying to solve power overcapacity, the

WEETP does not decrease total power capacity at the national level; while trying to solve fresh water undersupply, the SNWTP does not increase total water supply at the national level.

In addition, a solution deemed optimal at the national scale might demonstrate net negative benefits at the subnational scale. For example, it has been shown that the unification of electricity dispatch zones creates lower prices but also lowers demand for generators in net-importing zones, while net-exporting zones experience increased utilization hours but higher prices [87]. The resistance from Liaoning, Jilin, and Heilongjiang provincial governments to the 2003-2006 pilot electricity market experiment, which aimed to develop inter-provincial electricity flows to increase overall efficiency [87], illustrates this situation and the gap between national and provincial interests. After this pilot project failure, no more attempt to institutionalize regional electricity markets in China was made for a decade. In fact, the imbalance between centralized public policy design and decentralized policy implementation in China has even been regarded as creating additional pollution issues [86]. While provincial power dispatch is inefficient because it does not encourage synergies between diverse resources across regions [56], for example wind energy in Inner Mongolia and hydropower in Yunnan, the ambition of creating a national power dispatch system without profoundly reforming central-local government relations remains utopian [87]. This context suggests that optimal resource management planning be performed at a decentralized medium-scale, large enough to take advantage of interregional resource diversity, but small enough to account for local governance and dynamics. An example of such medium scale is the size of each of China's six regional power grids.

Looping back to the beginning of this section, the challenge behind power curtailment is not the release of resources per se since this power is produced by zero-carbon VREs and has no direct cost. It is rather the lost opportunity of value creation. On the one hand, since scarcity is a fundamental component of the derivation of price [301], abundant seawater and abundant power generation during off-peak hours are generally considered products of low or even negative value if the costs of power generation are factored in. On the other hand, the combination of these two low-value products—the use of electricity generated in excess from VREs to power desalination plants— produces fresh water, which is scarce in many regions of China and the world and, as a consequence, is of higher value. Unlike energy storage, water storage is not technically challenging and has, in fact, been performed for centuries. In this section, we explore the potential for regional grid-level planning and operation of power and fresh water supply systems as an alternative to national-scale WEETP and SNWTP. Using the North China Grid (NCG) as a case study, this study presents a methodology to evaluate whether, and at what conditions, the use of desalination as a deferrable load can enable NCG to reliably and cost-efficiently operate as an independent grid, self-reliant in power and fresh water supply.

While the literature is extensive on the use of renewable energy coupled with storage to power water treatment, the analysis of water treatment as a deferrable load to accommodate VRE fluctuations without energy storage has been less explored. Using daily data for renewable energy generation and power demand, Al-Nory et al. [302] derived an operation strategy to use excess renewable energy supply to desalinate and store water and found, in the case of Saudi Arabia, a 12% cost reduction caused by the system ability to produce excess water. Using hourly data, Tsai et al. [303] simulated and confirmed the operational viability of a system involving reservoir, hydropower, desalination plant and wind power in order to meet power and water demand in a Taiwanese city. Mentis et al. [304] found that, in order to solve water scarcity in three islands of the South Aegean sea, it is cost-efficient to build VRE-powered desalination plants and sell excess power to the main grid. Building on previous operational viability analyses of power-water coordination, the present study adds an evaluation of the additional economic value created. Particularly, it improves on the temporal resolution of [302], the spatial scope of [303] and the system scope of [304] in order to grasp the full potential and challenges of this inter-sectoral coordination.

3.3.1 Concept, Applicability and Methodology

3.3.1.1 Concepts

Wind and solar are virtually infinite sources of clean energy: their installed capacity can be scaled up to meet larger needs without the risk of resource depletion. However, their power availability is limited: in the absence of scalable storage systems or DR programs, large over-generation of power makes investment in VREs a risky bargain. Seawater resources are virtually infinite too. However, transforming seawater into fresh water is an energy-intensive process that can also be polluting when powered with electricity from fossil fuel-dominated grids. Unlike VREs, variable fresh water supply is not challenging since water storage is a common practice and has been performed for centuries. Since seawater can be retrieved at any time, extra VRE power can be used as soon as it is generated in order to power a desalination fleet and store fresh water until it is needed for consumption. While the value created by power curtailment is zero, additional value is created by the opportunity to supply fresh water when needed. Figure 3-6 visually explains such synergies between VREs and seawater treatment, and the resulting coordination, or nexus, opportunity.

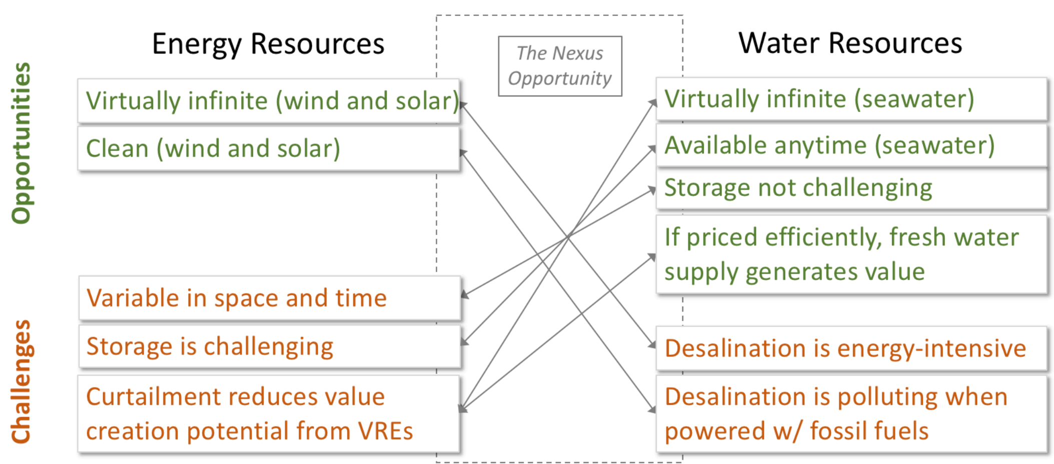

Figure 3-6 Challenges and opportunities of VRE power generation and seawater desalination. Inter-resource synergies offer potential for value creation.

3.3.1.2 Literature Review

As seawater salinity is typically five to six times larger than wastewater salinity, desalination is more energy-intensive than wastewater treatment. However, wastewater treatment has its own challenges, including endocrine disruption chemicals from hormones, painkillers and other drugs that can have considerable impacts on the wildlife [305] and on the quality of produced fresh water [306]. These elements are also present in seawater, but at much lower concentrations. In addition, environmental and safety constraints arise from the disposal of excess sludge from treatment plants that are located near urban areas. While also embedding negative impacts for the environment, post-desalination sludge disposal in the ocean has proved to be less challenging in practice. In addition, given the particular focus of this study on excess power, energy intensity is no longer a major selection criterion. Therefore, in the absence of perfect options and strict energy constraints, our analysis focuses on desalination. However, the water-power coordination concept is also applicable to wastewater treatment.

While novel seawater treatment technologies under development, such as forward osmosis, might present more advantages under variable power supply, the objective of this study is to evaluate the viability of operating desalination with excess power supply under proven technologies. A range of techniques for seawater desalination have proved their large-scale commercial feasibility under constant power supply, including thermal and membrane-based approaches. RO is the most widely used technology for desalination [307], and it is generally cheaper and more environmentally friendly than thermal approaches, even when those are powered with renewable energies [308].

RO has traditionally been used as a mean to desalinate water under steady-state conditions, including constant flow rate and pressure, with a constant power supply. As a consequence, many studies addressing off-grid desalination plants relying on VREs as their sole source of electricity supply include the use of batteries or other types of energy storage in order to artificially recreate constant power supply [308][309]. However, several studies, presented below, have explored the possibility to directly operate desalination plants with intermittent power supply, without the use of energy storage systems. The related literature, quite limited, can be divided into two categories: mathematical model/computer simulations and prototype testing.

Recognizing that capital and maintenance costs of batteries for RO systems can make them unattractive, Kumarasamy et al. [310] modeled operating strategies for two battery-less RO systems powered by solar energy: with and without a product buffer tank. While both configurations were found viable, results showed that permeate production was 28% higher with a buffer tank, since the tank acted as a surrogate energy storage device, storing energy during high power availability as lower concentration permeate. Through the use of an operational window as control strategy, Miranda et al. simulated the operation of a wind-powered RO system with no energy storage. The authors found that the system remained performant under wind fluctuations, with relatively low SEC, around 3.4 kWh/m^3 [311]—see Table 3-1 for a comparison with SEC values for thermal desalination processes.

Thomson et al. designed, simulated with Matlab-Simulink [312], then tested in a laboratory [313] a battery-less PV-powered seawater RO system coupled with a Clark pump for energy recovery. The simulation, performed over one entire year, predicted good quality of water, except after consecutive cloudy days where the resulting permeate salinity exceeded the guideline limit. It was noted by the authors that, given the specific design and assumptions, the system offered very little room for supply flexibility while straightforward techniques could be applied to palliate such problem. A similar system was then built and tested in a laboratory with an NaCl solution at 32,800 mg/L—close to seawater salinity—and operated during two cloudy days. The computed and laboratory-tested system components were not identical, leading, in this case, to a slightly higher experimental SEC than predicted. The demonstration showed that the product flow closely followed solar irradiance, the arrival of each cloud causing an immediate reduction or halt in product flow. The SEC remained around 4 kWh/m^3, except when power dropped below 15% of PV system peak rating. The authors found that intermittent power increased permeate salinity, as salt diffusion through the membrane continues during a break in production. While this led to a product tank salinity exceeding acceptable limits, less than 1% of the total volume was responsible for this. Therefore, a diverter valve could be fitted into the product line in order to remove high-salinity permeate while having a negligible impact on total production volume. The overall experience showed that it is possible to maintain excellent system performances under variable and intermittent power supplies by adding energy recovery devices such as Clark pump. It was noted, however, that the addition of components increases overall system complexity and may impact its reliability.

A series of experiments from Park, Richards and their research team, with similar prototype testing objectives, showed that RO systems used for brackish water can be operated within a safe operating window (SOW) with large power fluctuations and intermittency, without noticeable effects on the components or operation of the membrane [314]. The main limitation came from the permeate water salinity, which sometimes exceeded the guideline value at low power levels and, during power interruption, showed a spike upon system restart due to the diffusion of salts across the membrane (explained by the permeate water being drawn back into the membrane by osmotic suck-back [315]). While the initial off-time greatly influenced the concentration increase, as the salt diffused across the membrane, the concentration gradient reduced over time and the change in permeate concentration at longer off-time was not as significant [315]. The stabilization time—the time required for the permeate NaCl to return to its original value after restart—was shown to be proportional to salinity content of the feed water and inversely proportional to available power [314]. This latter observation is explained by the fact that higher power created higher transmembrane pressure (TMP), increasing the flux and reducing the amount of time required to purge the system. On the other hand, higher salinity increased the osmotic pressure of the feed that offset the TMP [315]. The authors therefore highlighted that, in order to reduce the impact of power supply intermittency on average permeate quality, it is more important to provide energy during very-short-term intermittent periods (60 seconds or less) than to smooth out longer periods of power break [315]. In another study, Richards et al. found that, at low power, minimum TMP value to compensate osmotic pressure increased while maximum TMP value to meet the maximum recovery constraint decreased, leading to a smaller area of the SOW [316]. The SOW's area became equal to zero when power decreased below the pump power lower limit. The same research team analyzed the impact on system performance under wind fluctuation and intermittency of adding supercapacitors for energy buffering. By using supercapacitors, the length of time when the permeate exceeded the salinity limit guideline was reduced by 77% [317]. However, it should be noted that the cumulative permeate salinity—the treated water stored in a tank—never exceeded the guideline limit during the 24-hour experiment, as the periods of time when the instantaneous permeate exceeded the salinity limit were limited, unlike Thomson et al. [313]. Therefore, adding supercapacitors did not constitute a hard constraint on producing potable water, but rather helped maintain an excellent system performance with fluctuating power supply. Adding one and three supercapacitor energy buffers increased the cumulative potable water production by 19% and 47%, respectively, while maintaining the SEC close to its steady-state value. The quantity of power available seemed to be a more important indicator of system performance than power variability. While under low solar irradiance, the system showed low flux and high NaCl concentration, including when powered by constant supply, under high irradiance the averaged performance results achieved under fluctuating irradiance were higher than for an equivalent irradiance in steady-state [318]. Higher frequencies led to faster recovery of good performance. Here again, the positive impact of short-term available power, for example through supercapacitors, was demonstrated.

Findings from the extensive research performed by Thomson et al., Park et al., and Richards et al. reveal that variable power supply for RO desalination does not dramatically impact energy consumption or components maintenance, and might even have positive effects on fouling. Its main downside compared to steady-state supply is that, at low power supply or during periods of no power, salt diffuses through the membrane, creating a risk for the permeate salinity to exceed the guideline value. Given the short time-scale—a few seconds—of such phenomenon and the small volume responsible for salinity increase—less than 1%—, solutions exist to overcome this challenge. The solution proposed by Richard et al. is the use of supercapacitors to provide short-term energy buffering without the need for energy storage. The solutions proposed by Thomson et al. is the use of a diverter valve to be fitted into the product line in order to remove high-salinity permeate while having a negligible impact on total production volume, or the use of high-rejection membrane elements that would improve the quality of the product but, at similar costs, at the expense of quantity [319].

The relative change in SEC between battery and battery-less systems seems to differ across designs and testing conditions, as shown by the antagonistic results of the two following studies. Mohamed et al. tested the performance of a PV-powered RO system to treat seawater with and without battery for energy recovery, and found SEC values of 4.3 kWh/m^3 and 4.6 kWh/m^3 for the battery and battery-less configurations, respectively [320]. Qiblawey et al. compared a household RO unit with no battery—following available solar power—and with battery—operating under steady-state power supply—to treat water with low total dissolved solids concentration, and found lower maximum SEC for the battery-less system [321]. However, in both studies, SEC values with and without battery remain close, suggesting that variable power supply does not impact SEC provided that a minimum quantity of power is being supplied—around 15% in [313]. The specific water cost in [320] was found to be higher in the battery configuration.

Carvalho et al. experimentally validated their model of a small-scale battery-less PV-powered RO plant designed to operate at variable flow/pressure in equatorial areas [322]. Joyce et al. [323], as well as Abdallah et al. [324], investigated variable power supply of RO plants through the development of small-scale experiments without batteries, and confirmed the favorable application of variable PV power supply for RO.

To summarize, the experimental literature on the topic, although limited, shows that it is possible to operate an RO plant with variable or intermittent power while maintaining good system performances and avoiding equipment damage. In fact, it is not power variability per se but periods of low power—even during a very short period—that creates the risk for desalinated water salinity to exceed acceptable quality guideline, usually set at 1000 mg/L [325]. Several measures exist to prevent this phenomenon. These measures, supercapacitors, high-rejection membrane, or diverter valve, increase capital and maintenance costs compared to a constant power configuration, although not considerably given that they are somewhat standard components and given the very limited time and/or volume they are expected to operate over.

Given the proven operational feasibility of RO plants under variable and intermittent power supply and the widespread utilization of RO technology around the world, providing large feedback, the rest of this analysis focuses on RO desalination technology.

3.3.1.3 Region Selected for the Analysis

Where it is available, conventional water supply such as surface or groundwater almost always demonstrates lower costs than desalination. As a consequence, deploying desalination at large scale only makes economic sense in regions where conventional fresh water sources are not available or where these sources are heavily polluted. Several regions in China face this double challenge, as mentioned in the introduction section.

China does not have a nationally interconnected electricity network but, rather, six regional synchronous grids with limited but growing interconnections [72], [326]. One of them, the NCG, serves Beijing, Tianjin, Hebei, Shanxi, Shandong and the Western part of Inner Mongolia [327], although some parts of Western Inner Mongolia (the "MengXi grid") fall into the jurisdiction of Inner Mongolia Power Grid Company, an independent grid operator. The literature usually includes the MengXi grid into NCG, therefore this assumption is used in the present study [72].

Electricity consumption in NCG is expected to be around 1516 TWh/year in 2020 [72]. By then, installed power capacity is expected to reach around 450 GW. Existing and planned capacity data per energy source is used to design this study's scenarios, presented in Table 3-3 in the next section. Large disparities in installed power sources exist between, on the one hand, Inner Mongolia and Hebei, where more than 34% of generated power comes from wind turbines, and on the other hand, the other four provinces, dominated at 78% on average by fossil fuel-burning plants. While NCG experienced electricity shortages in the past, recently installed capacity and transmission corridors have enabled the region to reach equilibrium between demand and supply [328].

NCG hosts six of the country's ten largest desalination plants for a current production capacity of 343,500 m^3/day and additional plans for a total capacity of 1,550,000 m^3/day by 2020 [29]. Yet, five of the six provinces experience water scarcity, and Inner Mongolia is at risk of future water shortages [244]. 53.5% of groundwater and 61.3% of surface water reserves in NCG are classified as quality class IV or lower, recommended for limited industrial use and no human contact [24]. Water consumption from residential, industrial and agricultural sectors in China exceed water resources. Current water supply in water-scarce provinces of NCG added up to 61.1 billion m^3 in 2016 [105]. The United Nations defines absolute water scarcity as an annual water supply below 500 m^3/capita/year [329]. Using this definition as a proxy to calculate water deficit, we find that an additional fresh water supply of 61.4 billion m^3/year is needed. This means that, to eradicate absolute water scarcity by 2020, supply must double in NCG. The provincial repartition of this deficit is as follows: 12% in Beijing, 27% in Hebei, 44% in Shandong, 8% in Shanxi and 9% in Tianjin.

With its intricate power and water challenges, its existing power infrastructure, and its small but growing desalination fleet, NCG provides an ideal laboratory to evaluate the feasibility of a self-reliant medium-size grid for power and water supply as an alternative to current national-scale interconnection projects.

3.3.1.4 Methodology

The DESEC model, inspired by and improving on both the DEEP and SWITCH-China models, is developed for this analysis. DESEC is an integrated programming model that optimizes installed power capacity and hourly dispatch schedule in a given region, calculates the resulting power generated in excess, and optimizes deferrable desalination capacity, by integrating technical and economic considerations. In particular, the model gives priority to meeting the projected power demand over powering desalination plants. The model includes four steps: (1) installed power capacity optimization to ensure operability of the system; (2) power dispatch optimization; (3) desalination capacity optimization; (4) water production and transport costs calculation.

Hourly capacity factors are used for wind and solar PV systems in Beijing, Hebei, West Inner Mongolia, Shandong, Shanxi, Tianjin. We use samples of six hourly data per day (every four hours) and one day per month. Projected hourly power demand in Beijing, Hebei, West Inner Mongolia, Shandong, Shanxi and Tianjin is time-synchronized with capacity factors in order to model realistic situations. Datasets for load and capacity factors come from the same sources as those presented in Chapter 2 and used in the SWITCH-China model [85]. Data sources for installed and planned power generation capacity for wind, solar, hydropower, nuclear, natural gas and coal are presented in the Scenarios section below. Inter-province transmission lines that exist or are planned to be built by 2020, including distance, maximum capacity and losses come from [85], [330], [331]. Other data sources, including for carbon intensity and techno-economic performances of power and water technologies, are provided in the DESEC model description below.

3.3.1.4.1 Step 1

The objective of this first step is to minimize the additional installed non-VRE power generation capacity and transmission capacity needed to meet NCG power needs in 2020 in each hour and in each province.

While existing capacity and plans for additional capacity to be built by 2020 are included in the model, our study makes the assumption that NCG will be self-reliant in power supply in 2020. This step ensures that the modeled electricity system is viable.

Objective function[5]:

$$\forall \boldsymbol{h} | \mathbf{1} \leq \boldsymbol{h} \leq \mathbf{72} \quad \min \sum\nolimits_{\boldsymbol{p},\boldsymbol{p}'} \left(\boldsymbol{IB}_{\boldsymbol{p},\boldsymbol{h}} + \boldsymbol{T}_{\boldsymbol{p}-\boldsymbol{p}',\boldsymbol{h}} \right) \qquad 3\text{-}16$$

Where $IB_{p,h}$ is the installed baseload capacity in province p in hour h, and $T_{p-p',h}$ is the electricity transmitted between province p and province p' in hour h.

Subject to the constraints:

– The electricity generated in all provinces in hour h must be higher or equal to the load:

$$\forall p, h \;\; \boldsymbol{IB}_{\boldsymbol{p},\boldsymbol{h}} \times CFB + IS_p \times CFS_{p,h} + IW_p \times CFW_{p,h} + \sum\nolimits_{p'=1}^{6} \boldsymbol{T}_{\boldsymbol{p}-\boldsymbol{p}',\boldsymbol{h}} \times \left(1 - LossT_{p-p'}\right) - L_{p,h} \geq 0 \qquad 3\text{-}17$$

where CFB is the availability factor of non-VRE systems, IS_p and IW_p are the installed solar PV and wind capacity in province p, $CFS_{p,h}$ and $CFW_{p,h}$ are the capacity factors for solar PVs and wind turbines in province p in hour r, $LossT_{p-p'}$ is the efficiency loss for transmission lines between provinces p and p'. It is assumed that 1% of power is lost over 200 km over which it is transmitted [332]. $L_{p,h}$ is the load in province p in hour h.

– The installed non-VRE capacity in province p in hour h must be higher or equal to the planned capacity in 2020:

$$\forall \boldsymbol{p}, \boldsymbol{h} \;\; \boldsymbol{IB}_{\boldsymbol{p},\boldsymbol{h}} \geq \boldsymbol{MinIB}_{\boldsymbol{p}} \qquad 3\text{-}18$$

– The electricity transmitted from province p to province p' in hour h must be lower than or equal to the maximum electricity that can be transmitted by the planned transmission capacity in 2020:

$$\forall \boldsymbol{p}, \boldsymbol{h} \;\; T_{p-p',h} \leq \boldsymbol{MaxIT}_{\boldsymbol{p}-\boldsymbol{p}'} \times \boldsymbol{\alpha} \qquad 3\text{-}19$$

[5] Non-VRE energy sources in NCG include coal, natural gas, nuclear and hydropower. Each energy is modeled explicitly because availability factors and carbon intensities vary across sources. However, since all of them are assumed to operate as baseload, their modeled behavior is identical. Therefore, for reading ease, the letter B in the rest of this section designates all non-VRE systems..

where the multiplication factor α sets the maximum allowed expansion of the transmission network compared to current plans.

- The electricity transmitted from province p to p' in hour h must equal the negative value of the electricity transmitted from province p' to p in hour h:
  $$\forall \boldsymbol{p}, \boldsymbol{h}\; T_{p-p',h} = -T_{p'-p,h} \quad \text{3-20}$$

- Additional non-VRE plant construction is not allowed in Beijing or Tianjin:
  $$\forall p \in \{Beijing, Tianjin\}\; \forall h\; \boldsymbol{IB_{p,h}} = MinIB_p \quad \text{3-21}$$

We define $IB_p = \max_{\boldsymbol{h}} IB_{p,h}$ 3-22

and $IT_{p-p'} = \frac{\max_{h} T_{p-p',h}}{\boldsymbol{LossT_{p-p'}}}$ 3-23

IB_p and $IT_{p-p'}$ give the minimum installed non-VRE capacity and minimum installed transmission capacity needed in order for the NCG region to be self-reliant with regards to power supply. In the following steps, we assume that IB_p and $IT_{p-p'}$ correspond to the installed capacity in NCG in 2020.

3.3.1.4.2 Step 2

Using previous results, this step minimizes the hourly generation and transmission of electricity to meet hourly power demand. This step allows to calculate extra power generated by the system in each hour.

Objective function:

$$\forall \boldsymbol{h} | \boldsymbol{1} \leq \boldsymbol{h} \leq \boldsymbol{72} \quad \min \sum_{\boldsymbol{p},\boldsymbol{p'}} \left(B_{p,h} + T_{p-p',h}\right) \quad \text{3-24}$$

Where Bp,h is the quantity of non-VRE electricity produced in province p in hour h in province p, and Tp-p' is the electricity transmitted between province p and province p' in hour h. All considered provinces are within NCG, as the region is assumed to operate fully independently.

Subject to the constraints:

- The electricity generated in province p in hour h must be higher or equal to the load:
  $$\forall \boldsymbol{p}, \boldsymbol{h}\; B_{p,h} + \boldsymbol{IS_p} \times \boldsymbol{CFS_{p,h}} + \boldsymbol{IW_p} \times \boldsymbol{CFW_{p,h}} + \sum_{\boldsymbol{p'=1}}^{\boldsymbol{6}} T_{p-p',h} \times \left(\boldsymbol{1} - \boldsymbol{LossT_{p-p'}}\right) - \boldsymbol{L_{p,h}} \geq \boldsymbol{0} \quad \text{3-25}$$

- The non-VRE electricity generated in province p in hour h must be higher than or equal to the nominal installed power capacity de-rated by a minimum capacity factor:
  $$\forall \boldsymbol{p}, \boldsymbol{h}\; B_{p,h} \geq IB_p \times \boldsymbol{MinCFB} \quad \text{3-26}$$

  where MinCFB (0.5 in 2015, lowest level since 1978 [72]) represents the minimum capacity factor at which non-VRE plants are allowed to operate for load maneuvering purposes.
- The non-VRE electricity generated in province p in hour h must be lower than or equal to its maximum value constrained by installed capacity:

$$\forall \boldsymbol{p}, \boldsymbol{h} \;\; B_{p,h} \leq IB_p \times \boldsymbol{CFB} \tag{3-27}$$

- The electricity transmitted from province p to province p' in hour h must be lower than or equal to its maximum value constrained by installed transmission lines:
  $$\forall \boldsymbol{p}, \boldsymbol{h} \;\; T_{p-p',h} \leq IT_{p-p'} \times (\boldsymbol{1} - \boldsymbol{LT}) \tag{3-28}$$

- The electricity transmitted from province p to p' in hour h must equal the negative value of the electricity transmitted from province p' to p in hour h:
  $$\forall \boldsymbol{p}, \boldsymbol{h} \; T_{p-p',h} = -T_{p\prime-p,h} \tag{3-29}$$

We define $G_{h,p} = B_{p,h} + \boldsymbol{IS_p} \times \boldsymbol{CFS_{p,h}} + \boldsymbol{IW_p} \times \boldsymbol{CFW_{p,h}} - \boldsymbol{TotalLoss}$ 3-30

$G_{h,p}$ is therefore the total quantity of useful electricity generated in province p in hour h.

The hourly power generated in excess in NCG is defined by:

$$Cur_h = \sum\nolimits_{\boldsymbol{p}} G_{h,p} - \boldsymbol{L_{h,p}} \tag{3-31}$$

In the absence of flexibility options or additional power demand—such as desalination—, this power is curtailed.

This step also calculates annual CO_2 emissions from the power sector:

$$CO2_y = \sum\nolimits_{\boldsymbol{p},\boldsymbol{h}} B_{p,h} \times \boldsymbol{CO2_B} + \boldsymbol{IS_p} \times \boldsymbol{CFS_{p,h}} \times \boldsymbol{CO2_S} + \boldsymbol{IW_p} \times \boldsymbol{CFW_{p,h}} \times \boldsymbol{CO2_W} \tag{3-32}$$

The carbon intensities of the various non-VRE sources comprised in B are obtained from [333] and made explicit in the model. The average carbon intensity of the power grid optimized by DESEC is therefore:

$$CO2int = \frac{CO2_y}{\sum_{\boldsymbol{p},\boldsymbol{h}} G_{h,p}} \tag{3-33}$$

3.3.1.4.3 Step 3

After the quantity of extra power per hour, i.e. the maximum power available for desalination in the framework of this analysis, has been calculated, this step optimizes the quantity of electricity used in each hour over the year to minimize the RO desalination plant capacity that can meet a specific fresh water production annual target. In other words, this model aims at minimizing the variance between hourly desalination production over all hours for a given annual target, in order to maximize the desalination plant utilization rate.

Objective function:

$$\forall \boldsymbol{s} | \boldsymbol{0} < \boldsymbol{s} \leq \boldsymbol{1} \; \mathbf{min} \left(\max_{\boldsymbol{h}} E_{h,s} \right) \tag{3-34}$$

where $E_{h,s}$ is the amount of energy allocated to desalination in hour h. s is the share of power generated in excess, calculated in the previous step, that is dedicated to powering desalination instead of being curtailed.

Subject to the constraints:

- $\boldsymbol{E_{h,s}}$ must be lower than the quantity of power generated in excess in hour h:

  $$E_{h,s} \leq Cur_h \quad (3\text{-}35)$$

- $\boldsymbol{E_{h,s}}$ must be higher than or equal to zero: $\boldsymbol{E_{h,s}} \geq 0$ 3-36
- The sum of $E_{h,s}$ over all hours must be equal to the desired portion s of the annual curtailment: $\sum_h \boldsymbol{E_{h,s}} = s \times \sum_h \boldsymbol{Cur_h}$ 3-37

We define se as the specific power use of desalination (3.51 kWh/m^3 [319]). te_p the specific power use of water transportation in province p, is defined by:

$$e_p = max\left(0, E_{flat} \times l_p + E_{lift} \times h_p \times \left(1 + \frac{L}{2}\right)\right) \quad (3\text{-}38)$$

where E_{flat} (*0.018 kJ*/m^3/m [262]) is the energy required by a pump to transport one cubic meter of water over 1 meter on a flat path, E_{lift} (*13.986 kJ* m^3/m [262]) is the energy required by a pump to lift one cubic meter of water one meter. l_p is the distance, therefore pipeline length, between the closest desalination site and province p. h_p is the altitude difference between those two points, therefore the pipeline total elevation. L (30% [264]) is the percentage of water lost through leakage.

The corresponding desalinated water production in hour h is equal to:

$$\boldsymbol{W_{s,h}} = \frac{\boldsymbol{E_{h,s}}}{se + te_p} \quad (3\text{-}39)$$

The total desalination capacity needed to accommodate the fresh water production, in m^3/hour, is:

$$\boldsymbol{Wcap_{s,h}} = \max_h \boldsymbol{W_{s,h}} \quad (3\text{-}40)$$

$W_{s,y}$ and $Wcap_{s,y}$ corresponds to the sum of $W_{s,h}$ and $Wcap_{s,h}$, respectively, over all hours of the year.

For each s, we define:

$$share_p = \frac{Wneed_{y,p}}{\sum_p Wneed_{y,p}} \quad (3\text{-}41)$$

where $Wneed_{y,p}$ is the water need in province p. $share_p$ is the relative share of water needs in province p compared to NCG's total water needs.

3.3.1.4.4 Step 4

This last step calculates the net present value of producing and transporting desalinated water. Here onward, calculations are made for a desired quantity of desalinated water per year, $W_{s,y}$, equal to or lower than the maximum desalination production, and its corresponding desalination capacity, $\boldsymbol{Wcap_{s,y}}$, as calculated above. For simplification purposes, we set $\boldsymbol{W_{s,y} = W_y}$ in this last step.

This step comprises desalinated water production cost and transportation cost calculations. It is similar to formulas used in section 3.2 of this chapter, although some data have been modified to be aligned with this section's context. In particular, we use a descriptive approach, from the decision-maker or investor's perspective. As explained in section 3.2, such approach usually warrants the use of a higher discount rate than the prescriptive approach.

Water desalination production costs:

The capital cost IC of a desalination plant is calculated using the following formula:

$$\boldsymbol{IC} = \frac{\boldsymbol{BU \times IO}}{\boldsymbol{1000}} \times \boldsymbol{Wcap_y} \times (1 + F_{co}) \times (1 + I)^{LT} \quad \text{3-42}$$

where BU is the base unit cost (\$950/m^3/day on average [252]), IO the addition of in and outfall specific cost factor (7% [334]), and Fco (0.105 [334]) the contingency cost factor. The discount rate I used in this study is 8% [335]. LT (12 months [334]) is the desalination plant construction lead-time.

Total O&M costs, including human resources and equipment are calculated as:

$$\boldsymbol{OMC_y} = (S_{lab} \times P_{lab} + S_{man} \times P_{man}) \times \boldsymbol{Wcap_y} + \left(SC_{OM-spare} + SC_{replace} + SC_{OM-pre} + SC_{OM-post}\right) \times \boldsymbol{W_y} \quad \text{3-43}$$

where S_{lab} (*\$23,190/year* [255]) and S_{man} (*\$43,481/year* [255]) are the annual salary of production engineers and product managers, respectively. P_{lab} and P_{man} are calculated based on formulas provided in [334]. $SC_{OM-spare}$ (*\$0.04*/m^3 [255]), $SC_{replace}$ (*\$0.09*/m^3 [255]), SC_{OM-pre} (*\$0.05*/m^3 [255]) and $SC_{OM-post}$ (*\$0.02*/m^3 [255]) are the specific O&M spare parts cost, membrane replacement cost, specific O&M chemicals cost for pre-treatment, and specific O&M chemicals cost for post-treatment, respectively.

The resulting cost per unit of time of the construction and operation of a desalination plant over its 25-year lifetime is the sum of its annual fixed charges and annual variable charges:

$$\boldsymbol{C_y} = \boldsymbol{IC} \times CRF_{desal} + \boldsymbol{OMC_y} \quad \text{3-44}$$

where CRF is the capital recovery factor for the water plant with a discount rate of 8% (0.071 for a plant lifetime of 25 years).

The specific production cost of one cubic meter of water is:

$$\boldsymbol{Wspc} = \frac{\boldsymbol{C_y}}{\boldsymbol{W_y}} \quad \text{3-45}$$

Water desalination transportation costs:

Water needs to eradicate absolute water scarcity in NCG are evaluated on a province-by-province basis. For simplification purposes, spatial coordinates of NCG province capitals are used as proxies for demand center locations. New desalination capacity is assumed to be built in places where desalination plants are already in operation in 2017 (Figure 3-7). These four locations are Qingdao Baifa in Shandong province, Tianjin Dagang Xinquan, as well as Huanghua and Caofeidian Industrial Park in Hebei [29]. As Inner Mongolia is not currently experiencing water scarcity, its desalination needs are assumed to be zero.

We calculate the economically-optimized diameter of the pipeline as follows:

$$\boldsymbol{D} = 2 \times \sqrt{\frac{\boldsymbol{W_y}}{\pi \times FS}} \qquad 3\text{-}46$$

where FS (1 m/s [265]) is the average water speed.

$$\boldsymbol{N} = \lfloor \frac{\boldsymbol{D}}{D_{max}} \rfloor \qquad 3\text{-}47$$

is the number of pipelines needed to transport water to the considered province from the closest desalination site. D_{max} is the average maximum diameter of water transmission mains designed by manufacturing companies (150 inches [268], [269]).

The corresponding fixed charge cost and the O&M cost per year are calculated as follows:

$$\boldsymbol{FP_{transp-y}} = l \times SC_{pipe} \times \boldsymbol{D} \times \boldsymbol{N} \times (1 + I)^{LT_p} \times CRF_{pipe} \qquad 3\text{-}48$$

$$\boldsymbol{OM_{transp-y}} = \boldsymbol{FP_{transp-y}} \times F_{OMp} \qquad 3\text{-}49$$

where SC_{pipe} (*\$160/m* [243]) is the cost of building one meter of a one-meter diameter pipeline. LT_p (*48 months*) is the pipeline construction lead time. CRF_{pipe} is the capital recovery factor for the pipeline with a discount rate of 8% and the pipeline's lifetime—set at 25 years, equal to the desalination plant lifetime plants, although in reality pipeline lifetime ranges between 30-100 years [266], [267]. F_{OMp} (*0.07* [334]) is the O&M cost factor for pipelines.

Finally, the water transport specific cost is:

$$\boldsymbol{Wstc} = \frac{\boldsymbol{FY_{transp-y}} + \boldsymbol{OM_{transp-y}} + \boldsymbol{EC_{transp-y}}}{\boldsymbol{W_y}} \qquad 3\text{-}50$$

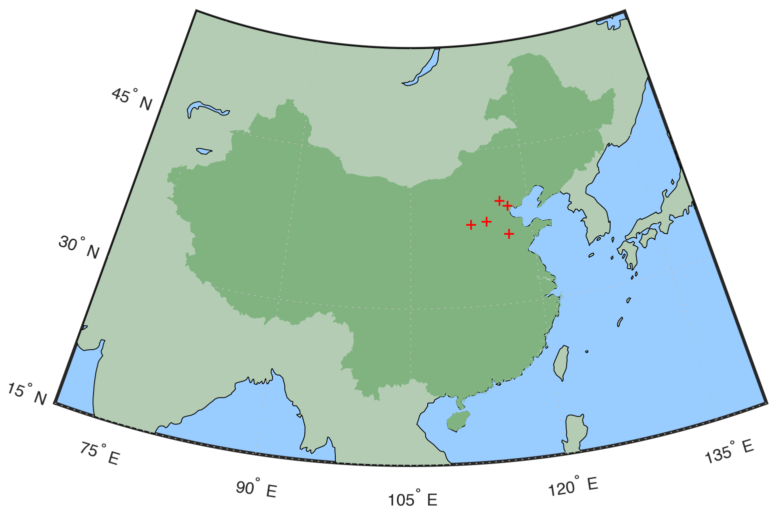

Figure 3-7 Location of capital cities of the NCG provinces (red crosses) used as proxies for water demand centers in the DESEC model.

3.3.1.5 Scenarios

Four scenarios for NCG's power and fresh water production are explored using the DESEC model. All scenarios share the same inputs regarding installed power capacity before 2017. Scenarios differ in their assumptions about the type, size and location of additional power capacity that will be built between 2017 and 2020, used as input data in the model. The first three scenarios are based on existing plans or target capacity deployment, including an increase in the share of wind. The fourth scenario, more hypothetical, explores the impact of developing sufficient VRE capacity to eradicate water scarcity in NCG by means of deferrable desalination. Scenarios are presented in Table 3-3. While, across scenarios, inputs only differ in their assumptions regarding installed power generation, prior to the DESEC optimization, these differences impact optimization results about power and desalination capacity and costs calculated by the model.

Table 3-3 Inputs used in the four scenarios explored by the DESEC optimization model.

Scenario number	Existing power generation capacity in NCG	Additional power generation construction by 2020 common across scenarios	Additional power generation construction by 2020 that differ across scenarios	Scenario description
BAU	Wind: 41 GW [336] PV: 18 GW [337] Hydro: 8 GW [338] Thermal: 286 GW [339]	Nuclear: 3 GW [65] PV: 23 GW [340]	Coal power: 56 GW [341] Wind: 23 GW—13th FYP [342]	Current plans for additional coal and wind power construction by 2020 are all carried out
BAU-MinNewCoal			Wind: 23 GW—13th FYP [342]	Current plans for additional coal power construction are cancelled, wind plans are carried out
MengXi			Wind power: 38.3 GW— MengXi grid target [343]	Additional wind capacity in Inner Mongolia
Water Scarcity Eradication			Wind power: 150 GW Solar power: 150 GW	Additional wind and solar capacity in Inner Mongolia to enable total supply 500m^3 of water /capita/year in NCG

The total wind capacity to be installed in Inner Mongolia in order to entirely meet NCG water needs (Water scarcity eradication scenario) is found by iteration and is approximative.

For each scenario, the DESEC optimization is performed over four one-year datasets. Each dataset represents one year of historical hourly wind and solar capacity factors.

3.3.2 RESULTS

While current plans for additional construction of coal power plants represent a total of 56 GW, we find that only 18.2 GW of additional baseload capacity would be needed for NCG to be self-reliant in power supply in 2020, provided that intra-NCG transmission capacity is deployed. Additional short- and medium-distance transmission lines within NCG enable reductions in fossil-fuel burning and in power curtailment.

According to current expansion plans, 13% of NCG power in 2020 will be generated by VREs, 29.5% of which will come from Inner Mongolia. Simulating over the DESEC datasets, we find that, under this electricity mix and in the absence of large scale energy storage, around 21.7 TWh of power will be generated in excess of the amount needed to meet the projected annual load in a **BAU** scenario, or 9.2% of annual power generation from VREs. When coal power deployment is limited to 18.2 GW, in the **BAU-MinNewCoal** scenario, excess electricity from the overall electricity mix decreases to 6.5 TWh/year. Extra power has to either be curtailed, transferred to demand centers out of NCG—provided that power is needed at the time it is transferred—or find another usage locally. Here, this other local usage is desalination.

The average SEC of RO desalination is assumed to be 3.5 kWh/m^3 [251]. The energy needed for water transportation via a pipeline network must be added to this number. The SEC of water transportation, assuming water is supplied from the closest desalination location, varies between 0.3 kWh/m^3 for supply to Tianjin and 5.9 kWh/m^3 for supply to Shanxi, given its long distance from the coast. The resulting total SEC for water desalination and transportation to demand centers, averaged over the needs and distances of each province, is 5.6 kWh/m^3.

As expected, scenarios with larger installed power capacity generate extra power during a larger number of hours over the course of a year. On average, power is generated in excess 17%, 8%, 21% and 68% of the time for the **BAU**, **BAU-MinNewCoal**, **MengXi** and **Water Scarcity Eradication** scenarios, respectively. In particular, we observe that, in scenarios with lower power capacity, extra power generation happens at times when VRE capacity factors are higher. VRE systems in the four scenarios are dominated by wind. Wind power frequency distributions tend to be leptokurtic—fat-tailed—defined as having a " propensity to produce outliers" [344], [345]. Frequency windows for low and high capacity factors are more homogeneously spread out. The left side of the distribution (low capacity factors) does not significantly impact results here since, at times of low wind power generation, curtailment is virtually reduced to zero. However, for any given amount of extra power generated annually, scenarios relying on high wind capacity factors need a larger desalination capacity to produce the same amount of water annually as situations with medium wind speeds. As a consequence, for given power and water demands, desalination plant annual utilization rates vary positively with installed power capacity. Similarly, utilization rates dramatically decrease when the desalination capacity is designed to accommodate the last few percent of annual extra power generation— i.e. infrequent, high capacity factors that do not fall within +/- three standard deviations of the mean of the wind power distribution.

When coal plans are all carried out, in the **BAU** scenario, up to 9% of NCG annual water deficit can be met under the simulated years. When only 18.2 GW of baseload is added, just enough to enable

NCG to be self-reliant in power supply in the **BAU-MinNewCoal** scenario, using excess power enables to meet up to 2.2% of NCG annual water needs only. Following the **MengXi** scenario would increase annual curtailment to 27.5 TWh, allowing to meet up to 9.1% of NCG's water needs. Therefore, while curtailment levels in planned power development can help alleviate part of NCG's water stress, much larger power generation is needed to actually eradicate absolute water scarcity in the region.

The **Water Scarcity Eradication** scenario explores the impact of installing additional VRE capacity in Inner Mongolia to increase fresh water supply to meet the 500 m^3/capita/year threshold. This scenario assumes that 150 GW of wind power and 150 GW of solar power are installed in Inner Mongolia. While the 2020 target year is too early to realistically believe that such levels of additional power generation from wind and solar can be achieved by then, the scale of such deployment, coupled with transmission network expansion, is technically feasible in the longer term as the potential capacity in Western Inner Mongolia has been found to be between 189 GW and 352 GW for wind, and between 858 GW and 9,488 GW for central PV [208], [209].

Increasing VRE capacity in the NCG electricity mix has a positive impact on decarbonization. From a baseline of 1,552 Megatons in the **BAU** scenario, annual CO_2 emissions decrease by 2%, 4% and 12% in the **BAU-MinNewCoal, MengXi** and **Water Scarcity Eradication** scenarios, respectively (Figure 3-8). The variation in carbon intensity of power generation across scenarios also impacts the carbon footprint of desalination. From 4.82 kg-CO2/m^3 of desalinated water in the **BAU** scenario, this number decreases by 1%, 4% and 24% in the **BAU-MinNewCoal, MengXi** and **Water Scarcity Eradication** scenarios, respectively.

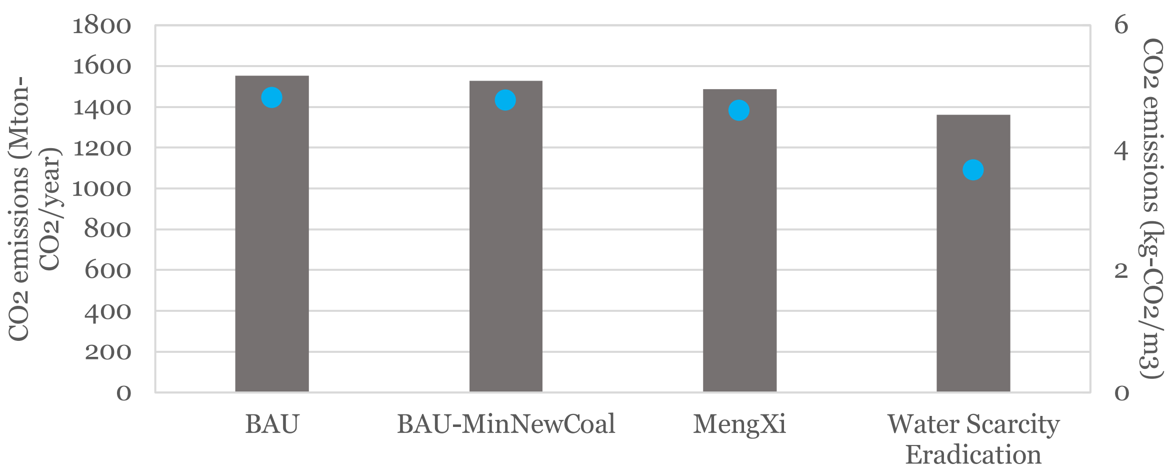

Sources: [32] (carbon footprint) and [333] (carbon intensity per energy source)

Figure 3-8 Annual carbon dioxide emissions from power generation in NCG (gray bars) and desalination carbon footprint (blue dots), including desalination plant construction, production and transport of desalinated water (model results).

While the share of VRE generation equals 14.3% and 14.5% in the **BAU** and **BAU-MinNewCoal** scenarios, respectively, the **Water Scarcity Eradication** scenario increases this number to 54.9%. Figure 3-9 below shows the hourly power dispatch schedule in NCG in 2020 in the **Water Scarcity Eradication** scenario coupled with deferrable desalination. The current NCG VRE mix is dominated by wind power. Wind capacity factors are highest from November to April. As a consequence, largest amounts of excess power are generated in the winter. In Figure 3-9, the desalination fleet size is optimized in the case where 99% of the total excess power generated must be accommodated for water desalination and transportation.

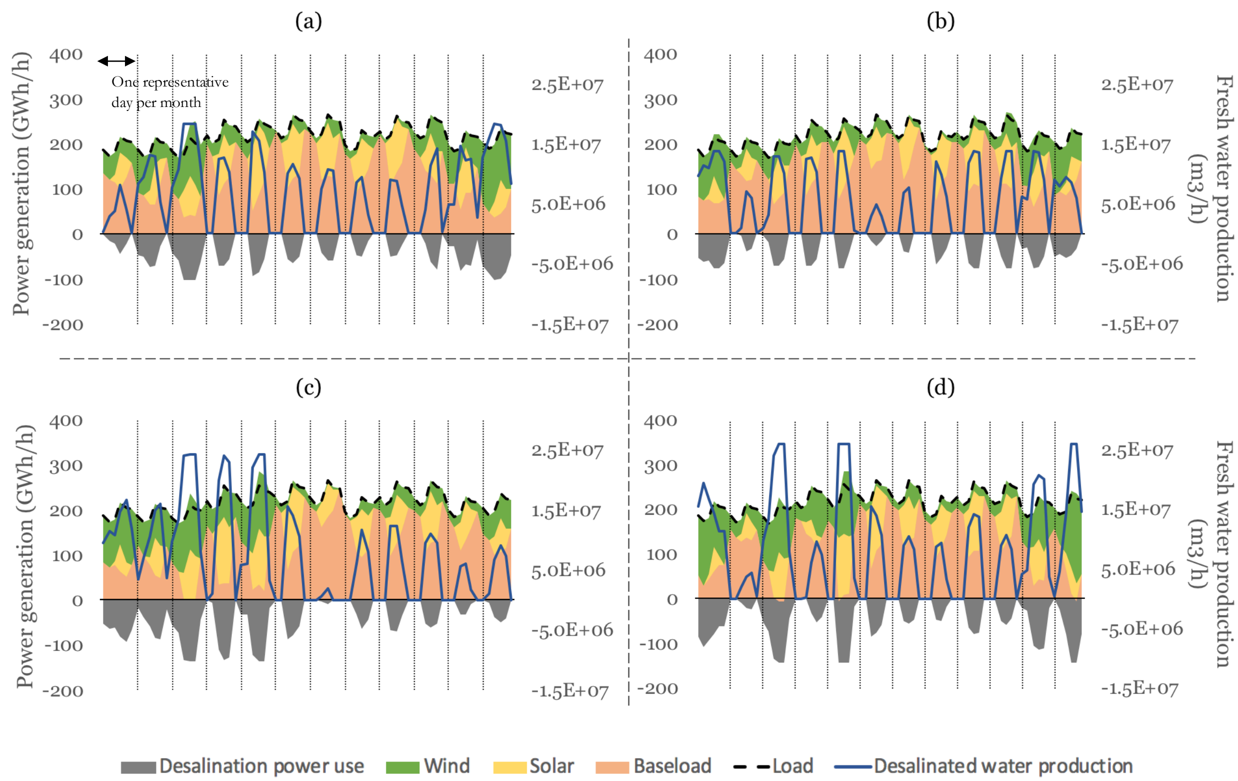

Figure 3-9 Simulated hourly power dispatch schedule in the NCG for the Water Scarcity Eradication scenario during four different years.

In the simulations presented in Figure 3-9, the model is forced to design an installed desalination capacity such that at least 99% of the excess electricity produced each year is used to power desalination plants. The resulting installed desalination capacity is 232 billion m^3/year, but the actual fresh water production, powered by when VRE generation exceeds the load, is 62.8, 51.6, 68.9 and 77.6 billion m^3/year over the four simulated years. On average, over the four yearly datasets, excess power resulting from the construction of 300 GW of VRE systems in Inner Mongolia can desalinate the equivalent of 1.04 times NCG's total water needs.

Wind and solar generation supplement each other quite well, since wind capacity factors are highest from November to April, while solar capacity factors are highest from May to September. On average, water desalination production is lower during the summer compared to the winter. Periods of low desalination mean that, in order to fully accommodate NCG water needs, the installed desalination capacity must be higher than if desalination production was evenly distributed across the year. As a result, while desalination plant utilization rates are close to 100% during a few months in years 3 and 4 (March, April, May in Figure 3-9. (c) and March, May and December in Figure 3-9. (d)), annual average utilization rates decrease when fresh water production target increases, negatively impacting costs. When the desalination capacity is sized to accommodate 100% of excess power, in every hour, annual desalination utilization rates vary between 6.5%, 2.7%, 8.2% in the **BAU**, **BAU-MinNewCoal,** and the **MengXi** scenarios, respectively. Deploying wind power capacity in NCG has a beneficial impact on utilization rates, since annual utilization rate equals 22.4% in the **Water Scarcity Eradication** scenario.

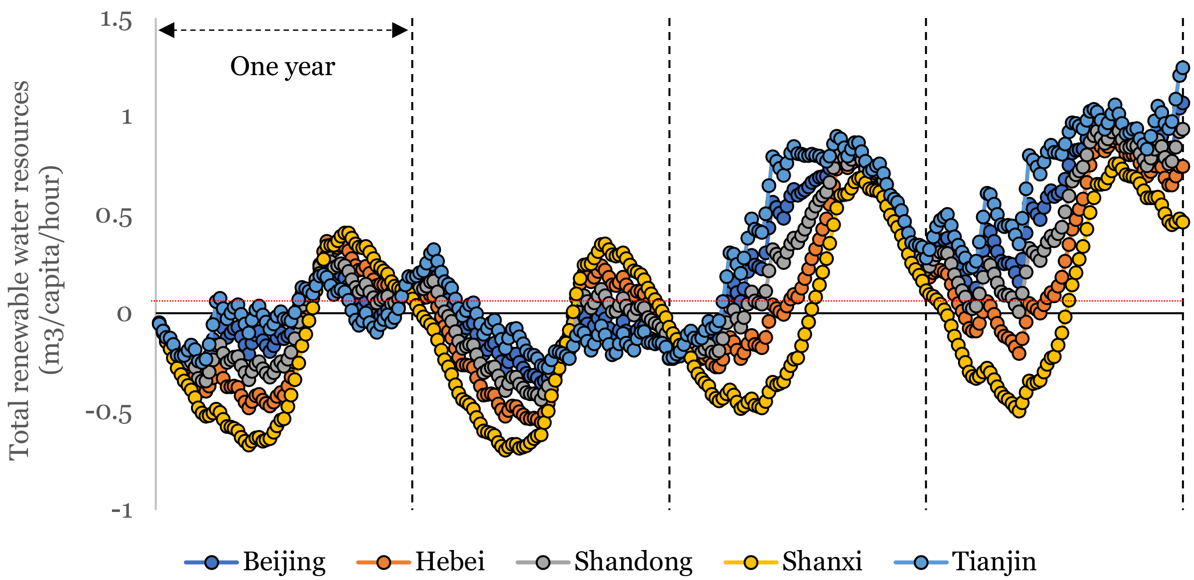

Source: China Water Risk & Unison Creative [244] *(current renewable energy supply) and* [346] *(precipitations)*

Figure 3-10 Cumulative net renewable fresh water resources available per capita by region, including existing supply weighted over monthly precipitation averages, and desalination supply DESEC results for the Water Scarcity Eradication scenario. The red dotted line represents the absolute water scarcity threshold, defined by the United Nations at 500 m^3/capita/year or 0.057 m^3/capita/hour.

Since three quarters of annual precipitations in NCG occur between May and August [346], water deficit is highest during winter months. Fresh water produced in excess during the summer can be stored until it is needed. When the desalination capacity is optimized to meet 100% of NCG needs over the course of a year, hourly fresh water supply oscillates around 500 m^3/capita/year—the absolute water scarcity threshold. When the DESEC simulation is successively run over the four one-year datasets, as illustrated in Figure 3-10 for the **Water Scarcity Eradication** scenario, the net cumulative water reserve has negative values from January to June, when conventional renewable water resources such as precipitations are low. In Figure 3-10, water supply is above the absolute scarcity eradication threshold during the second half of each year. When the desalination capacity is optimized to meet more than 100% of water needs, reservoirs fill up over time with fresh water produced in excess, and absolute water scarcity can be sustainably eradicated after a few years.

Economic calculations developed in this study include construction, O&M costs of desalination plants, and pipeline infrastructure deployment to transport water from coastal desalination plants to demand centers. An optimization is performed to determine the average diameter for water mains. In the absence of context-specific cost data, no significant economies of scale are considered when calculating desalination capacity costs in this study. For a given electricity mix, the specific cost of desalination varies as a function of the share of total excess power used for desalination, directly impacting plant utilization rate, and water transportation distance.

As mentioned in the first section of this chapter, state-controlled, unstable water prices in China are not an accurate proxy for the economic value of fresh water. At $0.75/m^3 and $1.15/m^3 on average for NCG residential and industrial sectors, respectively, water prices remain much lower than the global average of $2.06/m^3 in 2017 [347] despite the water crisis (NCG water prices are calculated based on [348] for Beijing, Tianjin and Jinan, and [217] for Shijiazhuang and Taiyuan). In the absence of an efficient market, it is difficult to determine the true monetary value of water. Several studies have calculated shadow water prices. A recent academic article on the topic in China found that the shadow price of industrial water varied, in 2012, between $0.77/m^3 in Xinjiang and $16.60/m^3 in Beijing, with an average of $8.97/m^3 across NCG [349]. Unlike current water prices, which are too low, shadow water prices are significantly higher than the global price average. Therefore, should a water market be established in NCG, prices would likely lie between current water prices and shadow prices of water. In the rest of this study, we compare the break-even point of desalinated water production and supply with current water prices and shadow water costs. Since this study focuses on eradicating absolute water scarcity, which can be assimilated to basic water needs of a society, it is assumed that water demand is inelastic.

For a given fresh water production target, higher installed power capacity leads to higher desalination plant utilization rate, hence lower capacity and costs, but higher power curtailment levels. There is therefore a trade-off between the average excess power to be curtailed, impacting the return-on-investment of VRE systems, and the specific cost of fresh water supply, impacting desalination break-even point and, eventually, the consumer. In practice we find that, for a given electricity mix, accommodating the last 10-15% of excess power dramatically increases desalination break-even point, especially at low deployment levels.

The specific cost of producing and transporting desalinated water is calculated using two approaches.

First, the costs of building and operating desalination plants, and transporting desalinated water to demand centers — weighted over province-level needs and distances — are calculated for each scenario and divided by the corresponding annual water production. Results are presented in Figure 3-11 (a). The **BAU-MinNewCoal** scenario, with the highest specific cost, features the smallest installed power capacity and lowest amount of extra power generated. The **BAU** scenario, with 37.8

GW more installed coal power than **BAU-MinNewCoal**, and the **MengXi** scenario, with 15.3 GW more wind capacity than **BAU-MinNewCoal** and 1 GW more coal power, share similar desalination specific costs, significantly lower than in the previous scenario. This further highlights that electricity mixes with minimal installed capacity, where excess power tends to be generated from higher wind speeds, have smaller desalination utilization rates and, eventually, higher costs. In contrast, the **Water Scarcity Eradication** scenario relies on a multitude of hours with low wind speeds to power its desalination fleet, leading to higher utilization rates, and therefore lower costs.

In a second approach, power costs are included in the calculations (Figure 3-11 (b)). Using electricity purchase as the metric to calculate power costs underestimates capacity sunk costs, especially in cases where extra power generated is not entirely used. Instead, we use the electricity mix found by the DESEC model in the **BAU-MinNewCoal** scenario as a baseline, since it represents the minimum installed capacity needed for NCG to be self-reliant in power supply in every hour over the four simulated years. The changes in power capacity between this baseline and the three other scenarios are included in the cost calculations by means of the LCOE of each energy system. LCOE data for coal, wind and solar PV systems in China are obtained from [350]. The installed power capacity and resulting costs in each scenario do not depend on the final amount of extra power used for desalination. Therefore, for low desalination production, total costs are much larger than in the baseline, over \$20/m^3 for **BAU** and **MengXi**, and \$16.7/m^3 for the **Water Scarcity Eradication** scenario. Costs per cubic meter significantly decrease as the desalination capacity and production increase. The combination of large additional installed coal capacity but low extra power levels, because coal plants operate at lower utilization rates to reduce overgeneration, make deferrable desalination prohibitively expensive in the **BAU** scenario, above the shadow price of industrial water at \$8.97/m^3 on average in NCG. Although bearing no additional costs from power capacity, the **BAU-MinNewCoal** scenario also shows very high costs. In the **MengXi** scenario, the specific cost decreases up to \$3.24/m^3, for an annual desalination production of 7% of NCG's water deficit, which is higher than the global average but significantly lower than some countries, such as Denmark. The **Water Scarcity Eradication** scenario curve in Figure 3.11. (b) includes the costs of building 300 GW of additional VRE capacity. Yet, with a specific cost of \$1.48/m^3 to meet 100% of NCG water needs, this scenario demonstrates smaller costs than the global price average and is, therefore, the least-cost approach among the cases presented in this study.

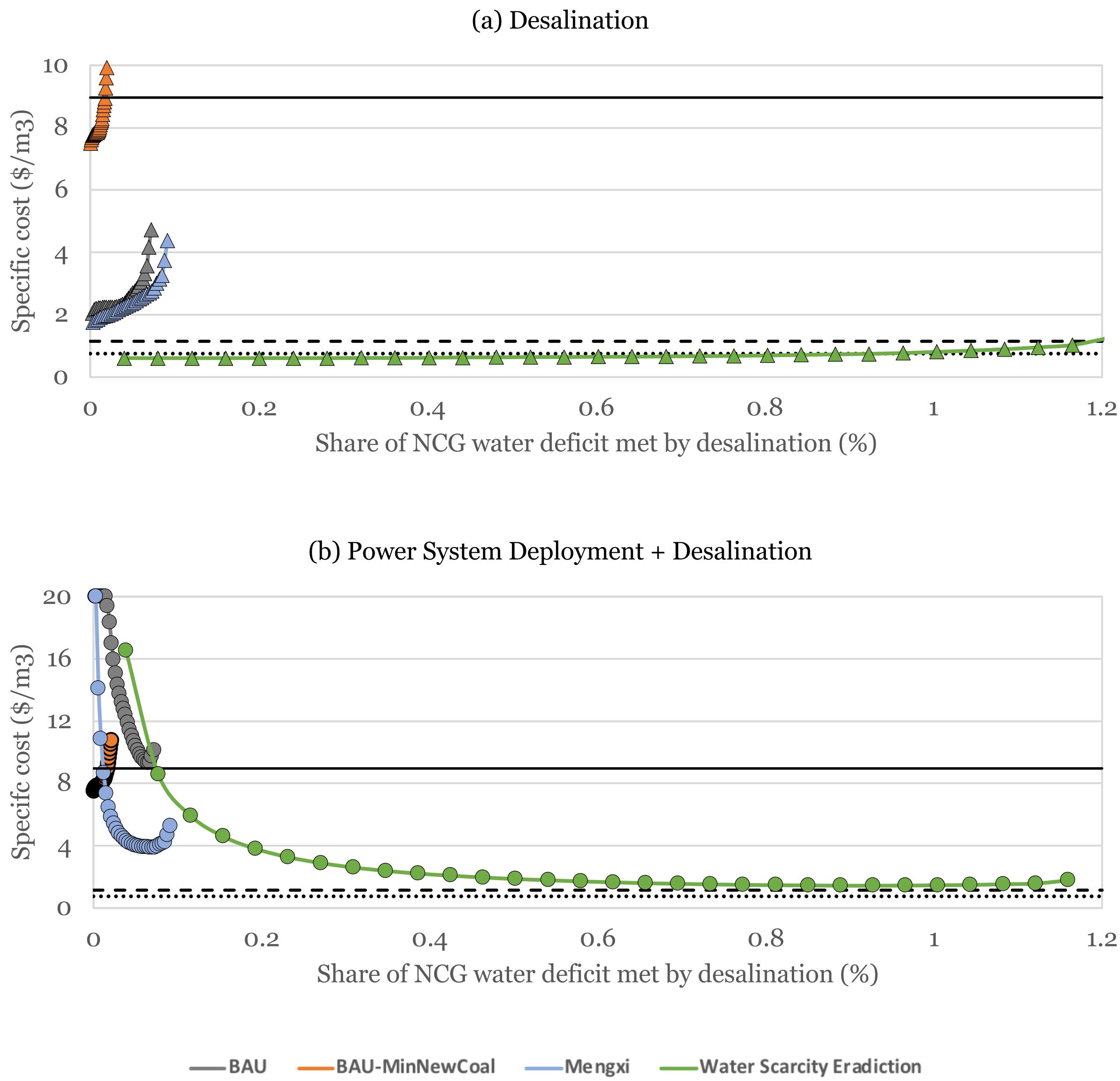

Figure 3-11 Deferrable desalination construction, operation and transportation costs In NCG.

(a) triangle markers: Specific costs of building and operating a desalination fleet and transporting water from desalination plans to demand centers, as a function of desalinated water production expressed as the share of NCG's water deficit (61.4 billion m^3 per year). (b) circle markers: To the desalination costs presented in (a) are added the costs of power system deployment, specific to each scenario, calculated relatively to the baseline of minimum needed capacity (DESEC results of the BAU-MinNewCoal scenario). The black, dashed and dotted lines represent average shadow price for industrial water, residential water price, and industrial water price, respectively.

3.3.3 CONCLUSION

Future climate change threats increase pressure on water resources, already challenged by economic and industrial development. At the same time, the deployment of wind and solar energy systems intensifies power waste around the world. By increasing the interdependence between regions, growing power transmission connectivity creates financial risks in investment, given the large investments needed to build long-distance transmission lines, and operational risks, by disconnecting power supply management decision-making from local techno-economic constraints. While household-level DR is still in its infancy, the use of variable power supply to operate industrial complexes, such as desalination plants, offers a load-response approach with better operability and sooner availability.

We proposed the development and use of desalination as a deferrable load to enable self-reliance in power and water supply at the subnational-grid level. We developed a methodology and the DESEC model to evaluate the relevance of this approach. Such methodology, while applied to NCG as a case study, can be used in any context. With its system-by-system, hour-by-hour, province-level, high resolution dataset and its successive optimization stages, DESEC is uniquely suited to explore the relevance of power-water coordination at the grid-level.

In this study, we analyzed the technical feasibility and economic efficiency of NCG operating as an independent grid for local power and water supply. The analysis showed that, by 2020, NCG can become self-reliant in power supply, provided that plans to increase short- to medium-distance transmission capacity between Inner Mongolia and the rest of NCG are carried out to accommodate Inner Mongolia's large installed wind power fleet. While 10% of NCG's current water deficit could be met while virtually reducing curtailment to zero by means of deferrable desalination, high fixed costs do not make this approach cost-efficient under business-as-usual power capacity.

Encouraging the coordination of power and desalinated water supply at a larger scale, within NCG, has a positive impact on both total costs and CO_2 emission reductions while effectively eradicating water scarcity in the region. More specifically, the deployment of 300 GW of VREs enables NCG to meet 100% of its water needs for a specific cost of water—including new power and desalination capacity construction, as well as water production and transport averaged across provinces and simulated years—of \$1.48/m^3. This price is higher than current, artificially low, water prices in NCG but smaller than the global average, especially among water-scarce countries. Importantly, it entirely covers new investment in VREs providing a new, more stable source of revenue for investors since power curtailment is no longer inevitable.

From a governance standpoint, this decentralized power-water coordination approach improves on national-level infrastructure deployment such as the SNWTP and WEETP for two reasons. First, it is aligned with the central government's reforms trend to break down national monopolies by strengthening regional-level resource management and coordination, which is currently being compromised by the development of a national grid. Second, it provides more flexibility to factor in local technical and economic constraints into capacity deployment planning, ensuring that long-term ambitious environmental targets set by the central government are realistic and successfully implemented at the regional level. While the local scope offered by this approach offers governance benefits, its cost structure and the overall scarcity context suggest that deferrable desalination be deployed at sufficiently large scale, within its geographic scope, to provide a sustainable solution to NCG's water stress rather than to be simply used as a backup solution during times of extreme water scarcity.

Developing a desalination fleet to be operated as a deferrable load does not merely constitute another industrial demand for electricity. Rather, it provides a technically feasible and economically efficient approach to solve water scarcity and power curtailment at once. In the short-term, it enables economic gains in NCG despite current overcapacity resulting from excessive coal plant construction. In the longer term, it offers a vehicle for cost-efficient deployment of VRE systems in the power sector, which are key levers—with nuclear power—of China's strategy toward decarbonization. Urgent governmental actions are needed to enable this strategy, and the success of the clean energy transition in general. These include the pursuit of medium-distance, *intra*-NCG power transmission deployment, reforms to enable realistic water pricing and efficient coordination of power and water utilities.

Further exploration should be performed to optimize the maneuverability of desalination plants at large scale and reservoir siting. More generally, the viability of this concept for other water treatment strategies, such as brackish water, urban wastewater, or polluted rivers and water discharges, for example the removal of high levels of lead and arsenic in Inner Mongolia, should be explored. Additional analyses should also be performed for other power grids in China and across the world. Looking further in the future, deferrable desalination could constitute a key lever to be accounted for in electricity mix expansion planning to enable meaningful CO_2 emission reductions and reach the 2°C target set by the IPCC.

This study encourages discussions around a new paradigm for sustainability: the development of distributed systems for resource management and supply—as smaller scales enable better account of local constraints by decision makers—and the inter-sectoral integration of resource management practices, in planning and operation, in order to achieve resilient and clean resource supply at lower risks.

CHAPITRE 4 NEW ENERGY VEHICLE DEPLOYMENT IN URBAN CHINA AND IMPACTS ON CO_2 EMISSIONS, COSTS AND ENERGY CONSUMPTION

4.1 INTRODUCTION

In 2015, the transportation sector only contributed to 9.4% of national CO_2 emissions in China and, as such, does not currently play a significant role in near-term targets for China's decarbonization strategy [351], [352]. As a consequence, its impact on national CO_2 emissions has been neglected, including by policy makers [353]. However, this sector is poised for considerable expansion over the next decades in China, including after 2030, year of the carbon peak target. In fact, despite a large increase in private car ownership over the last years (Figure 4-1), especially in urban areas, and despite China being the world's largest manufacturer of automobiles since 2008, the country still ranks globally low with regards to vehicle ownership, with 130 road motor vehicles per 1000 inhabitants [354], while the United States has 800 [355] and the European Union has an average of 480 [356]. Although it is likely that urban congestion constraints will maintain the number of cars at a lower level than observed in North America, the discrepancy in car ownership between China and other countries reveals that the country's current massive increase in vehicle ownership is likely to continue for a while. The majority of new car sales currently occurs in China's populated coastal regions — as shown by data on annual increase in the possession of private vehicles per province in [357] — where gasoline combustion aggravates levels of polluting emissions. The transportation sector is expected to become a new engine of provincial carbon dioxide emission growth [358], with the vast majority of passenger cars being fueled by gasoline [359]. This change challenges China's commitment to fighting climate change and aggravates national dependence on foreign crude oil, which already increased by 40% between 2005 and 2015 [360].

Yet, the typical short-distance commute in coastal Chinese provinces favors the use of NEVs, powered by electricity. Switching from gasoline to electricity in the urban transportation sector has the potential to decrease emissions, provided that the power sector pursues its clean energy transition. An additional promising aspect of NEVs is their low heat emission rate compared to Internal Combustion Engines Vehicles (ICEVs), which mitigates urban heat island effects and can significantly reduce electricity consumption from air conditioners in buildings [361]. The Chinese government has made the technological and market deployment of NEVs an official strategy of the country's sustainable development [362], [363] and has identified a "corner overtaking" (弯道超车) opportunity [20], [364]. Thanks to attractive pro-NEV subsidies and non-financial incentives—such as exemptions from restrictions on vehicle ownership in Beijing and Shanghai [365]—China became the world's largest market for NEVs for private cars and public buses in 2015 [366]. The stock of electric passenger cars in China was above 648,000 counts at the end of 2016 [367]. China has also become a global leader in electrification of public transportation, with 343,500 electric buses in circulation in 2016 [367].

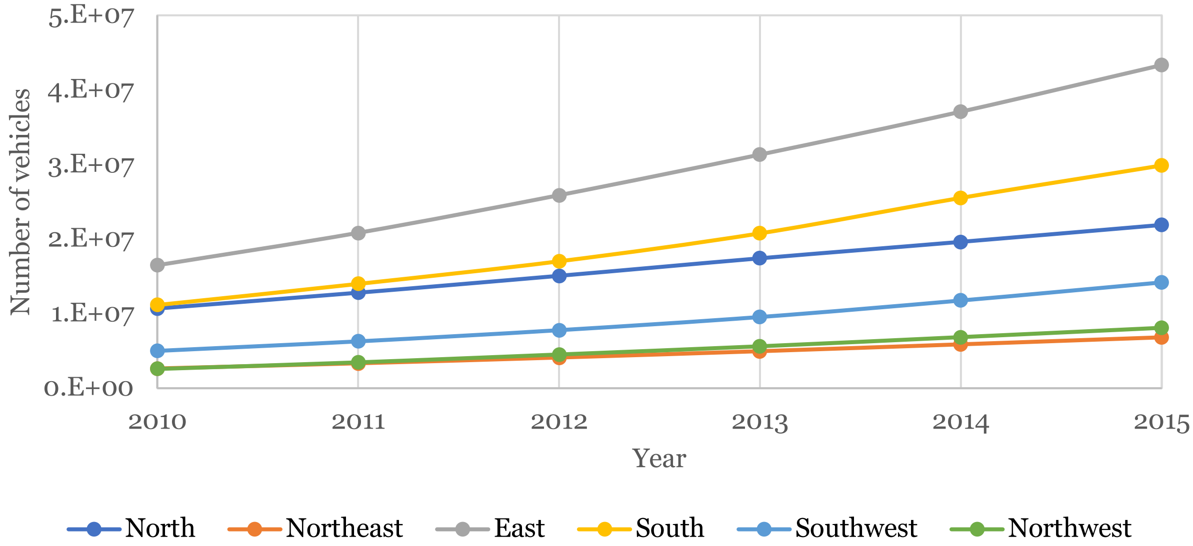

Source: National Bureau of Statistics of the People's Republic of China [357].

Figure 4-1 Possession of private passenger vehicles in China's six regions: North (Beijing Tianjin Hebei Shanxi Inner Mongolia), Northeast (Liaoning Jilin Heilongjiang), East (Shanghai Jiangsu Zhejiang Anhui Fujian Jiangxi Shandong), South (Henan Hubei Hunan Guangdong Guangxi Hainan), Southwest (Chongqing Sichuan Guizhou Yunnan Tibet), and Northwest (Shaanxi Gansu Qinghai Ningxia Xinjiang).

Over recent years, China's crude oil use has been decoupling from the industrial economy, becoming a consumer good [368]. In fact, while the transition toward electric buses and electric two-wheelers in China is on track, private NEV sales are still low and accounted for only 1.34% [369] of national car sales in 2015. This, as well as the progressive reduction in passenger NEV purchase subsidies in the current phase of the country's electric vehicle scheme, challenge the State Council's objective of reaching 5 million NEVs in China by 2020 [370], including 4.3 million private cars [366]. Urban passenger cars were only contributing to 10% of total CO_2 emissions from transportation in China in 2008 [371], [372], however they now represent 90% of total vehicle growth [373] and are therefore the main driver of the national expansion in transports. As China's transportation sector is poised for massive expansion in the next decades, the development of urban passenger cars is both an important threat and a promising lever to meeting the country's long-term commitment toward carbon dioxide emission reduction.

NEVs are only as clean as the electricity mix they are powered with. Therefore, the replacement of ICEV with electric cars powered by China's current electricity mix, dominated by coal, would not meaningfully impact national greenhouse gas emissions [374]. A combined transition toward an electric transportation fleet powered with clean energy sources simultaneously presents tremendous opportunities, as well as important and intricate challenges that China will have to start addressing in the next years.

The increasing pressure put by the transportation sector on the environment has been studied for several decades. Dargay [375] understood in 1997 the risk, in the absence of stringent policy measures, of the future increase in carbon dioxide emissions resulting from the projected growth in car ownership, as Asian countries' economies develop. Although the analysis underestimated China's rise in car ownership by a factor of three, Dargay's projections were already alarmist. Recent studies have analyzed the potential for energy use and carbon emission reduction of switching to NEVs. Yuan et al. [376] showed the correlation between factors such as NEV technology, driving range and driving speed, and the resulting energy consumption and well-to-wheel CO_2 emissions. The Union of Concerned Scientists [377] highlighted the role played by the electricity mix in NEV potential to reduce CO_2 emissions, and showed that, as a consequence, the net impact of NEV adoption on emissions varies significantly across regions of the United States. Meinrenken et al. [378] further stressed the importance of grid-carbon-intensity, among other factors, on achieving meaningful GHG emission reductions through electrification of the transportation sector. Mileva et al. [379] showed that the addition of electricity demand from NEVs will drive significant changes in the load curve, which must be addressed through adequate modifications of the power sector infrastructure.

Zhou et al. [380] noted the significant impact that financial and non-financial subsidies for NEV purchase have had on deploying electric buses and governmental vehicles in China, and its more mitigated impact on private NEV sales, limited by high purchase price—even with government incentives—and insufficient availability of charging infrastructure. However, Hao et al. [381] found that the anticipated decrease in electric vehicle manufacturing costs should allow NEVs to maintain competitiveness against conventional vehicles despite the gradual phasing-out of the subsidy mechanism.

Building deployment projections for NEVs and ICEVs and their impact on carbon dioxide emissions is a crucial step to better inform energy policies aiming at mitigating climate change. Pasaoglu et al. [382] highlighted that short-sighted electric vehicle deployment analyses, usually limited to short-time horizons, were a recurring caveat of the peer-reviewed literature. Therefore, looking at the 2050 horizon, Pasaoglu et al. analyzed the effects of four NEV deployment scenarios—built upon various oil and natural gas price evolutions. While these scenarios include decarbonization potentials of various intensities, allowing for a comparison of the correlation between NEV deployment and CO_2 emissions, they did not explicitly include China's official carbon targets. The IEA [366] built deployment scenarios for NEVs at the global level in line with specific carbon scenarios [383], yet limiting the study's horizon to 2030. Zheng et al. [384] built nine scenarios differing in various factors related to the transportation sector in China, and analyzed their ability to cap carbon emissions between 2030 and 2035. Since EV sales evolution over time were used as inputs rather than results of carbon targets, optimal deployment patterns to meet the 2030 carbon peak, and their sensitivity, are not available. Sorrentino et al. [385] found that, in order for the transportation sector to emit 30% less carbon emissions than today, BEV and PHEV technologies must evolve rapidly over time with aggressive penetration rates. This CO_2 emission reduction target, while applied to China in the study, does not correspond to an official carbon policy of the country.

A deeper analysis is needed to quantify the potential of transportation sector electrification in meeting China's long-term carbon dioxide emissions objective, and the resulting adequate NEV deployment scenario and policy to be implemented over time. This study proposes a methodology to evaluate the impacts on emissions, costs and fuel consumption of various NEV policies, and applies it to China's urban car fleet evolution over the 2050 horizon.

4.2 DATA AND METHODOLOGY

We analyze the evolution of China's urban private passenger vehicle fleet toward the double-objective of an electrified transportation system and a decarbonized electric power supply over the 2050 horizon. Projections built and used in this study are derived from both historical data and existing literature providing information about the future evolution of the variable of interests. Therefore, they embed uncertainty.

4.2.1 VEHICLE OWNERSHIP PROJECTIONS OVER THE 2050 HORIZON

Projections for population growth per province are calculated from the population at year-end per province for years 2010 to 2015, obtained from China Statistical Yearbook [357]. The proportion of urban population relative to rural population at year-end per province for years 2010 to 2015 is obtained from the same source. The population in urban areas is calculated by multiplying the proportion of urban population with the total population for years 2010 to 2015. Projections for future years are calculated by using a logistic function, in accordance with recent population growth observations in large cities [386]. The growth rate used in the logistic function corresponds to the average growth rate over the years 2010 to 2015. The urbanization saturation level is set at 0.8 [387].

The car ownership level per person for years 2010 to 2015 in each province is calculated by dividing the possession of private vehicles per province, obtained from [357], by the corresponding population.

The average household size used in this study is 3.34 persons in rural areas and 2.71 persons in urban areas [388] and is assumed to remain constant over the 2050 horizon. In the absence of available numbers for China, the ratio of the number of private vehicles between households in rural and urban areas is assumed to be 1.3, as found in the case of the United Kingdom [389]. The number of private vehicles per person in urban areas is:

$$N_{per\ capita-urban} = \frac{N_{per\ household-urban}}{Household\ size_{urban}} \qquad 4\text{-}1$$

and, similarly, for rural areas.

Therefore, the ratio of the number of private vehicles per person between urban and rural areas is:

$$R = \frac{N_{per\ capita-urban}}{N_{per\ capita-rural}} = \frac{N_{per\ household-urban}}{N_{per\ household-rural}} \times \frac{Household\ size_{rural}}{Household\ size_{urban}} \qquad 4\text{-}2$$

This ratio equals 0.95 and is assumed to remain constant. However, the share of urban versus rural population changes over time.

Urban vehicle ownership per capita in each province is:

$$V_p = \frac{Car\ ownership \times Pop}{Urban\ pop + (Pop - Urban\ pop)/R} \qquad 4\text{-}3$$

Several studies have found that the Gompertz function best fits historical data for car ownership [390] [391] [392]. In the absence of long-term deployment projections for urban car ownership and for electric vehicles from governmental Chinese sources, we use a Gompertz function to build car ownership projections. Annual GDP data are obtained from [393]. Urban car ownership per capita in province p and in year y is calculated using the following formula:

$$V_{p,y} = V^* \times e^{\alpha_p \cdot e^{\beta_p \cdot GDP_{p,y}}} \qquad 4\text{-}4$$

V* represents the car ownership saturation level, set at 450 per thousand inhabitants, corresponding to the medium value of the saturation level between a "low ownership scenario" and a "high ownership scenario" found in [391]. Historical α and β in each province are calculated over years 2010-2011, 2011-2012, 2012-2013, 2013-2014, and 2014-2015. The average value over the historical years considered is used in the Gompertz function for future years, for each province. This level is lower than in a majority of Western countries, as the high density of Chinese cities favors public transportation over private cars, and as many cities already suffer from congestion [394].

$\#V_{p,y}$, the number of circulating cars in urban areas per province per year over the 2050 horizon, is calculated by multiplying the urban car ownership rate by the urban population. It results in the total number of cars that are in operation in each province in each year, i.e. cars that were already circulating in previous years, plus new cars added to the road in the current year, minus cars that were retired — average useful car life is assumed to be 10 years [395].

4.2.2 CO_2 Emissions

In chapter 2 of this dissertation, we found, using the SWITCH-China model, the least-cost electricity mix trajectory over the 2050 horizon able to meet the country's existing carbon policies— the **BAU with Carbon Cap** scenario. This scenario included the 2020 carbon intensity target and the 2030 carbon peak commitment. Carbon intensity and costs corresponding to this modeled trajectory for the electricity mix serve as a basis to the present analysis. Since China's carbon intensive mix today results from its large and cheap coal resources, CO_2 emission reduction is rather negatively correlated with electricity cost reduction in the country. Given the cost-minimization objective of the SWITCH-China model, this scenario provides carbon intensity projections for electricity generation that are at or near the maximum carbon intensity value to meet the country's official carbon targets. More costly alternatives exist to reduce China's power sector emissions further, which are presented in chapter 2, but not used here.

Annual carbon emissions per NEV, $C_{NEV,y}$, are calculated as follows:

$$C_{NEV,y} = D \times E \times ce_y \qquad 4\text{-}5$$

Where D is the average annual driving distance of a private passenger car in urban areas (15,000 km/year [396]). E is the average electricity consumption per km (0.15 kWh/km [397]). ce_y is the carbon content of electricity in year y, based on the average national electricity mix composition from the **BAU with carbon cap** scenario of the SWITCH-China model, and assuming that coal plants and natural gas plants emit an average of 0.84 and 0.42 kilograms of CO_2 per kWh, respectively. It is assumed that the average annual carbon content of the electricity mix over the 2050 horizon is independent from the extent of the deployment of NEVs.

Annual carbon emissions per ICEV, $C_{ICEV,y}$, are calculated as follows:

$$C_{ICEV,y} = D \times \frac{G_{2015}}{100} \times \left(\prod_{i=2016}^{y} 1 + dG_i\right) \times cg_y \qquad 4\text{-}6$$

Where D is the same distance as used for NEVs, G_{2015} is the gasoline consumption per 100 km (6.90 L/100 km—34 mpg—in 2015 [398]). All ICEVs in this study are assumed to be fueled by gasoline, as is the vast majority of China's vehicle fleet [359]. dG_y is the annual relative decrease in gasoline consumption per km from year y-1 to year y ([399]), cg_y is the carbon content of gasoline in year y (2,210 g-CO_2/L [400]).

Calculations show that CO_2 emissions per ICEV are considerably higher than CO_2 emissions per NEV, in all years from 2017 to 2050. Actual future carbon intensity for electricity generation might differ from our projections. Higher values would increase CO_2 emissions per NEV. Yet, as mentioned above, they would not be consistent with China's existing CO_2 emission reduction targets.

4.2.3 New Energy Vehicle Deployment Scenarios

In order to compare the impacts of different NEV policies on carbon dioxide emissions and costs, four scenarios are created, presented in Table 4-1 below. The scenarios are based on the same urban passenger car projections presented in the beginning of this section but differ in the share of NEVs versus ICEVs added to the road every year, until 2050.

Data on annual NEV sales for years 2014 to 2017 come from [401]. The share of battery electric vehicles vs. plug-in hybrid electric vehicles in total NEV is assumed to remain constant at 75% vs. 25%, respectively.

The first scenario, **BAU**, serves as baseline: it assumes that the future share of NEV sales over total urban passenger vehicle sales will remain fixed at the 2016 level, which is 1.62%. The corresponding number of NEV circulating in year y, $\#NEV_{BAU,y}$, is:

$$\#NEV_{BAU,y} = \#NEV_{y-1} \times (1 - R) + \left(V_y - V_{y-1} \times (1 - R)\right) \times SNEV_{2016} \qquad 4\text{-}7$$

In the near term (2017 to 2030), the other three scenarios share the same NEV deployment projections, by extrapolating the recent growth in China's NEV sales that followed the implementation of new pro-NEV policy. This projection of future annual NEV sales is done through a polynomial regression with data from years 2014 to 2017 using the method of least squares (R^2 = 0.99988)

$$\forall y|2018 \leq y \leq 2030, SNEV_y = a \times y^2 + b \times y + c \quad 4\text{-}8$$

In the second scenario, **Current Policy Impact**, this extrapolation is applied until 2050.

The third scenario, **Min NEV under Carbon Cap**, highlights the role of CO_2 emission policies. In this scenario, carbon emissions are capped from 2030 on. NEV sales in each year from 2031 to 2050 are minimized such that emissions are maintained at the 2030 level.

$$\forall y|2030 < y,\ min\#NEV_y \quad 4\text{-}9$$

$$s.t.\ C_{NEV,y} \times \#NEV_y + C_{ICEV,y} \times \left(V_y - \#NEV_y\right) \leq C_{NEV,2030} \times \#NEV_{2030} + C_{ICEV,2030} \times (V_{2030} - \#NEV_{2030}) \quad 4\text{-}10$$

The right side of the inequality corresponds to carbon dioxide emissions from urban passenger cars in China in 2030.

As no date has been announced yet by the Chinese government with regards to ICEV ban, the fourth scenario, **2040 ICEV Sales Ban**, transposes France's ambitious objective to ban ICEV sales after 2040 to the case of China. The corresponding annual share of new NEV sales over new car sales is calculated using a logistic growth curve, and assuming that this share equals 99% in 2040:

$$\forall y|2030 < y, SNEV_y = \frac{L}{1+e^{-k(y-2015-x_0)}} \quad 4\text{-}11$$

Where L is the maximum value of new NEV sales share, it equals 100%. k is the steepness of the curve, calculated using the two following data points: SNEV2015 = 1.09% (historical data) and SNEV2040 = 99.00% (scenario assumption).

Table 4-1 Description of NEV deployment scenarios

	Annual urban passenger car ownership (2017-2050)	Annual NEV sale share (2017-2030)	Annual NEV sale share (2031-2050)
BAU	Gompertz model based on historical GDP and transport data at the province level.	Share of NEV in total car sales fixed at 2016 level.	
Current Policy Impact		Second-order polynomial regression based on historical sales.	
Min NEV under Carbon Cap		Second-order polynomial regression based on historical sales.	Minimization of NEV deployment under CO_2 emissions cap at 2030 levels.
2040 ICEV Sales Ban		Logistic growth based on historical sales and assuming 99% NEV sales share in 2040.	

Source: [402] *(NEV sale volumes in 2014, 2015 and 2016)*

4.2.4 Economic Analysis

For calculation convenience, and because NEV deployment scenarios modeled in this study occur at large scale—including the **BAU** scenario, which assumes that 200 million NEVs will circulate in 2050—it is assumed that vehicle and system costs are borne by the owner of the private passenger vehicle. Vehicle costs are divided into two categories: manufacturer's suggested retail price (MSRP), or car purchase price, and O&M costs. For NEVs, a third component is added, the average cost per vehicle of building and operating a charging infrastructure, namely public and home chargers. MSRP is supposed to be entirely paid for in the year of purchase, while O&M and charger costs are divided in equal yearly shares over the vehicle's lifetime. MSRP data are based on data from the Chinese state-owned manufacturer BAIC group.

The total costs of purchasing and operating an NEV, bought in year y, is:

$$K_{NEV,y} = \frac{MSRP_{NEV,y}}{(1+r)^{y-2016}} + \sum_{i=0}^{LT-1} \frac{D \times E \times K_{E,y+i} + OM_{NEV,y+i} + C_{NEV,y+i} \times T_{CO2,y+i} + K_{home-ch,y+i} + K_{public-ch,y+i}}{(1+r)^{y-2016+i}}$$

4-12

Where r is the discount rate (5% [351]). LT is the useful life of a vehicle (10 years [395]). $MSRP_{NEV,y}$ is the MSRP of an NEV in year y (Average price decrease between BAIC group's EV150 and EV200 in 1.5 years [403] is assumed to simulate NEV MSRP decrease, in the near-term. Once the NEV MSRP value reaches the value of ICE MSRP, in 2031 as calculated below and in line with projections from other sources [404], the decrease in NEV MSRP is assumed to diminish by 1% every year, until it plateaus in 2039. As a consequence, MSRP varies between $34,035 in 2015 and $9,931 in 2050. While a 71% MSRP reduction in 35 years is ambitious and can only happen contingently to battery technology breakthrough and large-scale deployment, it is in line with existing studies suggesting a 66-75% reduction in battery costs by 2030 [405], [406]). $OM_{NEV,t}$ corresponds to maintenance cost in year t. Maintenance includes tires and brakes. Brake maintenance assumed to occur only once during the first 160,000 km [407]. Since battery replacement is not usually necessary in the first ten years of a vehicle's life—the lifetime considered here—and for an average total driving distance of 150,000 km, battery replacement is not included in calculations [408], [409]. Maintenance costs are shared equally over the 10 years of the vehicle's lifetime in calculations—. $K_{E,t}$ is the electricity cost in year t (varies between $65.84 and $72.70/MWh [222]). $T_{CO2,t}$ is the carbon tax in $ per ton of CO_2. $K_{home\text{-}ch}$ is the average cost of a home charger per vehicle (varies between $1,200 [410] and $592/household. It is assumed that there is one home charger per household, or 2.71 persons in urban areas. In the absence of existing studies on the topic, a cost decrease of 2% per year is assumed.) $K_{public\text{-}ch}$ is the average cost of a public charger per vehicle (varies between $167 [410]and $117/vehicle. It is assumed that 45 cars can be charged per station at a time [411]. In the absence of existing studies on the topic, a cost decrease of 1% per year is assumed.)

The total costs of purchasing and operating an ICEV, bought in year y, is:

$$K_{ICEV,y} = \frac{MSRP_{ICEV,y}}{(1+r)^{y-2016}} + \sum_{i=0}^{LT-1} \frac{D \times \frac{G_{2015}}{100} \times (1+dG_{y+i}) \times K_{G,y+i} + OM_{NEV,y+i} + C_{NEV,y+i} \times T_{CO2,y+i}}{(1+r)^{y-2016+i}} \quad 4\text{-}13$$

Where $MSRP_{ICEV,y}$ is the MSRP of an ICEV in year y (assumed to remain fixed at $11,265 [412], the MSRP of BAIC group's E150, over the 2050 horizon since ICEV is a mature technology.) $K_{G,t}$ is the cost of gasoline in year t (varies between $0.60/L [413] and $2.39/L.) $OM_{ICEV,t}$ corresponds to maintenance cost in year t (machine oil change, automatic transmission fluid, spark plugs and wire, muffler, tires, and brakes maintenance [407], adding up to a total of $227/vehicle/year when maintenance costs are shared equally between years over the vehicle's lifetime.)

The evolution of NEV and ICEV net present costs over time is presented in Figure 4-2. NEVs will reach economic parity with comparable ICEVs around 2031. When battery replacement is excluded, maintenance costs for NEVs are significantly lower than for ICEVs [414], [415].

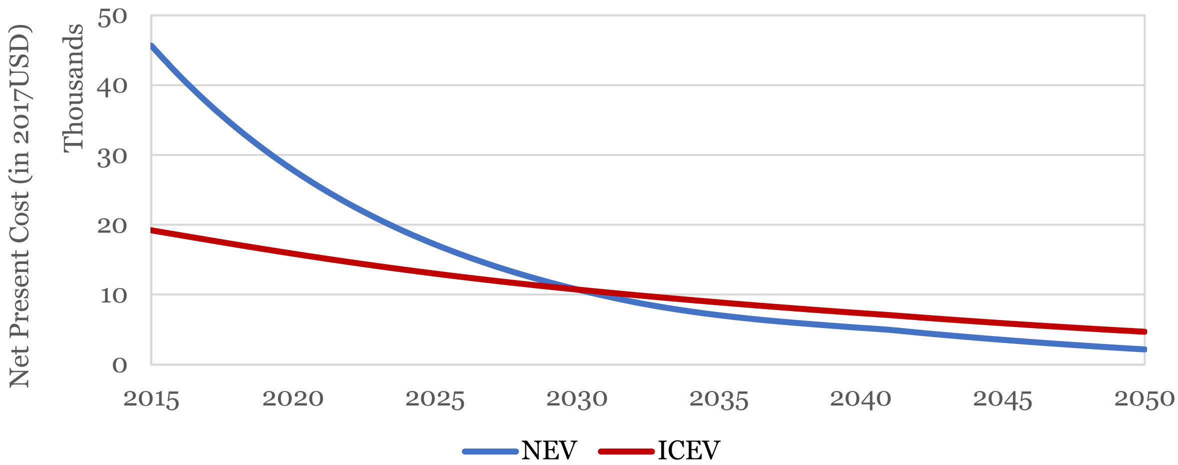

Figure 4-2 Net present cost per vehicle for NEVs and ICEVs using an annual discount rate of 5% and assuming that the average vehicle useful lifetime is 10 years.

4.2.5 Electricity consumption

Parking time probabilities in Shanghai are given in Figure 4-3.

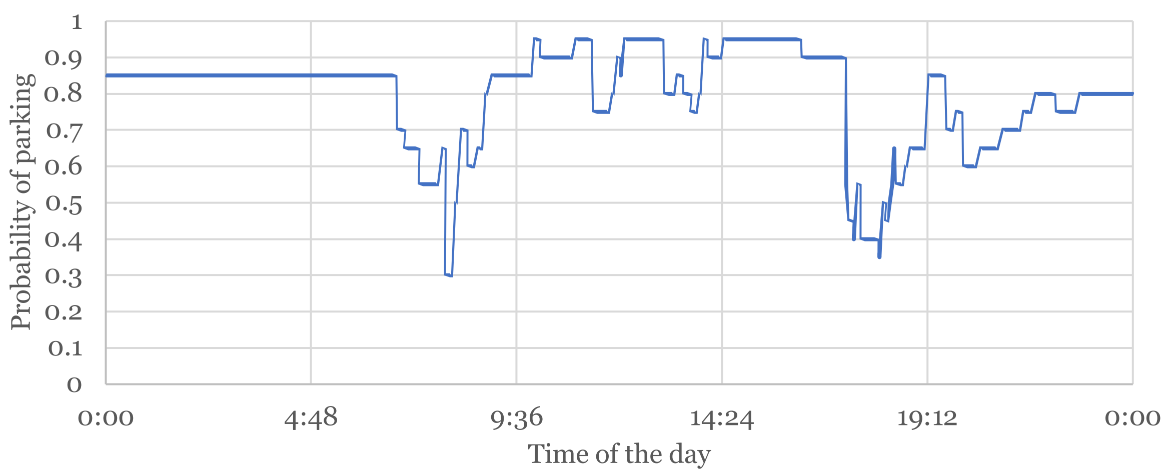

Source: Energy Research Institute of the National Reform and Development Commission [397]

Figure 4-3 Probability of parking at each time of the day for private vehicles in Shanghai.

Assuming that commute times during weekdays are 7-9 am and 5:30-7:30 pm, we make the following hypotheses with regards to probability of charging:

- The minimum probability of charging is 0.2 and occurs at 8am and 6:30pm (during commute hours).

- The probability of charging between 7:30pm and 7am (i.e. non-working time) is 1: all NEV owners are assumed to have access to home or residential charger, therefore only parking probability impacts the NEV charging load at night.
- The probability of charging between 9am and 5:30pm (working time) is 0.25 in 2015, 0.50 in 2025, 0.75 in 2035 and 1 in 2045, reflecting the gradual deployment of EV charger infrastructure at work and in commercial areas.
- The probability of charging varies linearly between minimum and maximum values during commute hours.

Besides temporal variations in probability of parking time and probability of charging, NEV power demand is assumed to be uniformly distributed throughout the day. Such assumption implies that smart charging measures are implemented to smooth out NEV power demand. The costs and technical characteristics of these measures are not detailed in this study.

Using the projected power load without electric vehicles for years 2015, 2025, 2035 and 2045, obtained from the SWITCH-China model [222], we calculate the average daily load profile of NEV charging at the national scale in China across the four NEV deployment scenarios in 2015, 2025, 2035 and 2045 (see Figure 4-4 for an example of the national daily load curve in 2045). It is assumed that private NEVs consume 15 kWh to travel 100 km and that the average driving distance per year is 15,000 km [396].

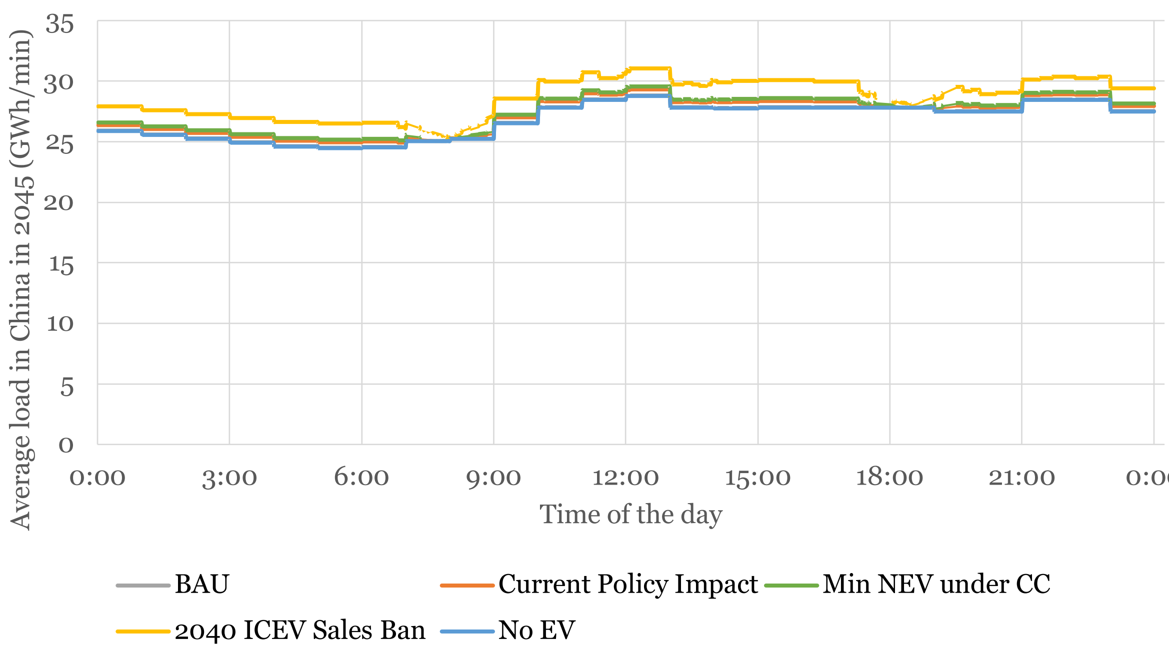

Figure 4-4 Daily national load in 2045 under the four NEV deployment scenarios and without electric vehicles, assuming that NEV charging load is smoothed out across the day but temporally constrained by probabilities of parking time and of charging.

These calculations are performed to grasp the extent of the impact of NEV deployment across the four NEV scenarios on the national load curve. Additional data would be needed to explore in more details the impact of NEV deployment on sources of electricity supply across regions and across hours, during weekdays vs. weekends, as well as on the costs and socio-technical feasibility of smart charging measures.

4.3 RESULTS

From about 100 million counts in 2017, the national fleet of urban private passenger cars increases over time and is expected to reach 400 million in 2030 and 570 million by 2050, with important disparities between provinces (Figure 4-5). Guangdong and Shandong will remain the provinces with the largest number of urban cars, and Tibet and Qinghai those with the smallest urban vehicle fleet. Between those two extremes, several provinces that already have high vehicle ownership levels, such as Zhejiang and Beijing, will be outpaced by other provinces, including Henan, Hebei, Sichuan, Hunan, around 2030. The national urban car ownership curve is currently in stage II of the Gompertz function and should enter its last stage around 2026, when the national average car ownership is 342 cars per 1,000 inhabitants.

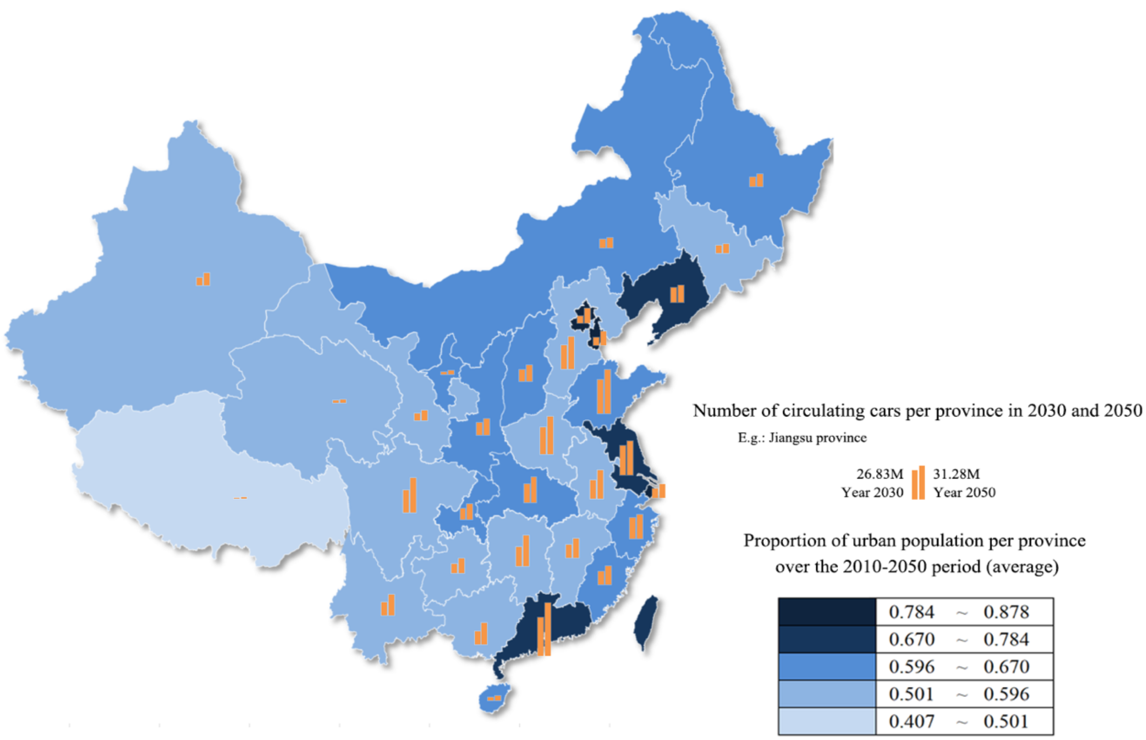

Sources: National Bureau of Statistics of the People's Republic of China [357] *(urban population share) and model results*

Figure 4-5 Average urban population share per province over the 2010-2015 period (colored areas) and number of private passenger cars on the road in urban areas per province in years 2030 and 2050 calculated with a Gompertz function (bar diagrams).

Should the future share of NEVs in annual car sales remain fixed at 2016 levels, as presented in the **BAU** scenario, up to 840,000 NEVs will be added to the road each year. NEVs will represent about 1.70% of total urban passenger vehicles in 2050 in the country (from 0.70% in 2016). Resulting national carbon dioxide emissions will continuously increase over the entire horizon, and will be 40% higher in 2050 than in 2030 (Figure 4-6).

Emission rates start to visibly vary across scenarios around 2025. The significant difference in scale between the reduction in carbon dioxide emissions from switching from ICEVs to NEVs—emitting a thousand times less carbon dioxide on average, under assumptions from the **BAU with Carbon Cap** scenario—and the increase in national CO_2 emissions from car ownership growth—several million cars a year—implies that a vast majority of vehicle sales after 2030 will have to be NEVs in order to cap emissions after that year.

In particular, CO_2 emissions from the urban passenger car sector will not peak by 2050 if the current share of NEV in total annual vehicle sales is maintained, as illustrated by the **BAU** scenario.

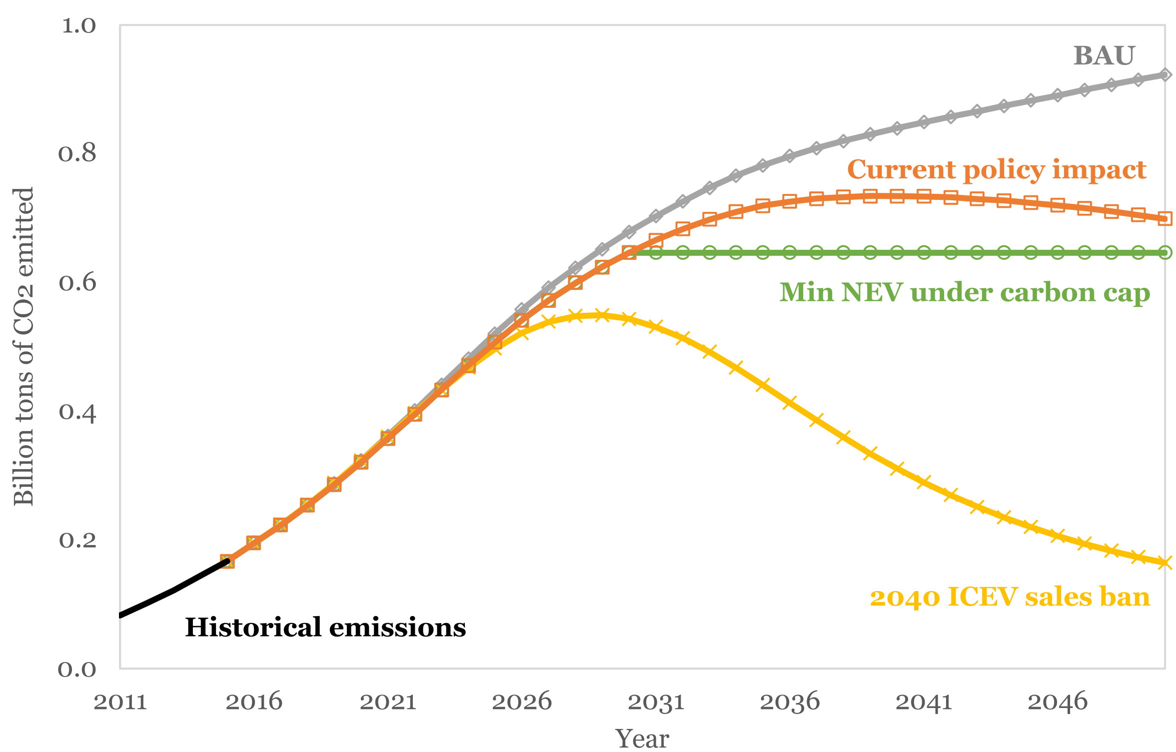

Figure 4-6 Projections of annual CO_2 emissions from urban private passenger vehicles in China under four NEV deployment scenarios (model results).

In fact, we find that about a third of urban passenger cars added to the road every year must be NEVs in order to cap carbon emissions after 2030. If, until then, the current increase in NEV sales enabled by public policies is maintained but not further expanded, stabilizing carbon emissions after 2030 would force a sharp and sudden increase in new NEV sales in 2031 compared to previous years, as shown by the **Min NEV under CC** curve in Figure 4-7. The annual increase in the share of NEV sales would then slow down in later years, as car ownership growth plateaus.

In the **Current Policy Impact** scenario, the number of NEVs on the road will fall short of, first, the 2020 target of 5 million NEVs as set by the State Council and reiterated by the Electric Vehicles Initiative and, second, the minimum deployment level needed to cap emissions after 2030. As a consequence, if the current pace at which NEV sales increase per year is maintained but not intensified by more stringent policy to further increase electric car deployment rate, CO_2 emissions will keep increasing after 2030, and will peak around 2040, or ten years after the official target.

When France's target is transposed to China, as demonstrated in the **2040 ICEV Sales Ban** scenario, emissions peak in 2027 with the carbon intensity assumptions described above.

A sensitivity analysis shows that, as the car ownership saturation level varies from 0.292 [416] to 0.807 [390], the peak year for CO_2 emissions varies between 2034 and 2050+, and between 2026 and 2028, for the **Current Policy Impact** and **2040 ICEV Sales Ban** scenarios, respectively.

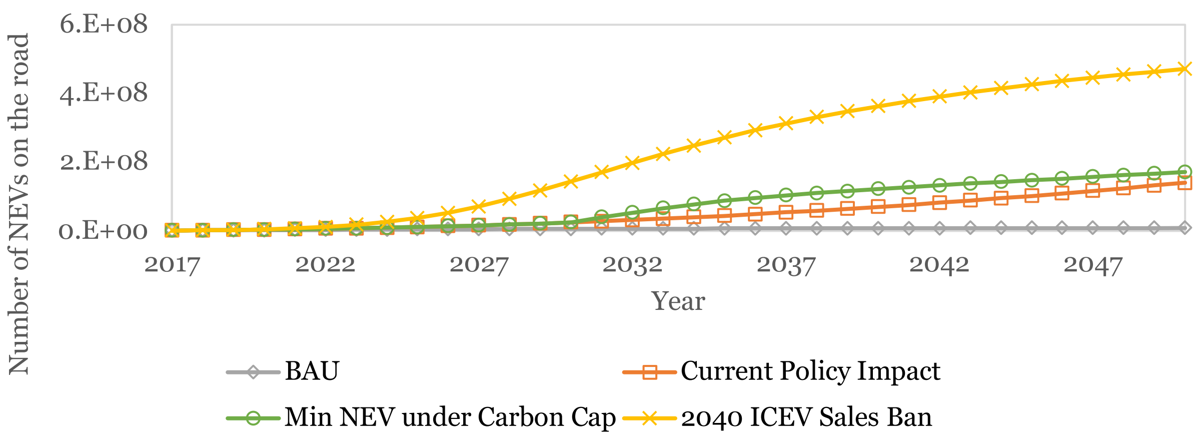

Figure 4-7 Modeled projections of circulating NEVs in China in the four scenarios.

The share of NEVs among circulating urban passenger cars in 2050 is 1.7%, 27.7%, 33.9% and 93.2% for the BAU, Current Policy Impact, Min NEV under Carbon Cap and 2040 ICEV Sales Ban, respectively. Only the green and yellow curves represent scenarios that are able to peak emissions by 2030.

Urban private passenger vehicle costs evolve similarly over time across scenarios (Figure 4-8). First, total costs increase as a consequence of both sharp increase in car ownership and increasing share of NEVs, which are more expensive than ICEVs in the near term. However, as the economics of both ICEVs and NEVs is expected to decrease over time, annual costs will reach a maximum around 2025-2026. As NEVs reach economic parity with comparable ICEVs around 2031, total costs are negatively correlated with NEV sales share after that year. From 2025 to 2050, total annual costs from urban passenger cars in China continuously decrease, although at a decreasing pace as NEV technology and market become more mature.

Costs in the **Current-Policy Impact** scenario are close to those of the **Min NEV under CC** scenario: while the increasing pace of NEV deployment enabled by current policies is not rapid enough to meet the carbon peak in 2030, there exist alternatives that, at similar costs, enable to cap CO_2 emissions after 2030. Despite higher costs in the medium term, annual costs in the **2040 ICEV Sales Ban** scenario fall below costs of the **BAU** scenario after 2032. Therefore, the **2040 ICEV Sales Ban** scenario requires stringent policies in the short run to encourage NEV adoption despite its higher costs relatively to ICEVs in the short run. Over the entire 2017-2050 period, total cumulative costs are highest in scenarios that do not meet the carbon peak in 2030. The **2040 ICEV Sales Ban** scenario shows lowest cumulative costs among all four scenarios.

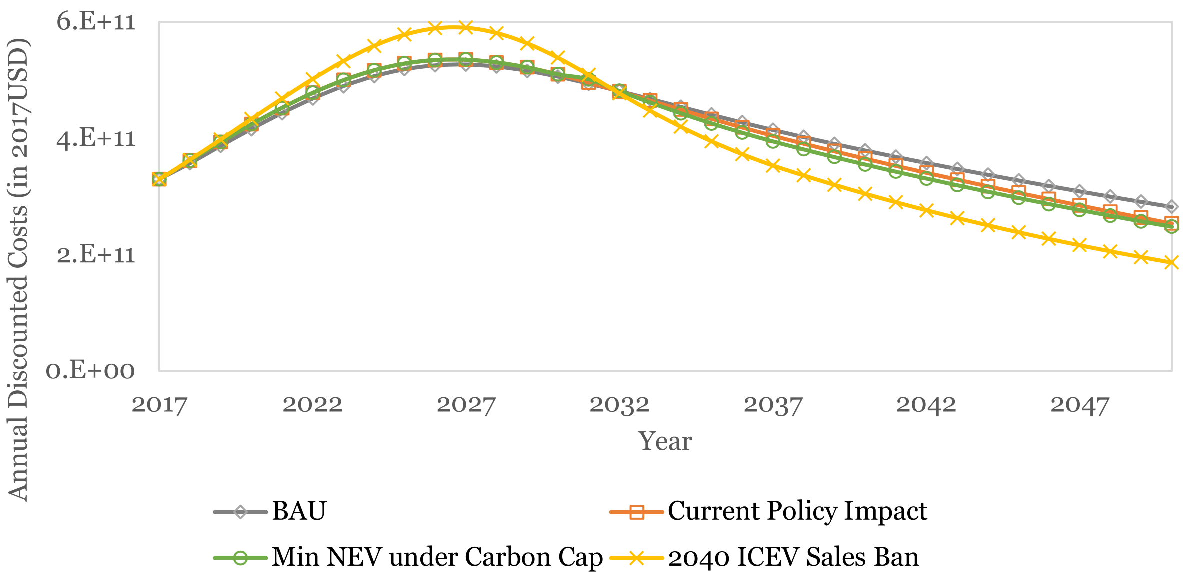

Figure 4-8 Net present cost of urban passenger vehicles (consumer and infrastructure levels) in China in the four scenarios using an annual discount rate of 5%.

Total annual discounted costs of the national urban passenger car fleet—ICEVs and NEVs—vary from $330 billion in 2017 to between $186 billion (2040 ICEV Sales Ban scenario) and $282 billion (BAU scenario) in 2050.

The national consumption of gasoline varies considerably across NEV deployment scenarios. In 2016, the annual gasoline consumption from urban passenger cars in China was 98 billion liters while its total motor gasoline production was 282 billion liters [417]. In 2050, the annual gasoline consumption varies by a factor of ten between the **BAU** (417 billion liters per year) and the **ICEV 2040 Sales Ban** (29 billion liters per year) scenarios. In the **Min NEV under Carbon Cap** scenario, gasoline consumption slowly decreases after 2030, from 290 billion liters in that year to 280 billion liters in 2050. Therefore, in scenarios where the 2030 carbon peak is not or barely met, China will have to considerably increase its national or foreign supply of crude oil and expand its current motor gasoline production. On the other hand, scenarios that encourage a pursued deployment of NEVs will allow for a progressive decrease of the current pressure on oil import.

Today, the load shape is rather flat across China due to the high share of industrial demand in overall power consumption [418]. The deployment of NEVs will gradually distort this flat shape over time. We calculate the daily load profile for NEV charging at the national level, making the optimistic assumption that smart charging measures will be implemented, although constrained by parking time probability and charging demand probability. Annual electricity consumption from NEVs will rise from 0.6 TWh in 2015 to between 18 TWh (**BAU**) and 958 TWh (**2040 ICEV Sales Ban**) in 2045, or on average +0.1% and +6.8% of the load in that year, respectively.

Besides temporal variations in probability of parking time and probability of charging, NEV power demand is assumed here to be uniformly distributed throughout the day. As a result, 32% of the daily charging load is met during the night, from midnight to 7am. If such smart charging measures are implemented to smooth out power demand, capping CO_2 emissions at their 2030 level would increase real-time national power demand by 2.4% on average throughout the day, in 2045. If ICEV sales are banned after 2040, real-time power demand can increase by up to 8.6% in 2045. However, the peak grid load could be much higher if no smart measures are implemented. In such case, the charging demand would be concentrated in specific hours—most likely late morning and evening hours—and an additional third of the daily load would have to be met during those few hours instead of being distributed across the night and early morning.

To meet the 2030 carbon peak in the urban passenger car sector, it will be necessary to adapt the current, rather inflexible, power grid either by providing large-scale storage able to release massive amount of electricity over a few hours in the morning and the evening, or by encouraging smart charging of NEVs [419], [420].

4.4 Conclusion

Given the particular nature of the 2030 CO_2 emissions peak target, the continuous decrease in carbon content of electricity will be a key enabler of the implementation of a carbon dioxide cap in the urban passenger transportation sector. However, it currently only varies by a few percent every year. In fact, the annual reduction in CO_2 emissions per NEV displacing ICEV is several orders of magnitude lower than the annual increase in CO_2 emissions from car ownership growth, from a few tons to several million tons. As a consequence, NEV deployment can only be efficient in meeting carbon targets if it is implemented at a considerably larger scale—between 15 and 20 million new NEVs every year after 2030—than it has been until today.

The Chinese government announced in September 2017 that it was working on a timetable to ban ICEV production and sales in a not-so-far future. Given the extent of current ICEV sales in the country—21 million new ICEVs sold in 2016, and 52 million expected to be sold in 2030 in a **BAU** scenario—, China must pave the way now to succeed in meeting such ambitious target in the next decades. To initiate a transition where ICEV sales are phased out by 2040, transposing France's target to China, we find that in the next ten years China will have to spend $0.4 trillion more than in a **BAU** scenario. In fact, whenever the temporal target for the ICEV ban, a large development of NEVs will undoubtedly require considerable additional investment in the short-term, as overall ICEV costs are expected to remain lower than NEV costs, including investment in new infrastructure, at least until 2031. However, over the 2050 horizon, the large-scale deployment of NEVs, along with a transition toward a cleaner power sector, becomes a cost-minimizing option to meet China's 2030 peak target while allowing urban passenger car growth at a reasonable level.

NEV deployment would also provide substantial non-financial benefits. In the past decades, China has been lagging behind in terms of technology R&D in the traditional automobile sector, as a majority of its ICEVs on the road are of foreign designs. The Chinese government has identified an opportunity for the country to take the lead at the global scale in NEV technology deployment—the "corner overtaking" strategy. Deploying NEVs would fuel this R&D strategy plan, which would in exchange finance additional technology programs.

The large-scale deployment of NEVs is found to be a promising pathway for China's decarbonization, given its positive impact on emissions reduction, long-term cost-efficiency, and its strategic aspect for national manufacturing and regional economic development. Yet, while governmental policy encouraging NEV purchase has helped their development in China, we find in this analysis that it has not been enough to initiate a meaningful car technology transition consistent with the country's environmental targets. In addition, quality issues and infrastructure limitations increasingly challenge the wide adoption of NEVs. In order to achieve China's double objective of technological excellence and large-scale deployment of NEVs, new policies are needed that are more inclusive and that favor inter-sectoral structural change.

China's electricity production and consumption landscape is evolving rapidly. The country has initiated reforms in the power sector, and the establishment of an interregional wholesale electricity market is near. Beyond industrial policy and purchase subsidies, an essential driver of the deployment of a globally leading NEV industry in China will be the initiation of national dynamic pricing in the retail electricity market, facilitating the integration of electric vehicles and the transition toward a cleaner power sector.

CHAPITRE 6 CONCLUSION

China has become the "world's factory" and lifted up several millions of people out of poverty through decades of market-oriented reforms. However, this socio-economic development, fueled by coal, has heavily impacted the environment. The "China Dream," as coined by the central government, reflects the conviction that there exists a successful path for the country to harmonize its recent economic development with radical environmental and social improvements. As challenges are as great as the opportunity—China is both the global largest polluter and largest developer of low-carbon energies—this transition is no easy task. Focusing on climate urgency, this study provides a fine-grain analysis of China's power sector decarbonization potential. Using large datasets of technical, economic and social factors, it proposes new modeling frameworks to analyze levers of the clean power transition, by quantifying and comparing their decarbonization potential, technical feasibility, and cost efficiency over time and across regions and sectors.

The centralized planning approach, personified by its chief planning agency the NDRC, is the country's main strength for building a sustainable future. However, central planning also has well-known disadvantages, such as risks of over-standardization and communication challenges between central decision-makers and local decision-implementers. The diversity of the national territory warrants a planning process that encourages synergetic use of various riches, across provinces and across sectors, while ensuring that the planning design process accounts for local, practical constraints. In particular, sector-specific, mega-engineering schemes, such as the WEETP and the SNWTP, increase financial, environmental and social risks and accentuate the development gap between Northeastern and Southwestern China. The belief behind the development of these massive projects rests upon the inexact idea that national-level geographic mismatch much be solved. China has a resource-rich territory, a chance for transiting to clean power. However, a closer look at regional resource disparities, and at the increasing importance of temporal disparities following larger VRE penetration, reveals the impossibility to enact this transition with a "one size fits all" policy. This study shows that there exist other, potentially unconventional, solutions for smaller-scale clean water and power supply that can be tailored to local characteristics, reducing technical and economic risks.

The high-resolution SWITCH-China model was developed and used to explore future province-level implications of meeting national-level CO_2 emission reduction and technology deployment objectives. SWITCH was uniquely built to recognize the grid operation challenge posed by VREs, expected to experience a double-digit growth in the next decades, and to select optimal flexibility measures to be implemented by comparing their technical, economic and environmental performances. Optimal energy source choices for China's future electricity mix were found to highly depend on how technological costs will evolve in the next years. As an example, when VRE system cost were projected to follow a steep decline in the next ten years, the model found it most economical to operate a rather inflexible mix with VREs and baseload plants, despite resulting high curtailment levels. In this scenario, natural gas was also favored in the near-future as a mature technology for rapidly bringing some flexibility to the grid, despite its high costs. In contrast, when longer-term carbon constraints were applied, large-scale storage was favored to accommodate intermittency. In particular, results showed that deep decarbonization, defined as an 80% reduction in CO_2 emissions by 2050 in line with the IPCC's 2°C target, is achievable through the concomitant deployment of nuclear—inland, encouraged by state programs for advanced nuclear technology design development—, coal with carbon CCS, VREs, in addition to interregional transmission lines and storage. Meeting this long-term goal would increase the costs of generating and supplying electricity by at least 30% compared to an unconstrained scenario. Many of these technologies have not reached a mature stage or have not been deployed at utility-scale today. The success of this transition will therefore depend on the country's ability to encourage technological and economic innovation.

A modular approach to reduce uncertainty, adaptable to traditional cost-minimizing approaches used by planning agencies, was proposed. By accounting for uncertainty on future costs, this study found that there exist alternatives to the least-cost strategy, which present slightly higher overall electricity costs, but much lower risks on costs. In particular, given the predominance of fossil fuel in the current electricity mix, the deployment of nuclear energy and VREs would decrease the overall risk on future costs through diversification, even when accounting for increased operational complexity resulting from VRE intermittency.

More generally, there exist a least-risk configuration size for the electricity mix infrastructure, at a sub-national but inter-provincial level. This configuration favors local usage of resources, especially wind and solar, ensuring a resilient system base for electricity supply by increasing autonomy, but also encourages the development of interprovincial transmission lines to decrease supply risks through diversification, up to a certain limit. While further investigation is needed to evaluate the size of these hypothetical zones, preliminary results showed that existing regional grids might actually be good candidates of this least-risk configuration. At the other end of official plans to build a national grid, this study suggests that regional grids should improve in self-reliance by coordinating resource management and supply across sectors. In fact, a radical rethinking of resource management practices is needed in China.

A majority of regions possess local resources that can be reliably used, provided that the infrastructure is upgraded. On the water side, given the current power overcapacity in China, a fraction of the heat in nuclear reactors could instead be used in thermal desalination plants. Using official nuclear power expansion plans, analyses described in this study showed that a nuclear desalination expansion program could enable the production of 20 km^3 of fresh water in 2030, doubling current renewable water resource supply in water-scarce provinces. Fresh water supply from desalination was found to be 1.5 times to 3.5 times more expensive than from the SNWTP, depending on the distance between the plant and the demand center, but its carbon intensity is six times lower. In addition, nuclear desalination—including both fresh water production and transportation from the coast to demand centers—was shown to be affordable even to households in the lowest income bracket.

Coordinating the power grid, including non-dispatchable VREs, with controllable RO desalination creates a local supply system of a virtually infinite source of fresh water for China's developed Eastern provinces, while decreasing power curtailment. Desalination, used as a deferrable load, can transform two low-value products, seawater and excess power, in a high-value product, fresh water. The DESEC model was developed and applied to the NCG region, suffering from an annual water deficit of 61.4 billion m^3. Results showed that the region can become self-reliant in power supply by 2020, without inter-regional transmission, provided that intra-NCG power connectivity is deployed. The general decarbonization and water scarcity context, and the specific cost structure, suggest that deferrable desalination be deployed at large scale to provide a sustainable solution to NCG's absolute water scarcity, clean energy transition and power curtailment at once. The resulting cost of supplying fresh water—including power and desalination systems construction, operation and water transportation—was calculated at $1.5/$m^3$, less than the global average water price.

Generally, this study found that optimal water supply strategies vary across water-scarce provinces. The Western route, rooted in China's Western region, could be dedicated to alleviating scarcity in inland provinces such as Gansu and Ningxia. On the other hand, nuclear- or grid-powered desalination should be favored in Eastern provinces, which either have a direct access to seawater such as Beijing and Shandong, or are adjacent to coastal provinces, such as Shanxi. In these regions, desalination was found to be affordable, more environmentally friendly and less disruptive for populations and landscapes than the SNWTP. In both cases, desalination presents the double opportunity of alleviating water scarcity while virtually eliminating curtailment from wind power.

In addition to clean power transition and water-power coordination, the transportation sector was analyzed as a potential decarbonization lever. In recent years, discussions have revolved around national CO_2 emissions peaking before the 2030 target thanks to measures implemented in mature industries. The transportation sector, poised for massive expansion, tells a different story. On average across provinces, urban car ownership is at Stage II of the deployment sigmoid curve and will not start plateauing before 2024 at the earliest. In addition, while electrification of public transportation has been impressive, urban passenger vehicles follow another trend. Despite China becoming the largest market for NEVs, NEV sales today represent less than 2% of total passenger car sales. Adopting a GDP-dependent Gompertz function to derive urban passenger car ownership projections until 2050, this study proposed a modeling framework to explore the deployment of NEVs and their impact on emissions, costs, and fuel consumption. Findings showed that their large-scale deployment cannot be enabled by short-term technology cost decrease alone. If the current annual increase in number of NEVs resulting from favorable policy were maintained but not amplified, CO_2 emissions from urban passenger cars would peak around 2040, or ten years past the official target. However, it is not too late to choose one of several alternative paths, with similar costs yet calling for more stringent policy, compliant with China's emission target. As the Chinese government currently works on a timetable to implement a ban on ICEV, France's 2040 ICEV sales ban target was applied in the China model. This scenario was found to enable the country to meet its emission goals at lower costs than a business-as-usual or other less stringent scenarios but demands larger near-term investments. In fact, results showed that, as long as a system transition is operated to limit power sector CO_2 emissions under the official 2020 and 2030 targets, large-scale vehicle electrification is the least-cost, least-CO_2-emission pathway for China's urban transportation expansion in the long run, provided that investment is made to encourage electric vehicle adoption in the near future.

More generally, through its central planning approach, the Chinese government has engaged the country in a long, steady march toward social, economic and environmental sustainability. Although many challenges remain, past achievements in poverty reduction, increased social services, higher industrial quality, and global lead in low-carbon technology development and deployment, have shown that the method is working. The ongoing success of the "Socialism with Chinese characteristics" is even more striking when compared with irrational, short-term, contradictory policies implemented in Western countries, following political fluctuation. Yet, stranded investments, such as ghost towns and underused power plants, show the limits of vertical planning when it is not informed by insights into local characteristics and constraints. Models developed, used and presented in this study, revealed the existence of viable, cost-efficient strategies to enable meaningful decarbonization, while alleviating water scarcity and urban gasoline pollution. These strategies cannot be achieved without combining central-scale coordination with local-scale implementation, in order to take advantage of China's diverse and rich territory while minimizing implementation risks. Results also revealed that massive investment is needed in R&D and infrastructure capacity deployment, and that utilities and institutions must be reformed to manage resources rationally, hand-in-hand. Developing more reliable models to help policy-makers grasp the potential consequences of different planning decisions and scenarios is a necessity. While models developed for this study analyzed the technical and economic relevance of decarbonization levers for electricity, water and transportation, future work should focus on including institutional and social uncertainty. In fact, pursuing power sector and resource management reforms—including price rationalization—, planning capital project expenditure through new financial mechanisms, and ensuring population participation in DR programs and new driving patterns, will be crucial to enable the clean energy transition in the decades to come.

REFERENCES

[1] World Nuclear Association, "Advanced Nuclear Power Reactors." [Online]. Available: http://www.world-nuclear.org/information-library/nuclear-fuel-cycle/nuclear-power-reactors/advanced-nuclear-power-reactors.aspx.

[2] International Atomic Energy Agency, "Advanced Reactors Information System (ARIS)." [Online]. Available: https://aris.iaea.org/.

[3] Q. Wang, "China needing a cautious approach to nuclear power strategy," *Energy Policy*, vol. 37, no. 7, pp. 2487–2491, 2009.

[4] World Nuclear Association, "China Nuclear Power," 2017. [Online]. Available: http://www.world-nuclear.org/information-library/country-profiles/countries-a-f/china-nuclear-power.aspx.

[5] Z. Zhang *et al.*, "The Shandong Shidao Bay 200 MWeHigh-Temperature Gas-Cooled Reactor Pebble-Bed Module (HTR-PM) Demonstration Power Plant: An Engineering and Technological Innovation," vol. 2, no. 1, pp. 112–118, 2016.

[6] D. Wang and Y. Lu, "Roles and prospect of nuclear power in China's energy supply strategy," *Nucl. Eng. Des.*, vol. 218, pp. 3–12, 2002.

[7] The World Bank, "The World Bank in China: Overview," 2017. [Online]. Available: http://www.worldbank.org/en/country/china/overview.

[8] D. Barton, Y. Chen, A. Jin, and McKInsey & Company, "Mapping China's middle class," 2017. [Online]. Available: http://www.mckinsey.com/industries/retail/our-insights/mapping-chinas-middle-class.

[9] S. Göss, "China's renewable energy revolution continues its long march," *Energy Post*, 13-Feb-2017.

[10] Y. Su, P. Tesfazion, and Z. Zhao, "Where are the migrants from? Inter- vs. intra-provincial rural-urban migration in China," *China Econ. Rev.*, vol. 47, no. August 2017, pp. 142–155, 2018.

[11] M. Sun and C. Cindy Fan, "China's permanent and temporary migrants: Differentials and changes, 1990–2000," *Prof. Geogr.*, vol. 63, no. 1, pp. 92–112, 2011.

[12] X. Guan, H. Wei, S. Lu, Q. Dai, and H. Su, "Assessment on the urbanization strategy in China: Achievements, challenges and reflections," *Habitat Int.*, vol. 71, no. December 2017, pp. 97–109, 2018.

[13] B. Su, A. Heshmati, Y. Geng, and X. Yu, "A review of the circular economy in China: Moving from rhetoric to implementation," *J. Clean. Prod.*, vol. 42, pp. 215–227, 2013.

[14] B. Yuan, S. Ren, and X. Chen, "The effects of urbanization, consumption ratio and consumption structure on residential indirect CO2 emissions in China: A regional comparative

analysis," *Appl. Energy*, vol. 140, pp. 94–106, 2015.

[15] B. Lin and J. Zhu, "Changes in urban air quality during urbanization in China," *J. Clean. Prod.*, vol. 188, pp. 312–321, 2018.

[16] K. Luo *et al.*, "Impacts of rapid urbanization on the water quality and macroinvertebrate communities of streams: A case study in Liangjiang New Area, China," *Sci. Total Environ.*, vol. 621, pp. 1601–1614, 2018.

[17] M. Liu, X. Liu, Y. Huang, Z. Ma, and J. Bi, "Epidemic transition of environmental health risk during China's urbanization," *Sci. Bull.*, vol. 62, no. 2, pp. 92–98, 2017.

[18] J. G. J. Olivier, K. M. Schure, and J. A. H. W. Peters, "Trends in Global CO2 and Total Greenhouse Gas Emissions: Summary of the 2017 report," 2017.

[19] D. Zhao, H. Chen, X. Li, and X. Ma, "Air pollution and its influential factors in China's hot spots," *J. Clean. Prod.*, vol. 185, 2018.

[20] STEPS centre, "Ecological Civilisation," 2015.

[21] G. Janssens-Maenhout *et al.*, "EDGAR v4.3.2 Global Atlas of the three major Greenhouse Gas Emissions for the period 1970–2012," *Earth System Science Data Discussions*, Aug-2017. [Online]. Available: https://www.earth-syst-sci-data-discuss.net/essd-2017-79/.

[22] X. Zhao, X. Yu, Y. Wang, and C. Fan, "Economic evaluation of health losses from air pollution in Beijing, China," *Environ. Sci. Pollut. Res.*, vol. 23, no. 12, pp. 11716–11728, 2016.

[23] D. Guan and K. Hubacek, "A new and integrated hydro-economic accounting and analytical framework for water resources: A case study for North China," *J. Environ. Manage.*, vol. 88, no. 4, pp. 1300–1313, 2008.

[24] D. Han, M. J. Currell, and G. Cao, "Deep challenges for China's war on water pollution," *Environ. Pollut.*, vol. 218, pp. 1222–1233, 2016.

[25] G. Shuzhong *et al.*, "Ensuring water resource security in China; the need for advances in evidence-based policy to support sustainable management," *Environ. Sci. Policy*, vol. 75, no. October 2016, pp. 65–69, 2017.

[26] Y. Qin, E. Curmi, G. M. Kopec, J. M. Allwood, and K. S. Richards, "China's energy-water nexus - assessment of the energy sector's compliance with the '3 Red Lines' industrial water policy," *Energy Policy*, vol. 82, no. 1, pp. 131–143, 2015.

[27] M. Flörke, E. Kynast, I. Bärlund, S. Eisner, F. Wimmer, and J. Alcamo, "Domestic and industrial water uses of the past 60 years as a mirror of socio-economic development: A global simulation study," *Glob. Environ. Chang.*, vol. 23, no. 1, pp. 144–156, 2013.

[28] United Nations and Food and Agriculture Organization, "AQUASTAT: China," 2012.

[29] X. Zheng, D. Chen, Q. Wang, and Z. Zhang, "Seawater desalination in China: Retrospect and prospect," *Chem. Eng. J.*, vol. 242, pp. 404–413, 2014.

[30] A. Wang, "New Year present for China seawater desalination: the national 13th Five-Year

Plan," 2016. [Online]. Available: http://www.umoregroup.com/project.aspx?id=2097.

[31] Desalination.biz, "China publishes details of country's desalination capacity," *Faversham House Group Ltd*, 19-Jul-2017.

[32] J. Liu, S. Chen, H. Wang, and X. Chen, "Calculation of Carbon Footprints for Water Diversion and Desalination Projects," *Energy Procedia*, vol. 75, pp. 2483–2494, 2015.

[33] J. Berkoff, "China : The South–North Water Transfer Project — is it justified ?," *Water Policy*, vol. 5, pp. 1–28, 2003.

[34] A. Jaffe and K. Schneider, "A Dry and Anxious North Awaits China's Giant, Unproven Water Transport Scheme," *Circle of Blue WaterNews*, 01-Mar-2011.

[35] Q. Tian, "Providing Sustainable Water Services to Cities : The Chinese Experiences."

[36] C. Lamb, "How should business react to China's water crisis?," *World Economic Forum*, 21-Jul-2016.

[37] N. P. Koptseva, "The Chinese Dream through the mirror of modern social research," vol. 2, pp. 374–393, 2016.

[38] X. Wei and Q. Li, "The Confucian Value of Harmony and its Influence on Chinese Social Interaction," *Cross-Cultural Commun.*, vol. 9, no. 1, pp. 60–66, 2013.

[39] Chinadaily.com.cn, "Scientific Outlook on Development," 08-Sep-2010.

[40] M. Avery, *From Bethune's Birthplace To The PR China*. 2013.

[41] J. Pan, *China's Environmental Governing and Ecological Civilization*. Heidelberg: Springer-Verlag Berlin Heidelberg, 2016.

[42] Q. Wang and X. Chen, "China's electricity market-oriented reform: From an absolute to a relative monopoly," *Energy Policy*, vol. 51, pp. 143–148, 2012.

[43] S. Xu and W. Chen, "The reform of electricity power sector in the PR of China," *Energy Policy*, vol. 34, no. 16, pp. 2455–2465, 2006.

[44] C. C. Ni, "Reform in China's Electric Power Industry - A Case Study of East China's Wholesale Electric Power Market," Institute of Electrical Engineers of Japan, 2006.

[45] H. W. Ngan, "Electricity regulation and electricity market reforms in China," *Energy Policy*, vol. 38, no. 5, pp. 2142–2148, 2010.

[46] B. An, W. Lin, A. Zhou, and W. Zhou, "China's Market-Oriented Reforms in the Energy and Environmental Sectors," p. 24, 2015.

[47] K. S. Gallagher, "Into the Dragon's Den," in *The Globalization of Clean Energy Technology lessons from China*, The MIT Press, 2014, p. 278.

[48] J. Kejun, H. Xiulian, L. Qiang, Z. Songli, and Z. Xing, "Modeling Development and Emission Scenario Analysis in China."

[49] M. Zeng, Y. Yang, L. Wang, and J. Sun, "The power industry reform in China 2015: Policies, evaluations and solutions," *Renew. Sustain. Energy Rev.*, vol. 57, pp. 94–110, 2016.

[50] "China Passes Renewable Energy Law," *Renewable Energy World*, 09-Mar-2005.

[51] *Law of the People's Republic of China on Prevention and Control of Radioactive Pollution*. Standing Committee of the National People's Congress, 2003.

[52] *Nuclear Safety Law of the People's Republic of China*. Standing Committee of the National People's Congress.

[53] "New nuclear safety law for China," *Nuclear Engineering International*, 06-Sep-2017.

[54] E. T. Yeh and J. I. Lewis, "State power and the logic of reform in china's electricity sector," *Pac. Aff.*, vol. 77, no. 3, pp. 437–465, 2004.

[55] S. Wilson, Y. Yang, and J. Kuang, "China's Electricity Sector," in *China's Domestic Transformation in a Global Context*, S. Ligang, R. Garnaut, C. Fang, and L. Johnston, Eds. 2006, pp. 175–211.

[56] M. G. Pollitt, C.-H. Yang, and H. Chen, "Reforming the Chinese Electricity Supply Sector: Lessons from International Experience," 2017.

[57] X. J. Yang, H. Hu, T. Tan, and J. Li, "China's renewable energy goals by 2050," *Environ. Dev.*, vol. 20, no. October, pp. 83–90, 2016.

[58] H. Bin Zhang, H. C. Dai, H. X. Lai, and W. T. Wang, "U.S. withdrawal from the Paris Agreement: Reasons, impacts, and China's response," *Adv. Clim. Chang. Res.*, vol. 8, no. 4, pp. 220–225, 2017.

[59] "2017 electricity & other energy statistics," *China Energy Portal | 中国能源门户*, 2018. [Online]. Available: https://chinaenergyportal.org/en/2017-electricity-energy-statistics/.

[60] K. Wu, *Energy economy in China : policy imperatives, market dynamics, and regional developments*. Singapore: World Scientific Publishing Co., Pte. Ltd., 2013.

[61] Statista from National Bureau of Statistics of China, "Power consumption in China in 2016, by region (in TWh)." [Online]. Available: https://www.statista.com/statistics/278792/power-consumption-in-china-by-region/.

[62] Lawrence Berkeley National Laboratory, *China Energy Databook Version 9.0*. Berkeley, 2016.

[63] Y. Zhang, N. Tang, Y. Niu, and X. Du, "Wind energy rejection in China: Current status, reasons and perspectives," *Renew. Sustain. Energy Rev.*, vol. 66, pp. 322–344, 2016.

[64] J. Byrne, Y.-D. Wang, A. Zhou, J. Tian, X. Zhang, and J. Wei, "A review of China's renewable energy policies and potentials," 2005.

[65] World Nuclear Association, "Nuclear Power in China," 2018. [Online]. Available: http://www.world-nuclear.org/information-library/country-profiles/countries-a-f/china-nuclear-power.aspx.

[66] "China's April power capacity near record even as Beijing curbs excess," *Reuters*, 16-May-2017.

[67] M. Zeng, S. Wang, J. Duan, J. Sun, P. Zhong, and Y. Zhang, "Review of nuclear power development in China: Environment analysis, historical stages, development status, problems and countermeasures," *Renew. Sustain. Energy Rev.*, vol. 59, pp. 1369–1383, 2016.

[68] World Nuclear News, "Nuclear growth revealed in China's new Five-Year Plan," World Nuclear News, 23-Mar-2016.

[69] J. Yang, Q. Liu, X. Li, and X. Cui, "Overview of Wind Power in China: Status and Future," *Sustainability*, vol. 9, no. 8, p. 1454, 2017.

[70] J. Tollefson, "CO2 emissions set to spike in 2017," *Nature*, vol. 551, no. 7680, p. 283, 2017.

[71] J. Yuan *et al.*, "Coal power overcapacity and investment bubble in China during 2015–2020," *Energy Policy*, vol. 97, pp. 136–144, 2016.

[72] J. Lin, F. Kahrl, and X. Liu, "A regional analysis of excess capacity in China's power systems," *Resour. Conserv. Recycl.*, vol. 129, no. November 2017, pp. 93–101, 2018.

[73] "China's 2016/2017 Restrictions on Development of Coal-Fired Power Capacity," *SourceWatch*. [Online]. Available: https://www.sourcewatch.org/index.php/China%27s_2016/2017_Restrictions_on_Development_of_Coal-Fired_Power_Capacity.

[74] Modern Markets Intelligence Inc. (MMI), "New ISO-NE rules would broaden economic dispatch," *PowerMarketsToday*.

[75] F. Kahrl, J. H. Williams, and J. Hu, "The political economy of electricity dispatch reform in China," *Energy Policy*, vol. 53, pp. 361–369, 2013.

[76] Y. Zhou and S. Lu, "China's Renewables Curtailment and Coal Assets Risk Map Research Findings and Map User Guide," 2017.

[77] G. Luo, E. Dan, X. Zhang, and Y. Guo, "Why the Wind Curtailment of Northwest China Remains High," *Sustainability*, vol. 10, no. 3, p. 570, 2018.

[78] "China wasted enough renewable energy to power Beijing for an entire year, says Greenpeace," *South China Morning Post*, 19-Apr-2017.

[79] C. Liu, "Facing Grid Constraints, China Puts a Chill on New Wind Energy Projects | InsideClimate News," *Inside Climate News*, 28-Mar-2016.

[80] L. Yuanyuan, "Wind Power Curtailment in China on the Mend," *Renewable Energy World*, 26-Jan-2018.

[81] NDRC, "Electric Power Development Planning (2016-2020)," pp. 1–41, 2017.

[82] "13th FYP development plan for the electricity sector," *China Energy Portal | 中国能源门户*, 2016. [Online]. Available: https://chinaenergyportal.org/en/13th-fyp-for-the-electricity-sector-full-text/.

[83] "China Seeks to Expand Electricity Networks," *Stratfor*, 2014. [Online]. Available:

https://worldview.stratfor.com/article/china-seeks-expand-electricity-networks.

[84] "China's West-East Electricity Transfer Project," *Wilson Center*. [Online]. Available: https://www.wilsoncenter.org/wilsonweekly/chinas-west-east-electricity-transfer-project.html.

[85] G. He *et al.*, "SWITCH-China: A Systems Approach to Decarbonizing China's Power System," *Environ. Sci. Technol.*, vol. 50, no. 11, 2016.

[86] R. Ran, "Understanding Blame Politics in China's Decentralized System of Environmental Governance: Actors, Strategies and Context," *China Q.*, vol. 231, no. August 2017, pp. 634–661, 2017.

[87] M. S. Ho, Z. Wang, and Z. Yu, "China's Power Generation Dispatch," 2017.

[88] T. Hancock, "China targets aggressive coal capacity cuts to 2020," *Financial Times*, Shanghai, 03-Jan-2017.

[89] J. Sultoon and P. Sharma, "China's coal policy: a victim of its own success?," *Financial Times*, 23-Mar-2017.

[90] X. Shi, B. Rioux, and P. Galkin, "Unintended consequences of China's coal capacity cut policy," *Energy Policy*, vol. 113, no. September 2017, pp. 478–486, 2018.

[91] A.-P. Avrin, G. He, and D. M. Kammen, "Assessing the impacts of nuclear desalination and geoengineering to address China's water shortages," *Desalination*, vol. 360, pp. 1–7, 2015.

[92] A.-P. Avrin, S. J. Moura, and D. M. Kammen, "Minimizing Cost Uncertainty with a New Methodology for Use In Policy Making : China's Electricity Pathways," in *Asia-Pacific Power and Energy Engineering Conference. IEEE/PES.*, 2016, pp. 1–7.

[93] A.-P. Avrin, G. He, and D. M. Kammen, "Relevance of Nuclear Desalination as an Alternative to Water Transfer Geoengineering Projects: Example of China," in *Renewable Energy Powered Desalination Handbook*, Elsevier, 2018, pp. 265–286.

[94] Y. Vogt, CEM, and MBA, "Top-down energy modeling," *Strateg. Plan. Energy Environ.*, vol. 22, no. 4, pp. 64–79, 2003.

[95] C. Böhringer and T. F. Rutherford, "Integrated assessment of energy policies: Decomposing top-down and bottom-up," *J. Econ. Dyn. Control*, vol. 33, no. 9, pp. 1648–1661, 2009.

[96] S. N. Chandramowli and F. A. Felder, "Impact of climate change on electricity systems and markets - A review of models and forecasts," *Sustain. Energy Technol. Assessments*, vol. 5, pp. 62–74, 2014.

[97] Q. Chen, C. Kang, Q. Xia, and J. Zhong, "Power generation expansion planning model towards low-carbon economy and its application in China," *Power Syst. IEEE Trans.*, vol. 25, no. 2, pp. 1117–1125, 2010.

[98] A. Krook-Riekkola, C. Berg, E. O. Ahlgren, and P. Söderholm, "Challenges in top-down and bottom-up soft-linking: Lessons from linking a Swedish energy system model with a CGE

model," *Energy*, vol. 141, pp. 803–817, 2017.

[99] C. Bataille, H. Waisman, M. Colombier, L. Segafredo, and J. Williams, "The Deep Decarbonization Pathways Project (DDPP): insights and emerging issues," *Clim. Policy*, vol. 16, no. sup1, pp. S1–S6, 2016.

[100] P. Sullivan, K. Eurek, and R. Margolis, "Advanced Methods for Incorporating Solar Energy Technologies into Electric Sector Capacity-expansion Models: Literature Review and Analysis," 2014.

[101] N. S. Pearre and L. G. Swan, "Technoeconomic feasibility of grid storage: Mapping electrical services and energy storage technologies," *Appl. Energy*, vol. 137, pp. 501–510, 2015.

[102] J. Wang, L. Feng, L. Zhao, and S. Snowden, "China's natural gas: Resources, production and its impacts," *Energy Policy*, vol. 55, no. 2013, pp. 690–698, 2013.

[103] X. Dong, G. Pi, Z. Ma, and C. Dong, "The reform of the natural gas industry in the PR of China," *Renew. Sustain. Energy Rev.*, vol. 73, no. June 2015, pp. 582–593, 2017.

[104] B. Li, H. Yin, and F. Wang, "Will China's 'dash for gas' halt in the future?," *Resour. Conserv. Recycl.*, vol. 134, no. April, pp. 303–312, 2018.

[105] 中华人民共和国国家统计局 (National Bureau of Statistics of the People's Republic of China), "China Statistical Yearbook 2017," 2017. [Online]. Available: http://www.stats.gov.cn/tjsj/ndsj/2017/indexeh.htm.

[106] X. Dong and Z. Kong, "The impact of China's natural gas import risks on the national economy," *J. Nat. Gas Sci. Eng.*, vol. 36, pp. 97–107, 2016.

[107] H. Aolin and D. Qing, "On natural gas pricing reform in China," *Nat. Gas Ind. B*, vol. 2, no. 4, pp. 374–382, 2015.

[108] Y. Qin, F. Tong, G. Yang, and D. L. Mauzerall, "Challenges of using natural gas as a carbon mitigation option in China," *Energy Policy*, vol. 117, no. July 2017, pp. 457–462, 2018.

[109] R. A. Alvarez, S. W. Pacala, J. J. Winebrake, W. L. Chameides, and S. P. Hamburg, "Greater focus needed on methane leakage from natural gas infrastructure," *Proc. Natl. Acad. Sci.*, vol. 109, no. 17, pp. 6435–6440, 2012.

[110] C. Cany, C. Mansilla, G. Mathonnière, and P. da Costa, "Nuclear power supply: Going against the misconceptions. Evidence of nuclear flexibility from the French experience," *Energy*, vol. 151, pp. 289–296, 2018.

[111] International Atomic Energy Agency, "Non-baseload Operation in Nuclear Power Plants: Load Following and Frequency Control Modes of Flexible Operation," Vienna, 2018.

[112] Q. Yue, J. He, L. Stamford, and A. Azapagic, "Nuclear Power in China: An Analysis of the Current and Near-Future Uranium Flows," *Energy Technol.*, vol. 5, no. 5, pp. 681–691, 2017.

[113] K. Sun, S. Yuan, and Y. Qiu, "Development of UHV Power Transmission in China," in *Ultra-high Voltage AC/DC Power Transmission*, H. Zhou, W. Qiu, K. Sun, J. Chen, X. Deng, F. Qian,

D. Wang, Z. Bincai, J. Li, S. Li, Y. Qiu, and J. Yu, Eds. 2018.

[114] X. Li, "Decarbonizing China's power system with wind power : the past and the future," 2015.

[115] U.S. Department of Energy, "Global Energy Storage Database," 2018. [Online]. Available: http://www.energystorageexchange.org/projects/data_visualization.

[116] P. Denholm and G. L. Kulcinski, "Life cycle energy requirements and greenhouse gas emissions from large scale energy storage systems," *Energy Convers. Manag.*, vol. 45, no. 13–14, pp. 2153–2172, 2004.

[117] A. Berrada, K. Loudiyi, and I. Zorkani, "Profitability, risk, and financial modeling of energy storage in residential and large scale applications," *Energy*, vol. 119, pp. 94–109, 2017.

[118] Q. Gangliang, "Development of Pumped Storage Power Station in China," in *World Hydropower Congress*, 2017.

[119] W. Chandler *et al.*, "China's Future Generation: Assessing the Maximum Potential for Renewable Power Sources in China to 2050," 2014.

[120] C. J. Yang, "Opportunities and barriers to demand response in China," *Resour. Conserv. Recycl.*, vol. 121, pp. 51–55, 2017.

[121] P. Guo, V. O. K. Li, and J. C. K. Lam, "Smart demand response in China: Challenges and drivers," *Energy Policy*, vol. 107, no. December 2015, pp. 1–10, 2017.

[122] Y. Yu, "How to fit demand side management (DSM) into current Chinese electricity system reform?," *Energy Econ.*, vol. 34, no. 2, pp. 549–557, 2012.

[123] Z. Zhao, C. Yu, M. Yew, and M. Liu, "Demand side management: A green way to power Beijing," *J. Renew. Sustain. Energy*, vol. 7, no. 4, p. 041505, 2015.

[124] U.S. Department of Commerce, "2016 Top Markets Report Smart Grid: Country Case Study - China," 2016.

[125] A. Martens, "The energetic feasibility of CHP compared to the separate production of heat and power," *Appl. Therm. Eng.*, vol. 18, no. 11, pp. 935–946, 1998.

[126] J. Hui, W. Cai, M. Ye, and C. Wang, "Clean Generation Technologies in Chinese Power Sector: Penetration Thresholds and Supporting Policies," *Energy Procedia*, vol. 75, pp. 2807–2812, 2015.

[127] Energy Research Institute of Academy of Macroeconomic Research/NDRC and China National Renewable Energy Centre, "China Renewable Energy Outlook," 2017.

[128] The World Bank, "World Bank and ESMAP: long-term partners in China's energy transition," 2017.

[129] R. Spencer, P. Meier, and N. Berrah, "Scaling Up Renewable Energy in China : Economic Modeling Method and Application," no. 11, pp. 1–4, 2007.

[130] Energy Sector Management Assistance Program (ESMAP), World Bank Institute, and Department For International Development (DFID), "Planning for a Low Carbon Future,"

2012.

[131] China Energy Group, "China 2050 Demand Resources Energy Analysis Model (DREAM)." [Online]. Available: https://china.lbl.gov/tools/dream.

[132] N. Zhou, N. Z. Khanna, D. Fridley, and E. Franconi, "Transformative pathway for Chinese buildings by 2050," *Eceee 2015*, pp. 1373–1384, 2015.

[133] N. Z. Jiang Lin, David Fridley, Hongyou Lu, Lynn Price and Energy, "Near-term trends in China's coal consumption," 2018.

[134] H. Harvey, S. Aggarwal, C. Busch, J. Rissman, R. Orvis, and H. Kennan, "Climate and energy policy solutions for China," 2016.

[135] "China | Energy Policy Solutions," *Energy Innovation*, 2018. [Online]. Available: https://china.energypolicy.solutions/.

[136] International Energy Agency, "Energy Technology Perspectives 2017," 2017.

[137] Energy Research Institute (ERI) of the National Development and Reform Commission (NDRC), "Integrated Energy and Environment Policy Assessment Model for China (IPAC)." [Online]. Available: http://www.ipac-model.org/.

[138] K. J. Jiang, X. Zhuang, C. M. He, J. Liu, X. Y. Xu, and S. Chen, "China's low-carbon investment pathway under the 2 °C scenario," *Adv. Clim. Chang. Res.*, vol. 7, no. 4, pp. 229–234, 2016.

[139] K. Jiang and H. Chenmin, "Energy Options and Predictions for China," in *Future Energy: Improved, Sustainable and Clean Options for our Planet*, 2nd ed., 2013, pp. 679–692.

[140] Q. Chen, C. Kang, Q. Xia, and D. Guan, "Preliminary exploration on low-carbon technology roadmap of China's power sector," *Energy*, vol. 36, no. 3, pp. 1500–1512, 2011.

[141] Q. Wu and C. Peng, "Scenario Analysis of Carbon Emissions of China's Electric Power Industry Up to 2030," *Energies*, vol. 9, no. 12, p. 988, 2016.

[142] W. Cai, C. Wang, K. Wang, Y. Zhang, and J. Chen, "Scenario analysis on CO2 emissions reduction potential in China's electricity sector," *Energy Policy*, vol. 35, no. 12, pp. 6445–6456, 2007.

[143] L. Cai, J. Guo, and L. Zhu, "China's future power structure analysis based on LEAP," *Energy Sources, Part A Recover. Util. Environ. Eff.*, vol. 35, no. 22, pp. 2113–2122, 2013.

[144] P. Mischke, "China's 'energy revolution': measuring the status quo, modelling regional dynamics and assessing global impacts," 2015.

[145] Z. Guo, L. Ma, P. Liu, I. Jones, and Z. Li, "A long-term multi-region load-dispatch model based on grid structures for the optimal planning of China's power sector," *Comput. Chem. Eng.*, vol. 102, pp. 52–63, 2017.

[146] P. De Laquil, C. Wenying, and E. D. Larson, "Modeling China's energy future," *Energy Sustain. Dev.*, vol. 7, no. 4, pp. 40–56, 2003.

[147] Grantham Institute for Climate Change and International Institute for Applied Systems Analysis, "China's energy technologies to 2050," 2012.

[148] Q. Liu, M. Shi, and K. Jiang, "New power generation technology options under the greenhouse gases mitigation scenario in China," *Energy Policy*, vol. 37, no. 6, pp. 2440–2449, 2009.

[149] B. W. Yi, J. H. Xu, and Y. Fan, "Inter-regional power grid planning up to 2030 in China considering renewable energy development and regional pollutant control: A multi-region bottom-up optimization model," *Appl. Energy*, vol. 184, pp. 641–658, 2016.

[150] D. Zhang, P. Liu, L. Ma, Z. Li, and W. Ni, "A multi-period modelling and optimization approach to the planning of China's power sector with consideration of carbon dioxide mitigation," *Comput. Chem. Eng.*, vol. 37, pp. 227–247, 2012.

[151] D. Zhang, P. Liu, L. Ma, and Z. Li, "A multi-period optimization model for optimal planning of China's power sector with consideration of carbon mitigation-The optimal pathway under uncertain parametric conditions," *Comput. Chem. Eng.*, vol. 50, pp. 196–206, 2013.

[152] D. Zhang, P. Liu, L. Ma, and Z. Li, "A multi-period optimization model for planning of China's power sector with consideration of carbon dioxide mitigation-The importance of continuous and stable carbon mitigation policy," *Energy Policy*, vol. 58, pp. 319–328, 2013.

[153] J. Liu, W. Chen, and D. Liu, "Scenario analysis of China's future energy demand based on TIMES model system," *Energy Procedia*, vol. 5, pp. 1803–1808, 2011.

[154] W. Chen, X. Yin, and H. Zhang, "Towards low carbon development in China: a comparison of national and global models," *Clim. Change*, vol. 136, no. 1, pp. 95–108, 2016.

[155] P. Mischke and K. B. Karlsson, "Modelling tools to evaluate China's future energy system - A review of the Chinese perspective," *Energy*, vol. 69, pp. 132–143, 2014.

[156] M. Fripp, "Optimal Investment in Wind and Solar Power in California (Ph.D. dissertation)," University of California, Berkeley, United States, 2008.

[157] M. Fripp, "Switch: a planning tool for power systems with large shares of intermittent renewable energy.," *Environ. Sci. Technol.*, vol. 46, no. 11, pp. 6371–8, Jun. 2012.

[158] J. Nelson *et al.*, "High-resolution modeling of the western North American power system demonstrates low-cost and low-carbon futures," *Energy Policy*, vol. 43, pp. 436–447, Apr. 2012.

[159] D. P. De Leon Barido, J. Johnston, M. V Moncada, D. Callaway, and D. M. Kammen, "Evidence and future scenarios of a low-carbon energy transition in Central America: A case study in Nicaragua," *Environ. Res. Lett.*, vol. 10, no. 10, 2015.

[160] National Development and Reform Commission of China, "Enhanced Actions on Climate Change: China's intended nationally determined contributions," 2015.

[161] "China Overview," *Climate Action Tracker*, 2017. [Online]. Available: https://climateactiontracker.org/countries/china/.

[162] G. Gisela, "China's shift to clean energies," 2015.

[163] "Wind Development 12th Five Year Plan," National Energy Administration, National Development and Reform Commission, 2012.

[164] China National Energy Administration, "Solar Power Development 12th Five-year Plan," Beijing, Jul. 2012.

[165] The White House Office of the Press Secretary, "U.S.-China Joint Announcement on Climate Change," Beijing, 12-Nov-2014.

[166] China State Council, "Energy Development Strategy Action Plan (2014-2020)," Beijing, Jun. 2014.

[167] China State Council, "On promoting the health development of solar PV industry," Beijing, 24, Jul. 2013.

[168] U.S. Department of Energy, "SunShot Vision Study," Washington D.C., 2012.

[169] I. Gur, K. Sawyer, and R. Prasher, "Searching for a Better Thermal Battery," *Science (80-.).*, vol. 335, no. 6075, pp. 1454–1455, 2012.

[170] *Climate Change 2007: Impacts, Adaptation and Vulnerability*. Cambridge, UK: Cambridge University Press, 2007.

[171] A. Y. Lo, "Carbon emissions trading in China," *Nat. Clim. Chang.*, vol. 2, no. 11, pp. 765–766, Nov. 2012.

[172] National Development and Reform Commission of China, *Notice on Carbon Emission Trading Pilot Program*, vol. 2601. 2011.

[173] H. Harvey and H. Min, "The China Carbon Market Just Launched, And It's The World's Largest. Here's How It Can Succeed.," *Forbes*, 19-Dec-2017.

[174] S. Mufson, "With cap and trade plan, China adopts emissions policy that couldn't get through U.S. Congress," *The Washington Post*, 28-Sep-2015.

[175] G. Nelson, "China's Cap-and-Trade Plan," *China Business Review*, 02-Jul-2014.

[176] A. Rathi and E. Huang, "China is launching the world's largest carbon market," *Quartz*, 18-Dec-2017.

[177] ICAP, "Emissions Trading Worldwide: Status Report 2018," 2018.

[178] H. Liu and Z. Li, "Carbon Cap-and-Trade in China: A Comprehensive Framework," *Emerg. Mark. Financ. Trade*, vol. 53, no. 5, pp. 1152–1169, 2017.

[179] W. Xing, A. Wang, Q. Yan, and S. Chen, "A study of China's uranium resources security issues: Based on analysis of China's nuclear power development trend," *Ann. Nucl. Energy*, vol. 110, pp. 1156–1164, 2017.

[180] R. Mu, J. Zuo, and X. Yuan, "China's approach to nuclear safety - From the perspective of policy and institutional system," *Energy Policy*, vol. 76, pp. 161–172, 2015.

[181] Y. Zhou, C. Rengifo, P. Chen, and J. Hinze, "Is China ready for its nuclear expansion?," *Energy Policy*, vol. 39, no. 2, pp. 771–781, 2011.

[182] "China passes new law to strengthen nuclear safety," *South China Morning Post*, 01-Sep-2017.

[183] M. C. Lott and S.-I. Kim, "Technology Roadmap: Energy storage," 2014.

[184] International Energy Agency, "Energy Technology Perspectives 2014," 2014.

[185] G. He, J. Lin, and A. Yuan, "Economic Rebalancing and Electricity Demand in China," Lawrence Berkeley National Laboratory, LBNL-1003799, Nov. 2015.

[186] F. D. Munoz, A. H. van der Weijde, B. F. Hobbs, and J.-P. Watson, "Does risk aversion affect transmission and generation planning? A Western North America case study," 2017.

[187] F. D. Munoz, J. P. Watson, and B. F. Hobbs, "Optimizing Your Options: Extracting the Full Economic Value of Transmission When Planning Under Uncertainty," 2015.

[188] Bloomberg New Energy Finance; Swiss Re, "Profiling the Risks in Solar and Wind: A case for new risk management approaches in the renewable energy sector," 2013.

[189] L. Schrattenholzer, "Energy Planning Methodologies and Tools," 2005.

[190] G. He *et al.*, "A System's Approach to Decarbonize China's Power System," *Environ. Sci. Technol.*, 2016.

[191] A. Mileva, J. H. Nelson, J. Johnston, and D. M. Kammen, "SunShot solar power reduces costs and uncertainty in future low-carbon electricity systems.," *Environ. Sci. Technol.*, vol. 47, no. 16, pp. 9053–60, Aug. 2013.

[192] National Renewable Energy Laboratory, "Getting Started Guide for HOMER Version 2.1," 2005.

[193] N. N. Taleb, *The black swan: The impact of the highly improbable.*, Random Hou. New York, 2007.

[194] S. E. Clark and T. T. Yates, "How efficient is your frontier?," no. November, pp. 1–5, 2003.

[195] F. deLlano-Paz, A. Calvo-Silvosa, S. I. Antelo, and I. Soares, "Energy planning and modern portfolio theory: A review," *Renew. Sustain. Energy Rev.*, vol. 77, no. March 2016, pp. 636–651, 2017.

[196] H. Markowitz, "Portfolio selection," *J. Finance*, vol. 7, no. 1, pp. 77–91, 1952.

[197] D. Bar-Lev and S. Katz, "A portfolio approach to fossil fuel procurement in the electric utility industry," *J. Finance*, vol. 31, no. 3, pp. 933–947, Jun. 1976.

[198] E. Delarue, C. De Jonghe, R. Belmans, and W. D'haeseleer, "Applying portfolio theory to the electricity sector: Energy versus power," *Energy Econ.*, vol. 33, no. 1, pp. 12–23, 2011.

[199] F. Kienzle, G. Koeppel, P. Stricker, and G. Andersson, "Efficient electricity production portfolios taking into account physical boundaries," *Methods*, pp. 1–17.

[200] J. I. Muñoz, A. a. Sánchez de la Nieta, J. Contreras, and J. L. Bernal-Agustín, "Optimal investment portfolio in renewable energy: The Spanish case," *Energy Policy*, vol. 37, pp. 5273–5284, 2009.

[201] A. Bhattacharya and S. Kojima, "Power sector investment risk and renewable energy: A Japanese case study using portfolio risk optimization method," *Energy Policy*, vol. 40, pp. 69–80, 2012.

[202] H. Markowitz, "Mean-variance approximations to expected utility," *Eur. J. Oper. Res.*, vol. 234, no. 2, pp. 346–355, 2014.

[203] U.S. Energy Information Administration (EIA), "Levelized Cost and Levelized Avoided Cost of New Generation Resources in the Annual Energy Outlook 2016," 2016. [Online]. Available: http://www.eia.gov/forecasts/aeo/electricity_generation.cfm.

[204] California Energy Commission, "A mean-variance portfolio optimization of California's generation mix to 2020: achieving California's 33 percent renewable portfolio standard goal," 2007.

[205] World Energy Council and Bloomberg New Energy Finance, "World Energy Perspective - Cost of Energy Technologies," 2013.

[206] L. Zhu and Y. Fan, "Optimization of China's generating portfolio and policy implications based on portfolio theory," *Energy*, vol. 35, no. 3, pp. 1391–1402, 2010.

[207] J. C. Jansen, L. W. M. Beurskens, and X. van Tilburg, "Application of portfolio analysis to the Dutch generating mix. Reference case and two renewables cases : year 2030 - SE and GE scenario," no. February, pp. 5–67, 2006.

[208] G. He and D. M. Kammen, "Where, when and how much wind is available? A provincial-scale wind resource assessment for China," *Energy Policy*, vol. 74, no. C, pp. 116–122, 2014.

[209] G. He and D. M. Kammen, "Where, when and how much solar is available? A provincial-scale solar resource assessment for China," *Renew. Energy*, vol. 85, pp. 74–82, 2016.

[210] X. Zhang, V. J. Karplus, T. Qi, D. Zhang, and J. He, "Carbon emissions in China: How far can new efforts bend the curve?," *Energy Econ.*, vol. 54, no. 267, pp. 388–395, 2016.

[211] D. Shemie and K. Vigerstol, "China has a water crisis - how can it be solved?," *World Economic Forum*, 29-Apr-2016.

[212] L. Lin, "China's water pollution will be more difficult to fix than its dirty air," *China Dialogue*, 17-Feb-2014.

[213] "Renewable internal freshwater resources per capita (cubic meters) | Data," 2017. [Online]. Available: http://data.worldbank.org/indicator/ER.H2O.INTR.PC.

[214] L. Addams, G. Boccaletti, M. Kerlin, and M. Stuchtey, "Charting Our Water Future: Economic frameworks to inform decision-making," 2009.

[215] "Climate change threatens our water," *China.org.cn*, 23-Apr-2011.

[216] S. Renzetti and D. P. Dupont, *Water Pricing Experiences and Innovations*. 2015.

[217] D. Doré, G. Peiyuan, A.-S. Nette, and J. An, "Water in China," 2010.

[218] China Water Risk, "China's Water Crisis Part I – Introduction," no. March, p. 13, 2010.

[219] J. Barnett, S. Rogers, M. Webber, B. Finlayson, and M. Wang, "Transfer project cannot meet China's water needs," *Nature*, vol. 527, pp. 295–297, 2015.

[220] "Google Maps." [Online]. Available: https://maps.google.com/.

[221] Bureau of South-to-North Water Transfer Planning Designing and management - Ministry of Water Resources, "欢迎浏览 '中 国 南 水 北 调' 网站 - South-to-North Water Diversion," 2017. [Online]. Available: http://www.nsbd.gov.cn.

[222] G. He *et al.*, "SWITCH-China: A Systems Approach to Decarbonize China's Power System," *Environ. Sci. Technol.*, May 2016.

[223] L. Zhang, L. Xie, H.-L. Chen, and C.-J. Gao, "Progress and prospects of seawater desalination in China," *Desalination*, vol. 182, no. 1–3, pp. 13–18, Nov. 2005.

[224] Y. Zhou and R. S. J. Tol, "Implications of desalination for water resources in China - an economic perspective," *Desalination*, vol. 164, pp. 225–240, 2004.

[225] R. Deng, L. Xie, H. Lin, J. Liu, and W. Han, "Integration of thermal energy and seawater desalination," *Energy*, vol. 35, no. 11, pp. 4368–4374, Nov. 2010.

[226] Q. Zou and X. Liu, "Economic effects analysis of seawater desalination in China with input-output technology," *Desalination*, vol. 380, pp. 18–28, 2016.

[227] M. M. Megahed, "Feasibility of nuclear power and desalination on El-Dabaa site," *Desalination*, vol. 246, no. 1–3, pp. 238–256, Sep. 2009.

[228] P. Gleick, "Water and Energy," *Annu. Rev. Energy Environ.*, vol. 19, no. 1, pp. 267–299, Jan. 1994.

[229] M. Methnani, "Influence of fuel costs on seawater desalination options," *Desalination*, vol. 205, no. May 2006, pp. 332–339, 2007.

[230] T. Younos and K. E. Tulou, "Energy Needs, Consumption and Sources," *J. Contemp. Water Res. Educ.*, vol. 132, no. 1, pp. 27–38, May 2009.

[231] J. Kupitz and M. J. Crijns, "Perspectives desalination of nuclear energy for seawater," *Desalination*, vol. 99, pp. 299–327, 1994.

[232] R. S. Faibish and T. Konishi, "Nuclear desalination: a viable option for producing freshwater," *Desalination*, vol. 157, no. 1–3, pp. 241–252, Aug. 2003.

[233] M. M. Megahed, "Nuclear desalination: history and prospects," *Desalination*, vol. 135, no. 1–3, pp. 169–185, Apr. 2001.

[234] International Atomic Energy Agency, "Status of design concepts of nuclear desalination

plants," no. November, 2002.

[235] D. Wang, D. Dong, W. Zheng, D. Zhang, and L. Wang, "The 200 MW nuclear heating reactor and its possible application in seawater desalination," *Desalination*, vol. 99, no. 2–3, pp. 383–399, Dec. 1994.

[236] H. Jia and Y. Zhang, "Nuclear seawater desalination plant coupled with 200 MW heating reactor," *Int. J. Nucl. Desalin.*, vol. 3, no. 2, p. 230, 2008.

[237] L. Tian, Y. Wang, and J. Guo, "Economic analysis of a 2x200 MW nuclear heating reactor for seawater desalination by multi-effect distillation (MED)," *Desalination*, vol. 152, pp. 223–228, 2002.

[238] International Atomic Energy Agency, "Desalination Economic Evaluation Program (DEEP-3.0): User's manual," *Comput. Man. Ser.*, vol. 19, 2006.

[239] International Atomic Energy Agency, "Examining the economics of seawater desalination using the DEEP code," Vienna, 2000.

[240] International Atomic Energy Agency, "DEEP 5 User Manual," 2013.

[241] International Atomic Energy Agency, "PRIS: Power Reactor Information System - Country Details (China)," 2017. [Online]. Available: http://www.iaea.org/pris/CountryStatistics/CountryDetails.aspx?current=CN.

[242] Y. Zhou and R. S. J. Tol, "Evaluating the costs of desalination and water transport," no. Vc, pp. 1–16, 2004.

[243] International Atomic Energy Agency, "Economics of Nuclear Desalination: New Developments and Site Specific Studies," Vienna, 2007.

[244] China Water Risk and Unison Creative, "Who's Running Dry?," 2013. [Online]. Available: http://chinawaterrisk.org/big-picture/whos-running-dry/.

[245] American Water Works Association, *Desalination of seawater, manual of water supply practices*. Denver: American Water Works Association, 2011.

[246] International Atomic Energy Agency, "Optimization of the coupling of nuclear reactors and desalination systems," Vienna, 2005.

[247] M. A. Darwish, "Cogeneration Power-Desalination Plants," *Desalination*, vol. 69, pp. 27–46, 1988.

[248] J. Tonner, "Barriers to Thermal Desalination in the United States," 2008.

[249] International Atomic Energy Agency, "Introduction of Nuclear Desalination: a guidebook," Vienna, 2000.

[250] Energy Sector Management Assistance Program; The World Bank, "Central America Regional Programmatic Study For The Energy Sector: Managing An Electricity Shortfall," 2010.

[251] International Atomic Energy Agency, "Desalination Economic Evaluation Program (DEEP)."

Vienna, 2011.

[252] University of Palermo, *Seawater Desalination: Conventional and Renewable Energy Processes*. Palermo: Springer, 2009.

[253] D. Fridley, N. Zheng, N. Zhou, J. Ke, A. Hasanbeigi, and L. Price, "China Energy and Emissions Paths to 2030," 2011.

[254] McKinsey & Company, "China's green revolution," 2009.

[255] Kelly Services, "Salary guide," 2016.

[256] Carlsbad Desalination Project, "Carlsbad Desalination Project | FAQs," 2017. [Online]. Available: http://carlsbaddesal.com/faqs.

[257] Department of Environment and Primary Industries Victoria State Government, "DEPI - Desalination jobs and contracts," 2017. [Online]. Available: http://www.depi.vic.gov.au/water/urban-water/desalination-project/desalination-background/desalination-jobs-and-contracts.

[258] C. C. Ni, "China's Electric Power Industry and Its Trends," 2006.

[259] Beijing Internati, "Guide to Heating, Electricity, Water, and Gas Policies and Procedures," 2012. [Online]. Available: http://www.ebeijing.gov.cn/feature_2/GuideToHeatingElectricityWaterAndGas/PriceGuide/t1107813.htm.

[260] China.org.cn, "China's power consumption slows further," Xinhua, 17-Oct-2012.

[261] M. a. Delucchi and M. Z. Jacobson, "Providing all global energy with wind, water, and solar power, Part II: Reliability, system and transmission costs, and policies," *Energy Policy*, vol. 39, no. 3, pp. 1170–1190, Mar. 2011.

[262] J. Anderson, "Potential impacts of desalination development on energy consumption," Brussels, 2008.

[263] B. Liberman, "The importance of energy recovery devices in reverse osmosis desalination."

[264] M. Yang and C.-F. Weng, "China's Recycled Water/Water Treatment Industry in the Age of Water Crisis," in *China's Industrial Development in the 21st Century*, M. Yang and H. Yu, Eds. 2011.

[265] Saskatchewan Environment, "Water Pipeline Design Guidelines," 2004.

[266] F. Du, G. Woods, and D. Kang, "Life Cycle Analysis for Water and Wastewater Pipe Materials," *J. Environ. Eng.*, vol. 139, no. May, pp. 703–711, 2012.

[267] J. West, "There's A Perfect Pipe For Every Water And | Municipal Sewer and Water," *Municipal Sewer and Water Magazine*, 2014.

[268] AMERICAN Cast Iron Pipe Company, "Water Transmission," 2018. [Online]. Available: http://www.american-usa.com/industries/water-and-wastewater/water-transmission.

[269] Northwest Pipe Company, "Water Transmission," 2018. [Online]. Available: http://www.nwpipe.com/product-category/industries-markets/water-transmission/.

[270] Inflation.eu, "Historic CPI inflation China," 2016. [Online]. Available: http://www.inflation.eu/inflation-rates/china/historic-inflation/cpi-inflation-china.aspx.

[271] J. Zhao, H. Ni, X. Peng, J. Li, G. Chen, and J. Liu, "Impact of water price reform on water conservation and economic growth in China," *Econ. Anal. Policy*, vol. 51, pp. 90–103, 2016.

[272] R. Rutkowski, "The Economics of H2O: Water Price Reforms in China," *Peterson Institute for International Economics*, 22-Jul-2014.

[273] L. Zhong and A. P. J. Mol, "Water Price Reforms in China: Policy-Making and Implementation," *Water Resour. Manag.*, vol. 24, no. 2, pp. 377–396, May 2009.

[274] D. Shen and J. Wu, "State of the Art Review: Water pricing reform in China," *Int. J. Water Resour. Dev.*, vol. 33, no. 2, pp. 198–232, 2017.

[275] X. Yang, J. F. Donzier, and C. Noel, "Une Comparaison de la Politique de l'Eau en France et en Chine Deuxième Partie : Autorisation , Protection et Financement," 2012.

[276] G. J. Browder, S. Xie, Y. Kim, L. Gu, and M. E. Fan, "Improving the performance of China's urban water utilities," *World Bank*, 2007.

[277] Water Engineering and Development Centre (WEDC), Water Sector Development Project (WSDP), and Department For International Development (DFID), "China Water Sector Briefing Note Series: Assessing Ability and Willingness to Pay Briefing," pp. 1–6, 2003.

[278] National Bureau of Statistics of China, "China Statistical Yearbook 2015," 2016. [Online]. Available: http://www.stats.gov.cn/tjsj/ndsj/2015/indexeh.htm.

[279] M. Falkenmark, J. Lundqvist, and C. Widstrand, "Macro-scale water scarcity requires micro-scale approaches. Aspects of vulnerability in semi-arid development.," *Nat. Resour. Forum*, vol. 13, no. 4, pp. 258–67, Nov. 1989.

[280] "Food and Agriculture Organization of the United Nations - Water scarcity," 2014. [Online]. Available: http://www.fao.org/nr/water/topics_scarcity.html.

[281] 中华人民共和国人力资源和社会保障部 (Ministry of Human Resources and Social Security of the People's Republic of China), "全国各地区月最低工资标准情况 (Monthly minimum wage standards per region)," 28-Sep-2015.

[282] J. Hawksworth and C. Lambe, "Global wage projections to 2030, PWC," 2013.

[283] World Nuclear Association, "Nuclear Desalination," 2018. [Online]. Available: http://www.world-nuclear.org/information-library/non-power-nuclear-applications/industry/nuclear-desalination.aspx.

[284] The Urban China Initiative, G. Xiao, L. Xue, and J. Woetzel, "The Urban Sustainability Index : A New Tool for Measuring China ' s Cities," 2010.

[285] "Photo Slideshow: China Completes Second Line of South-North Water Transfer Project - Circle of Blue," 2017. [Online]. Available: http://www.circleofblue.org/2015/world/photo-slideshow-china-completes-second-line-south-north-water-transfer/.

[286] Bureau of South-to-North Water Transfer Planning Designing and Management - Ministry of Water Resources, "南水北调工程总体规划内容简介," 2008. [Online]. Available: http://nsbd.mwr.gov.cn/nsbdgcjs/ztbj/201211/t20121129_333896.html.

[287] Bureau of South-to-North Water Transfer Planning Designing and management - Ministry of Water Resources, "南水北调东线工程规划（２００１年修订）简介," 2008. [Online]. Available: http://nsbd.mwr.gov.cn/nsbdgcjs/ztbj/201211/t20121129_333895.html.

[288] Bureau of South-to-North Water Transfer Planning Designing and management - Ministry of Water Resources, "欢迎浏览 '中 国 南 水 北 调' 网站," 2017. [Online]. Available: http://www.nsbd.gov.cn/zx/gcgh/200308/t20030825_195174.html.

[289] M. L. Mallonée, "The South-North Water Transfer Project: a Cost-Benefit Analysis," 2016.

[290] M. Fontseré, "LCA software : Practical example using SimaPro." Girona, 2012.

[291] O. Edenhofer, R. Pichs Madruga, and Y. Sokona, *Renewable Energy Sources and Climate Change Mitigation (Special Report of the Intergovernmental Panel on Climate Change)*, vol. 6, no. 4. 2012.

[292] J. Swartz, "China's National Emissions Trading System: Implications for Carbon Markets and Trade," 2016.

[293] X. Ge, "State and Trends of Shenzhen Carbon Market," in *14th IEA-IETA-EPRI Annual Workshop on Greenhouse Gas Emission Trading*, 2014.

[294] Global Clean Water Desalination Alliance, "Global Clean Water Desalination Alliance - Concept Paper," 2015.

[295] International Atomic Energy Agency, "Nuclear Technology Review," Vienna, 2004.

[296] D. P. Schlachtberger, S. Becker, S. Schramm, and M. Greiner, "Backup flexibility classes in emerging large-scale renewable electricity systems," *Energy Convers. Manag.*, vol. 125, pp. 336–346, 2016.

[297] D. Pescia, "Flexibility in thermal power plants with a focus on existing coal-fired power plants," Berlin, 2017.

[298] F. Xia and F. Song, "The uneven development of wind power in China: Determinants and the role of supporting policies," *Energy Econ.*, vol. 67, pp. 278–286, 2017.

[299] Statista, "Cumulative installed solar power capacity in China as of 2016, by region (in megawatts)," 2016. [Online]. Available: https://www.statista.com/statistics/673390/china-cumulative-installed-capacity-of-solar-power-by-region/.

[300] National Energy Administration, "Wind Grid Operation in the First Three Quarters of 2017," 2017. [Online]. Available: http://www.nea.gov.cn/2017-10/31/c_136717648.htm.

[301] "Valuing abundance – breaking the tyranny of resource scarcity | Guardian Sustainable Business | The Guardian," 2012. [Online]. Available: https://www.theguardian.com/sustainable-business/blog/valuing-abundance-breaking-resource-scarcity.

[302] M. Al-Nory and M. El-Beltagy, "An energy management approach for renewable energy integration with power generation and water desalination," *Renew. Energy*, vol. 72, pp. 377–385, 2014.

[303] Y. C. Tsai, C. P. Chiu, F. K. Ko, T. C. Chen, and J. T. Yang, "Desalination plants and renewables combined to solve power and water issues," *Energy*, vol. 113, pp. 1018–1030, 2016.

[304] D. Mentis *et al.*, "Desalination using renewable energy sources on the arid islands of South Aegean Sea," *Energy*, vol. 94, pp. 262–272, 2016.

[305] N. J. Niemuth and R. D. Klaper, "Emerging wastewater contaminant metformin causes intersex and reduced fecundity in fish," *Chemosphere*, vol. 135, pp. 38–45, 2015.

[306] P. Schröder *et al.*, "Status of hormones and painkillers in wastewater effluents across several European states—considerations for the EU watch list concerning estradiols and diclofenac," *Environ. Sci. Pollut. Res.*, vol. 23, no. 13, pp. 12835–12866, 2016.

[307] A. Rodríguez-Calvo, G. A. Silva-Castro, F. Osorio, J. González-López, and C. Calvo, "Reverse osmosis seawater desalination: current status of membrane systems," *Desalin. Water Treat.*, vol. 56, no. 4, pp. 849–861, 2015.

[308] M. T. Ali, H. E. S. Fath, and P. R. Armstrong, "A comprehensive techno-economical review of indirect solar desalination," *Renew. Sustain. Energy Rev.*, vol. 15, no. 8, pp. 4187–4199, 2011.

[309] W. Lai, Q. Ma, H. Lu, S. Weng, J. Fan, and H. Fang, "Effects of wind intermittence and fluctuation on reverse osmosis desalination process and solution strategies," *Desalination*, vol. 395, pp. 17–27, 2016.

[310] S. Kumarasamy, S. Narasimhan, and S. Narasimhan, "Optimal operation of battery-less solar powered reverse osmosis plant for desalination," *Desalination*, vol. 375, pp. 89–99, 2015.

[311] M. S. Miranda and D. Infield, "A wind-powered seawater reverse-osmosis system without batteries," *Desalination*, vol. 153, pp. 9–16, 2002.

[312] M. Thomson and D. Infield, "A photovoltaic-powered seawater reverse-osmosis without batteries," vol. 153, 2002.

[313] M. Thomson and D. Infield, "Laboratory demonstration of a photovoltaic-powered seawater reverse-osmosis system without batteries," *Desalination*, vol. 183, no. 1–3, pp. 105–111, 2005.

[314] G. L. Park, A. I. Schäfer, and B. S. Richards, "Renewable energy powered membrane technology: The effect of wind speed fluctuations on the performance of a wind-powered membrane system for brackish water desalination," *J. Memb. Sci.*, vol. 370, no. 1–2, pp. 34–44, 2011.

[315] G. L. Park, A. I. Schäfer, and B. S. Richards, "The effect of intermittent operation on a wind-

powered membrane system for brackish water desalination," *Water Sci. Technol.*, vol. 65, no. 5, pp. 867–874, 2012.

[316] B. S. Richards, G. L. Park, T. Pietzsch, and A. I. Schäfer, "Renewable energy powered membrane technology: Safe operating window of a brackish water desalination system," *J. Memb. Sci.*, vol. 468, pp. 400–409, 2014.

[317] B. S. Richards, G. L. Park, T. Pietzsch, and A. I. Schäfer, "Renewable energy powered membrane technology: Brackish water desalination system operated using real wind fluctuations and energy buffering," *J. Memb. Sci.*, vol. 468, pp. 400–409, 2014.

[318] B. S. Richards, D. P. S. Capão, W. G. Früh, and A. I. Schäfer, "Renewable energy powered membrane technology: Impact of solar irradiance fluctuations on performance of a brackish water reverse osmosis system," *Sep. Purif. Technol.*, vol. 156, pp. 379–390, 2015.

[319] M. Thomson, "Reverse-Osmosis Desalination of Seawater Powered by Photovoltaics Without Batteries," 2003.

[320] E. S. Mohamed, G. Papadakis, E. Mathioulakis, and V. Belessiotis, "A direct coupled photovoltaic seawater reverse osmosis desalination system toward battery based systems - a technical and economical experimental comparative study," *Desalination*, vol. 221, no. 1–3, pp. 17–22, 2008.

[321] H. Qiblawey, F. Banat, and Q. Al-Nasser, "Laboratory setup for water purification using household PV-driven reverse osmosis unit," *Desalin. Water Treat.*, vol. 7, no. 1–3, pp. 53–59, 2009.

[322] P. Cesar *et al.*, "Mathematical Model of a Photovoltaic Powered Reverse Osmosis Plant without Batteries," in *Energy*, 2005, no. February, pp. 15–17.

[323] A. Joyce, D. Loureiro, C. Rodrigues, and S. Castro, "Small reverse osmosis units using PV systems for water purification in rural places," *Desalination*, vol. 137, no. 1–3, pp. 39–44, 2001.

[324] S. Abdallah, M. Abu-Hilal, and M. S. Mohsen, "Performance of a photovoltaic powered reverse osmosis system under local climatic conditions," *Desalination*, vol. 183, no. 1–3, pp. 95–104, 2005.

[325] South Australia Environment Protection Authority, "Salinity." [Online]. Available: http://www.epa.sa.gov.au/environmental_info/water_quality/threats/salinity.

[326] G. Brunekreeft, T. Luhmann, T. Menz, S.-U. Müller, and P. Recknagel, "China's way from conventional power grids towards smart grids," in *Regulatory Pathways For Smart Grid Development in China*, 2015, pp. 19–43.

[327] J. Pittock, K. Hussey, and S. Dovers, Eds., *Climate, Energy and Water*. Cambridge: Cambridge University Press, 2015.

[328] Z. Ming, P. Lilin, F. Qiannan, and Z. Yingjie, "Trans-regional electricity transmission in China: Status, issues and strategies," *Renew. Sustain. Energy Rev.*, vol. 66, pp. 572–583, 2016.

[329] United Nations, "International Decade for Action 'Water for Life' 2005-2015. Focus Areas:

Water scarcity," 2014. [Online]. Available: http://www.un.org/waterforlifedecade/scarcity.shtml.

[330] Z. Guo, L. Ma, P. Liu, I. Jones, and Z. Li, "A multi-regional modelling and optimization approach to China's power generation and transmission planning," *Energy*, 2016.

[331] A. Guo, "SGCC: all eight UHVDC lines come on stream to combat air pollution," *sxcoal.com*, 27-Dec-2017.

[332] SERC, "Annual Report on Electricity Regulation (2011)," State Electricity Regulatory Commission, Beijing, May 2012.

[333] World Energy Council, "Comparison of Energy Systems Using Life Cycle Assessment," 2004.

[334] International Atomic Energy Agency, "Desalination Economic Evaluation Program (DEEP) 4-5." 2011.

[335] M. Papapetrou, A. Cipollina, U. La Commare, G. Micale, G. Zaragoza, and G. Kosmadakis, "Assessment of methodologies and data used to calculate desalination costs," *Desalination*, vol. 419, no. March, pp. 8–19, 2017.

[336] Statista from CEC, "Installed capacity of wind power generation in China in 2015, by region (in MW)," 2018. [Online]. Available: https://www.statista.com/statistics/302350/china-installed-wind-power-capacity-by-region/.

[337] Statista from National Energy Administration (China), "Cumulative installed solar power capacity in China as of 2016, by region (in megawatts)," 2018. [Online]. Available: https://www.statista.com/statistics/673390/china-cumulative-installed-capacity-of-solar-power-by-region/.

[338] Statista from CEC, "Installed capacity of hydroelectric power generation in China in 2015, by region (in GW)," 2018. [Online]. Available: https://www.statista.com/statistics/302327/china-installed-hydropower-capacity-by-region/.

[339] Statista from CEC, "Installed capacity of thermoelectric power generation in China in 2015, by region (in GW)," 2018. [Online]. Available: https://www.statista.com/statistics/302332/china-installed-thermal-power-capacity-by-region/.

[340] "China's Cumulative PV Installations Could Reach 250GW by 2020," *PV Energy Trend*, Aug-2017.

[341] Greenpeace, "Is China doubling down on its coal power bubble? (Update)," 2016.

[342] J. Gosens, T. Kåberger, and Y. Wang, "China's next renewable energy revolution: goals and mechanisms in the 13th Five Year Plan for energy," *Energy Sci. Eng.*, vol. 5, no. 3, pp. 141–155, 2017.

[343] B. K. Sahu, "Wind energy developments and policies in China: A short review," *Renew. Sustain. Energy Rev.*, vol. 81, no. May 2017, pp. 1393–1405, 2018.

[344] B. Hodge, D. Lew, M. Milligan, E. Gómez-lázaro, D. Flynn, and J. Dobschinski, "Wind Power Forecasting Error Distributions: An International Comparison," 2011.

[345] P. H. Westfall, "Kurtosis as Peakedness, 1905 - 2014. R.I.P.," *Am. Stat.*, vol. 68, no. 3, pp. 191–195, 2014.

[346] Kelly, "China Weather Guide," *China Highlights*. [Online]. Available: https://www.chinahighlights.com/weather/.

[347] G. Yom-Tov, "No End in Sight: Gloabl Water Tariffs Increasing 3.91% in 2017," *GYT Analytics*, 08-Nov-2017.

[348] Y. Che and Z. Shang, "Chapter 6 Water Pricing in China: Impact of Socioeconomic Development," in *Water Pricing Experiences and Innovations*, vol. 9, no. 500, 2015.

[349] W. Wang, H. Xie, N. Zhang, and D. Xiang, "Sustainable water use and water shadow price in China's urban industry," *Resour. Conserv. Recycl.*, vol. 128, pp. 489–498, 2018.

[350] International Energy Agency and Nuclear Energy Agency, "Projected Costs of Generating Electricity," 2015.

[351] A. Gambhir, L. K. C. Tse, D. Tong, and R. Martinez-Botas, "Reducing China's road transport sector CO2 emissions to 2050: Technologies, costs and decomposition analysis," *Appl. Energy*, vol. 157, pp. 905–917, 2015.

[352] EDGAR - Emission Database For Global Atmospheric Research, "CO2 time series 1990-2015 per region/country," 2017. .

[353] F. Li, Z. Xu, and H. Ma, "Can China achieve its CO2 emissions peak by 2030?," *Ecol. Indic.*, vol. 84, no. 37, pp. 337–344, 2018.

[354] "2015汽车保有量再创新高达1.72亿辆 平均百户家庭31辆--人民网汽车--人民网." [Online]. Available: http://auto.people.com.cn/n1/2016/0126/c1005-28086267.html.

[355] "United States Transport Stats: NationMaster.com." [Online]. Available: http://www.nationmaster.com/country-info/profiles/United-States/Transport.

[356] Statista, "Passenger cars per capita in the EU | Statistics," 2017. [Online]. Available: https://www.statista.com/statistics/607540/car-per-capita-eu/.

[357] National Bureau of Statistics of the People's Republic of China, "China Statistical Yearbook 2011 to 2016." [Online]. Available: http://www.stats.gov.cn/tjsj/ndsj/.

[358] B. Ye, J. Jiang, C. Li, L. Miao, and J. Tang, "Quantification and driving force analysis of provincial-level carbon emissions in China Intergovernmental Panel on Climate Change," *Appl. Energy*, vol. 198, pp. 223–238, 2017.

[359] G. Collins, "China's Evolving Oil Demand Slowing Overall Growth, Gasoline Replacing Diesel as Demand Driver, Refined Product Exports Rising Substantially," 2016.

[360] J. Du and D. Ouyang, "Progress of Chinese electric vehicles industrialization in 2015: A

review," *Appl. Energy*, vol. 188, pp. 529–546, 2017.

[361] C. Li *et al.*, "Hidden Benefits of Electric Vehicles for Addressing Climate Change," *Sci. Rep.*, vol. 5, no. 1, p. 9213, 2015.

[362] "国务院关于印发'十二五'国家战略性新兴产业发展规划的通知," 2017. [Online]. Available: http://www.gov.cn/zwgk/2012-07/20/content_2187770.htm.

[363] "国务院关于印发节能与新能源汽车产业发展规划（2012—2020年）的通知," 2017. [Online]. Available: http://www.gov.cn/zwgk/2012-07/09/content_2179032.htm.

[364] L. Yang, J. Xu, and P. Neuhäusler, "Electric vehicle technology in China: An exploratory patent analysis," *World Pat. Inf.*, vol. 35, no. 4, pp. 305–312, 2013.

[365] Y. Wang, D. Sperling, G. Tal, and H. Fang, "China's electric car surge," *Energy Policy*, vol. 102, no. December 2016, pp. 486–490, 2017.

[366] International Energy Agency, "Global EV Outlook 2016: Beyond one million electric cars," 2016.

[367] International Energy Agency, "Global EV Outlook 2017: Two million and counting," 2017.

[368] China SignPost, "Rising Gasoline Demand Means China's Crude Oil Use is Decoupling from the Industrial Economy | China SignPost™," 2016. [Online]. Available: http://www.chinasignpost.com/2016/06/03/rising-gasoline-demand-means-chinas-crude-oil-use-is-decoupling-from-the-industrial-economy/.

[369] "Chen Quanshi: EV industry to face the first recession next year." [Online]. Available: http://www.urldata.xyz/p/oqqg/Chen-Quanshi-EV-industry-to-face-the-first-recession-next-year.html.

[370] "国务院关于印发节能与新能源汽车产业发展规划（2012—2020年）的通知." [Online]. Available: http://www.gov.cn/zwgk/2012-07/09/content_2179032.htm.

[371] ifeu – Institute for Energy and Environmental Research Heidelberg, "Transport in China : Energy Consumption and Emissions of Different Transport Modes," 2008.

[372] J. Wu, "The Transport Contribution to CO2 in China." pp. 1–27, 2015.

[373] "Cars a threat to China's 2030 CO2 peak | China Dialogue," 2015. [Online]. Available: https://www.chinadialogue.net/article/show/single/en/8115-Cars-a-threat-to-China-s-2-3-CO2-peak.

[374] J. Hofmann, D. Guan, K. Chalvatzis, and H. Huo, "Assessment of electrical vehicles as a successful driver for reducing CO2 emissions in China," *Appl. Energy*, vol. 184, pp. 995–1003, 2016.

[375] J. Dargay and D. Gatel, "Vehicle ownership to 2015: implications for energy use and emissions. .," *Energy Policy*, vol. 25, no. 14, pp. 1121–1127, 1997.

[376] X. Yuan, L. Li, H. Gou, and T. Dong, "Energy and environmental impact of battery electric

vehicle range in China," *Appl. Energy*, vol. 157, pp. 75–84, 2015.

[377] D. Anair and A. Mahmassani, "State of charge: Electric vehicles' global warming emissions and fuel-cost savings across the United States," 2012.

[378] C. J. Meinrenken and K. S. Lackner, "Fleet view of electrified transportation reveals smaller potential to reduce GHG emissions," *Appl. Energy*, vol. 138, pp. 393–403, 2015.

[379] A. Mileva, J. Johnston, J. H. Nelson, and D. M. Kammen, "Power system balancing for deep decarbonization of the electricity sector," *Appl. Energy*, vol. 162, pp. 1001–1009, 2016.

[380] Y. Zhou, M. Wang, H. Hao, L. Johnson, H. Wang, and H. Hao, "Plug-in electric vehicle market penetration and incentives: a global review," *Mitig. Adapt. Strateg. Glob. Chang.*, vol. 20, no. 5, pp. 777–795, 2015.

[381] H. Hao, X. Ou, J. Du, H. Wang, and M. Ouyang, "China's electric vehicle subsidy scheme: Rationale and impacts," *Energy Policy*, vol. 73, pp. 722–732, 2014.

[382] G. Pasaoglu, M. Honselaar, and C. Thiel, "Potential vehicle fleet CO 2 reductions and cost implications for various vehicle technology deployment scenarios in Europe," *Energy Policy*, vol. 40, no. 1, pp. 404–421, 2012.

[383] International Energy Agency, "Scenarios and projections - Energy Technology Perspectives," 2017. [Online]. Available: http://www.iea.org/publications/scenariosandprojections/.

[384] B. Zheng *et al.*, "How will greenhouse gas emissions from motor vehicles be constrained in China around 2030?," *Appl. Energy*, vol. 156, no. November 2014, pp. 230–240, 2015.

[385] M. Sorrentino, G. Rizzo, and L. Sorrentino, "A study aimed at assessing the potential impact of vehicle electrification on grid infrastructure and road-traffic green house emissions," *Appl. Energy*, vol. 120, pp. 31–40, 2014.

[386] G. F. Mulligan, "Logistic population growth in the world's largest cities," *Geogr. Anal.*, vol. 38, no. 4, pp. 344–370, 2006.

[387] G. Chaolin, W. Liya, and I. Cook, "Progress in research on Chinese urbanization," *Front. Archit. Res.*, vol. 1, no. 2, pp. 101–149, 2012.

[388] Z. Hu and X. Peng, "Household changes in contemporary China: an analysis based on the four recent censuses," *J. Chinese Sociol.*, vol. 2, no. 1, p. 9, 2015.

[389] J. M. Dargay, "Determinants of car ownership in rural and urban areas: a pseudo-panel analysis," *Transp. Res. Part E*, vol. 38, no. 5, pp. 351–366, 2002.

[390] T. Wu, M. Zhang, and X. Ou, "Analysis of future vehicle energy demand in China based on a Gompertz function method and computable general equilibrium model," *Energies*, vol. 7, no. 11, pp. 7454–7482, 2014.

[391] H. Huo and M. Wang, "Modeling future vehicle sales and stock in China," *Energy Policy*, vol. 43, pp. 17–29, 2012.

[392] J. Dargay and D. Gately, "Income's effect on car and vehicle ownership, worldwide: 1960–

2015," *Transp. Res. Part A Policy Pract.*, vol. 33, no. 2, pp. 101–138, 1999.

[393] T. Wu, H. Zhao, and X. Ou, "Vehicle ownership analysis based on GDP per capita in China: 1963-2050," *Sustain.*, vol. 6, no. 8, pp. 4877–4899, 2014.

[394] U.S. Energy Information Administration, "Issues in International Energy Consumption Analysis : Chinese Transportation Fuel Demand," 2014.

[395] R. Haddock and S. Torok, "The road ahead - China's Passenger Vehicle Market In 2015," 2008.

[396] W. Han, "Challenges facing auto industry in China," 2014.

[397] Natural Resources Defense Council, "The Potential of Grid Integration of Electric Vehicles in Shanghai," no. 38, 2016.

[398] H. Hao, S. Wang, Z. Liu, and F. Zhao, "The impact of stepped fuel economy targets on automaker's light-weighting strategy: The China case," *Energy*, vol. 94, pp. 755–765, 2016.

[399] A. Gambhir *et al.*, "A hybrid modelling approach to develop scenarios for China's carbon dioxide emissions to 2050," *Energy Policy*, vol. 59, pp. 614–632, 2013.

[400] "Learn the facts: Fuel consumption and CO2 | Natural Resources Canada," 2017. [Online]. Available: http://www.nrcan.gc.ca/energy/efficiency/transportation/cars-light-trucks/buying/16770.

[401] EV Volumes.com, "China NEV Volumes years 2014-2017," 2017. [Online]. Available: http://www.ev-volumes.com/country/china/.

[402] EV-Volumes - The Electric Vehicle World Sales Database, "China Plug-in Sales 2016 Q4 and Full Year," 2016. [Online]. Available: http://www.ev-volumes.com/country/china/.

[403] China Auto Web, "Chinese-Made Electric Cars," 2017. [Online]. Available: http://chinaautoweb.com/electric-cars/.

[404] Bloomberg New Energy Finance, "Electric Vehicle Outlook," 2017.

[405] G. Berckmans, M. Messagie, J. Smekens, N. Omar, L. Vanhaverbeke, and J. Van Mierlo, "Cost projection of state of the art lithium-ion batteries for electric vehicles up to 2030," *Energies*, vol. 10, no. 9, 2017.

[406] J. RISSMAN, "The Future of Electric Vehicles in the US," 2017.

[407] Inside EVs, "EV vs ICE Maintenance – The First 100,000 miles," 2012. [Online]. Available: http://insideevs.com/ev-vs-ice-maintenance-the-first-100000-miles/.

[408] Z. Wu, M. Wang, J. Zheng, X. Sun, M. Zhao, and X. Wang, "Life cycle greenhouse gas emission reduction potential of battery electric vehicle," *J. Clean. Prod.*, vol. 190, pp. 462–470, 2018.

[409] K. Lagowski, "What You Should Know About Today's Electric Car Batteries," *Fleetcarma*, Mar-2017.

[410] GreenBiz, "RMI: What's the true cost of EV charging stations?," 2014. [Online]. Available:

https://www.greenbiz.com/blog/2014/05/07/rmi-whats-true-cost-ev-charging-stations.

[411] China.org.cn, “Shandong builds 1st large electric car charging station,” 2010. [Online]. Available: http://www.china.org.cn/business/2010-04/11/content_19790544.htm.

[412] H. Hao, M. Wang, Y. Zhou, H. Wang, and M. Ouyang, “Levelized costs of conventional and battery electric vehicles in china: Beijing experiences,” *Mitig. Adapt. Strateg. Glob. Chang.*, vol. 20, no. 7, pp. 1229–1246, 2015.

[413] Trading Economics, “China Gasoline Prices | 1995-2017 | Data | Chart | Calendar | Forecast,” 2017. [Online]. Available: https://tradingeconomics.com/china/gasoline-prices.

[414] B. Propfe *et al.*, “Cost Analysis of Plug-in Hybrid Electric Vehicles including Maintenance & Repair Costs and Resale Values Implementing Agreement on Hybrid and Electric Vehicles,” vol. 5, p. 6862, 2012.

[415] D. Bakker, “Battery Electric Vehicles,” University of Utrecht, 2010.

[416] H. Huo, M. Wang, L. Johnson, and D. He, “Projection of Chinese Motor Vehicle Growth, Oil Demand, and CO_2 Emissions Through 2050,” *Transp. Res. Rec. J. Transp. Res. Board*, vol. 2038, pp. 69–77, 2007.

[417] U.S. Energy Information Administration (EIA), “International Energy Statistics - China - Production of motor gasoline,” 2017. [Online]. Available: https://www.eia.gov/beta/international/data/browser/.

[418] M. Madrigal and K. Porter, *Operating and Planning Electricity Grids with Variable Renewable Generation: Review of Emerging Lessons from Selected Operational Experiences and Desktop Studies*. World Bank Publications, 2013.

[419] Z. Luo, Z. Hu, Y. Song, Z. Xu, and H. Lu, “Optimal coordination of plug-in electric vehicles in power grids with cost-benefit analysis - Part I: Enabling techniques,” *IEEE Trans. Power Syst.*, vol. 28, no. 4, pp. 3546–3555, 2013.

[420] Z. Luo, Z. Hu, Y. Song, Z. Xu, and H. Lu, “Optimal Coordination of Plug-in Electric Vehicles in Power Grids With Cost-Benefit Analysis - Part II: A Case Study in China,” *Power Syst. IEEE Trans.*, vol. 28, no. 4, pp. 3556–3565, 2013.